PROTONS IN THE INNER RADIATION BELT

Gerhard Haerendel

Translation of "Protonen im inneren Strahlungsgürtel."
Fortschritte der Physik, Vol. 12, pp. 271-346, 1964.

NATIONAL AERONAUTICS AND SPACE ADMINISTRATION
WASHINGTON NOVEMBER 1965

NASA TT F-8771

[From: Fortschritte der Physik, 1964, Vol. 12, pp. 271-346.]

by Gerhard Haerendel

Division for Extraterrestrial Physics, Max Planck

Institute for Physics and Astrophysics, Munich.

PROTONS IN THE INNER RADIATION BELT

Table of Contents

Abstract

11606

The proton distribution at the lower limit of the radiation belt is calculated numerically as an equilibrium between replenishment through the decay of the albedo neutrons of the cosmic radiation and losses through collision in the upper atmosphere. The calculations of the particle orbits in the terrestrial magnetic field made by Jensen (1960) are utilized to take the mean of the atmospheric density over the particle motion. With this model and the atmospheric-density curve derived from the orbital changes of artificial satellite, the observed distribution of protons above 30 MeV can be satisfactorily represented for a flux density of about 10^3 cm^{-2} s^{-1}, provided we assume a neutron flux which is greater above 30 MeV by a factor of about 7 than the one found theoretically by Hess (1961). At higher values of the flux density, comparison with observations compels us to introduce losses by reason of the finite duration of captivity in the terrestrial magnetic field. It is made understandable that impairment or disturbance ("Verletzung") of the adiabatic invariants linked to the longitudinal drift, and caused by hydromagnetic waves is responsible for this. The theoretically derived time scale of this process and its dependence on energy and locus correspond to the requirements resulting from observation. On this basis, an interpretation of the minimum at a distance of twice the radius of the earth and of the variations in time is given.

Author

1 - Introduction

The phenomena grouped under the designation "terrestrial radiation belt" or "Van-Allen Belt" (from its discoverer) have in common that the terrestrial magnetic field keeps the high-energy electrons, protons and light nuclei captive in a narrowly restricted volume for intervals of time which are very long by comparison to the simple transit time. Somewhat different from the

circumstances in plasma experiments, the reaction of the captured particles on the magnetic field appears to be rather low because of their low density (Dessler, Vestine 1960). The other features of this formation such as its behavior in time, the loss processes and the replenishment have by no means a uniform character which is manifested in the occurrence of different spatial maxima and minima of distribution but the intensity of the latter greatly depends on the type of the measuring instruments utilized and the instant of measurement.

The protons above 1 MeV in the vicinity of the earth at the present time probably constitute the best understood component of the radiation belt. The suggestion made by Christofilos (cf. Van-Allen, 1959) immediately after the discovery of the radiation belt in 1958 that the replenishment is provided through the albedo neutrons of cosmic radiation -- these are secondary particles from an altitude of about 10-30 km which find their way into space -- has been subsequently discussed in detail and has in general been evaluated positively (first estimations by Singer, 1958; Kellogg, 1959 and Vernov et al, 1959). The strongest support for this theory was found in the rather satisfactory concordance of the spectrum between 30 and 200 MeV, measured by Freden and White (1959) with nuclear-emulsion plates, with the spectrum of equilibrium which may be expected with only collision losses and on the basis of present knowledge on the albedo neutrons (Hess, 1959; Freden, White, 1960). The observations of Naugle and Kniffen (1961) and Pizzela, McIlwain and Van Allen (1962-a) showed beyond this that, outside of the field lines with a distance of about 1.7 terrestrial radii measured in the equatorial plane, there must occasionally be added a very intensive neutron flux with a very much steeper spectrum to this continuous and almost constant flux of albedo neutrons of the galactic components of cosmic radiation, during the incidence of high-

energy solar particles in the magnetic-pole regions (Lenchek, Singer 1962, a,b; Lenchek 1962). Other promising possibilities of proton replenishment at low altitudes have not so far been found.

In regard to the losses of the captured protons, we must distinguish between two regions. In the vicinity of the surface of the earth, collisions obviously predominate in the determination of the life span because the increase of radiation with increasing altitude can be understood only as a consequence of the decrease of atmospheric density. Since the penetrating components of the radiation, i.e., the protons, decreases, however, already again beyond 1.5 terrestrial radii, as was shown by the measurements of Van Allen and Frank, (1959-a,b); Fan, Meyer and Simpson, (1961); Ginzburg, et al (1962); and Pizzela, et al (1962-a), there must here be added other loss processes which can be found only in the impairment of the three adiabatic invariants controlling particle motion and due to spatial inhomogeneity and variations in time of the magnetic field. The first suggestions in this direction were made by Singer, (1959) and Welch and Whitaker, (1959).

The theory of the captured protons has thus arrived at a point which makes a detailed quantitative investigation desirable. The question whether the flow of the albedo neutrons of cosmic radiation is actually sufficient for maintaining the stationary proton distribution measured in the vicinity of the earth and in low latitudes can be tested only there where the losses can be calculated <u>a priori</u> with satisfactory accuracy, i.e, at the lower limit of the radiation belt. The scale of the drop of atmospheric density, however, is here smaller by one order of magnitude than the differences of altitude through which the captured particles travel on their periodic orbit around the earth. This means that a relatively small error in the orbit description involves a high unreliability in the atmospheric density averaged over the particle motion

and consequently of the life span in relation to collisions which is an unreliability affecting the statements on the validity of the albedo hypothesis at the present time. The similarity existing in a certain range of energy between the energy spectrum measured and a theoretical spectrum which was derived from exclusive consideration of the collisions, could be entirely accidental. At higher altitudes (1,000 km and more) where the scale height of atmospheric density becomes much larger, we cannot say with certainty what the loss processes are which determine distribution. The collision intervals merely play the role of an upper limit. Here there is necessary on the other hand a satisfactory knowledge of the intensity of the proton-source intensity in order to draw conclusions on the time scale of the losses and eventually on their nature from comparison with the measured distribution of intensity.

The program suggested by this consideration was carried out in sec. 7 of this study. Prior to this, sec. 2 represents, in preparation for the model calculations, the bases of motion of the particles captured in the terrestrial magnetic field and the resulting manner of description of a distribution. For arbitrary particles, there is also valid further the derivation of the terms from a Fokker-Planck equation (sec. 3) with which the effect of the collisions on a distribution function can be expressed. However, the coefficients are indicated only for protons in view of the intended use. Sec. 4 intends to obtain a priori a concept of the time scales of the variations which are produced by the magnetic field in a given distribution. Sec. 5 describes the details of an adequately realistic description of orbit which enter into the averaging of the atmospheric density over the particle motion utilized in the following and sec. 6 describes the geometric aspects of proton capture upon decay of the albedo neutrons in the terrestrial magnetic field. With this and with the concepts on the flux of albedo neutrons from the lower atmosphere

obtained from the literature, the stationary proton distribution at low latitudes and low altitude has been calculated numerically and compared with the observations. On the assumption that the intensity of the proton source changes only slightly as far as field lines with a distance from the equator of 1.7 terrestrial radii, rough estimates of life span at higher altitudes were derived and correlated with the concepts sketched in sec. 4. The discontinuous injection possible beyond this limit under solar proton phenomena has not been treated here because it is still extraordinarily difficult to obtain satisfactory estimates of the neutron flux which then issues from the polar caps (such an attempt was undertaken by Lenchek, 1962). As a conclusion from the determination of time scales so carried out, there is finally attempted an interpretation of the minimum of distribution at a distance from the equator of about two terrestrial radii and of the behavior in time measured with Explorer VII (Pizzela, 1962-a).

2 - Demonstration of Particle Distribution

2.1 - Constants of Motion and Adiabatic Invariants

The magnetic field of the earth can be compared in satisfactory approximation to the field of a dipole. This is a special case of the general cylinder-symmetrical magnetic field in which we can postulate, in the absence of other forces, 2 integrals of the equation of motion of a particle with charge Ze and mass m (Luest and Schlueter 1957), i.e., the theorems of energy and of generalized angular momentum:

$$|v| = \text{const.} \tag{2.1}$$

$$sv_\varphi - \frac{Ze}{mc} F(s,z) = 2\gamma = \text{const.} \tag{2.2}$$

in which s, φ, z = cylinder coordinates are used as basis; v_φ = azimuthal component of velocity ; $2\pi F(s,z)$ = magnetic flux at altitude z through a circular surface orthogonal and concentric to the z-axis of symmetry; c = velocity of

light; 2γ = constant introduced by Stoermer in 1906 in the integration of the particle orbits in the dipole field which is equal to the angular momentum and/or the z-axis for F = 0. Because it is necessary that $|v_\varphi| \leqq |v|$, (2.1) and (2.2) can be combined into an inequality

$$\frac{1}{s}\left|\frac{Z|e|}{mc}F(s,z) + 2\gamma\right| \leqq |v|, \tag{2.3}$$

which subdivides space for a given particle, i.e., for the choice once made of the constants $|v|$ and 2γ, into permitted and prohibited areas (Stoermer, 1955). For the case where the "meridional" field component which can be derived separately from F(s, z), has closed field lines and the energy of the particle is not too high, (2.3) determines a finite volume which the particle cannot leave (Luest and Schlueter, 1957).

This is true precisely for a dipole field of the intensity of the terrestrial field and the particle energies observed in the radiation belt. Substitution of the numerical values in (2.2) shows that the value of 2γ is determined almost completely by the magnetic flux so that the permitted area can be characterized roughly by

$$F(s,z) \approx \text{const} \tag{2.4}$$

Read as equation, (2.4) describes a field line in a meridian plane. The thickness of the permitted area along this field line -- an example is sketched in fig. 2.1 -- results from (2.3) for small $|v|$ as equal to the diameter of the circle of gyration determined by local field intensity.

However, the laws of conservation do not indicate anything in regard to restriction of motion in the permitted area in the direction of the field. This is obtained with an approximation method developed by Alfven (1950) in which the actual motion, in analogy to the motion in the homogeneous field, is divided into two components also in the slightly inhomogeneous field or

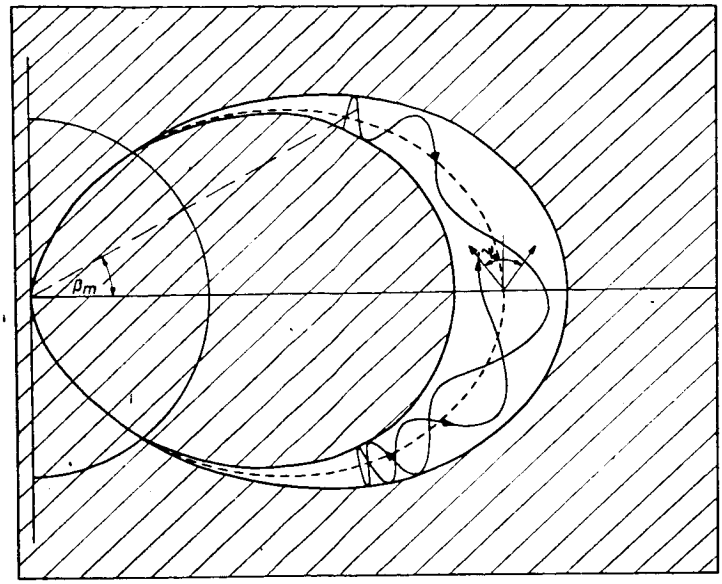

Fig. 2.1 - Orbit of charged particle captured in dipole field, projected on meridian plane and limits of area permissible according to Stoermer where ψ_o is the angle of inclination at the Equator.

the field slowly variable in time of which the one which does not spiral and essentially follows the field lines, is ascribed to a hypothetical particle, the guiding center whereas the other component, the gyration, performed by the true particle in the static system of the guiding center is, in this approximation, a circular motion of the frequency $\omega_g = (Z|e|B)/mc$. An extra force $\mathfrak{K} = -\mu$ grad B with the magnetic moment

$$\mu = \frac{p_g^2}{2 m_0 B} \tag{2.5}$$

in which p_g = impulse of gyratory motion; m_o = mass at rest; $B = |\mathfrak{B}|$ at the locus of the guiding center. μ corresponds to the magnetic moment of a circular current equivalent to the circulating charge and is constant in the border case

$$\frac{1}{\omega_g B}\left|\frac{d\mathfrak{B}}{dt}\right| \to 0 \tag{2.6}$$

μ is an adiabatic invariant. The action of the extra force attempting to displace the guiding center from regions of higher field intensity can be described in a very simple equation if we couple (2.5) with the energy postulate (2.1) and introduce the angle of orbital inclination ψ through $p_g = p \sin \psi$ (fig. 2.1)

$$\frac{\sin^2 \psi}{B} = \text{const.} \tag{2.7}$$

In the trivial inequality $\sin^2 \psi \leqq 1$, there now appears a restriction of motion along the field. If the constant in (2.7) has been once established, perhaps by the angle ψ_o and the field intensity B_o in the equatorial plane, there then results in $B_m = B_o \sin^{-2} \psi_o$ the maximum attainable field intensity in which the particle is forced into inversion, is "reflected." The relation of the velocity components parallel and perpendicular to the field and the radius of the circle of gyration

$$R_g = \frac{pc}{Z|e|B} \sin \psi \tag{2.8}$$

are determined over its entire path as pure function of the field intensity B. The result of this is that the particles, in a field like that of a dipole, execute an oscillation along the field lines between the two conjugated points of the field intensity B_m which is superposed, by reason of the field gradient and the centrifugal force occurring during oscillation, by a slow drift perpendicular to the latter with the velocity

$$v_D = \frac{\mathfrak{B}}{B^2} \times \left(\frac{\mu c}{Ze\gamma} \cdot \text{grad } B + \frac{pc}{ZeB} \cos \psi \frac{d\mathfrak{B}}{dt} \right) \tag{2.9}$$

(for a vanishing electric field, Schlueter 1959); $\gamma = (1 - v^2/c^2)^{-1/2}$. This drift slowly impels the particle around the axis of symmetry in the permitted area.

However, the terrestrial field is by no means ideal rotation-symmetrical and is moreover subject to variations in time so that the motion integrals (2.1) and (2.2) do not actually exist. At sufficiently small and slow interferences with the field, their place is taken by two further adiabatic invariants which are given through the phase volume of the other two periodic components of motion, oscillation and drift.

The first adiabatic invariant was found by M. Rosenbluth (Chew, Goldberger, Low 1955). It is generally written as the path integral extending over one oscillation period of the impulse component parallel to the field

$$J = \oint p_{\parallel} \, dl. \tag{2.10}$$

With an initially still assumed constancy in time of the field, i.e., at constant energy of the particle, the integrand in (2.10) is a pure function of locus according to (2.7). Consequently, there exists, between the integration limits B_m determined by μ, in general only a self-contained surface, the so-called invariant surface on which the integral assumes a given value J.

In the realistic case of slight time-dependent disturbances of the field in which the relative variation of the field during a drift period is, however, very small as against 1, it is possible for the guiding center to migrate, due to the change of particle energy, from one invariant surface to the adjacent one but only so that, in addition to μ and J, also the magnetic flux Φ enveloping the actually covered surface remains constant (Northrop and Teller, 1960). This means that the particles captured in the terrestrial field can follow slight variations to some extent but remain bound on the whole to a mean invariant surface and consequently cannot escape either inward or outward nor change -- which would be necessarily correlated with this -- their energy irreversibly.

The quality of adiabatic invariance will be discussed in sec. 4 but is assumed as unlimited for the time being. However, in that case, we can completely disregard the time-dependency of the field and also neglect, when the accuracy of the spatial structures does not need to be too high, the deviations from rotation-symmetry, i.e., return to the static dipole field in which motion is controlled essentially by the two magnitudes of conservation (2.1) and (2.2) and the adiabatic invariant μ.

2.2 - Motion of Charged Particles in the Magnetic Dipole Field

Let us here describe the magnetic dipole field in polar coordinates r, φ, λ, where the magnetic latitude β is counted starting from the equatorial plane. We then obtain for the field intensity the expression

$$B = \frac{M}{R_e^3} \cdot \frac{\sqrt{1 + 3 \sin^2 \beta}}{r^3}. \tag{2.11}$$

($M = 8.06 \times 10^{25}$ Gauss x cm^3; $R_e = 6{,}370$ km), for the equation of a field line

$$r = \varrho \cos^2 \beta \tag{2.12}$$

and the inclination

$$\cos i = \frac{\cos \beta}{\sqrt{1 + 3 \sin^2 \beta}}. \tag{2.13}$$

In the following, let us introduce the abbreviation

$$\zeta = \sin \beta \tag{2.14}$$

with which the relation of the equatorial field intensity B_o to $B(\zeta)$ is written according to (2.11) and (2.12) as

$$b^3(\zeta) = \frac{B_0}{B(\zeta)} = \frac{(1 - \zeta^2)^3}{\sqrt{1 + 3\zeta^2}} \tag{2.15}$$

The existence of three invariants of motion in the terrestrial field discussed in the preceding section will find its expression hereinafter by three parameters:

$$\alpha = \frac{E}{m^2 c_0} = \frac{\text{kinetic energy}}{\text{energy at rest}}$$

ρ = equatorial distance of the invariant surface (2.16)

$\eta = \sin \psi_0$ = sine of angle of inclination of equatorial orbit.

These parameters are sufficient to define the important features of particle motion. Since the life spans (cf. subsec. 3.3) are in general so long that the particles travel many times over even their longest orbital period, the drift, the phases (the angle ξ in the circle of gyration, φ and λ) coordinated with the three periodic components can remain indeterminate. All values of ξ and λ are equally probable in the motion and we need indicate a probability of locus merely for ζ. It is proportional to the transit time $dl/v_{\parallel}$ in the path interval

$$dl = R_e \rho \sqrt{1 + 3\zeta^2}\, d\zeta \tag{2.17}$$

along a field line. With (2.15), there follows from (2.7)

$$\sin \psi = |b^{-1}(\zeta)|\, \eta \tag{2.18}$$

and $v_{\parallel} = v \sqrt{1 - b^{-2}(\zeta) \cdot \eta^2}$. The constants R_e, ρ, v contained in $dl/v_{\parallel}$ are cancelled out under normalization and the probability of locus between ζ and $\zeta + d\zeta$ reads

$$w(\eta, \zeta)\, d\zeta = \frac{1}{\mathfrak{N}(\eta)} \cdot \frac{\sqrt{1 + 3\zeta^2}\, d\zeta}{\sqrt{1 - \eta^2 b^{-2}(\zeta)}}, \tag{2.19}$$

in which the normalization constant $\mathfrak{N}(\eta)$ is determined by

$$\int_{-\zeta_m(\eta)}^{\zeta_m(\eta)} w(\eta, \zeta)\, d\zeta = 1 \tag{2.20}$$

$$\mathfrak{N}(\eta) = 2{,}6 - 1{,}12 \cdot \eta. \tag{2.21}$$

is a satisfactory numerical representation.

$\pm \zeta_m(\eta)$ designate the latitudes of the reflection points ["Spiegelpunkte"] determined by the angle of inclination of the equatorial orbit; they result from (2.18) for $|\sin \psi| = 1$:

$$\eta = |b(\pm \zeta_m)|. \tag{2.22}$$

Since Ψ always lies between 0 and π, η is positive and the relation (2.18) between ψ and η is ambiguous. This is very appropriate for the present problem because it expresses the symmetry of each local angular distribution to $\Psi = \pi/2$ necessary for all the cases considered here. For the oscillation period, we obtain the expression

$$T_{osc} = 2\frac{\varrho R_e}{v}\mathfrak{N}(\eta) = 4{,}25\cdot 10^{-2}\,\varrho\,\frac{\alpha+1}{\sqrt{\alpha(\alpha+2)}}\mathfrak{N}(\eta) \quad [\mathrm{s}], \tag{2.23}$$

because the relativistic velocity is $v = c\sqrt{\alpha(\alpha+2)}/(\alpha+1)$. For the sake of completeness, we shall also indicate the gyration frequency ν_g and the gyration radius R_g for protons:

$$\nu_g = \frac{1}{2\pi}\cdot\frac{eB}{mc} = 4{,}8\cdot 10^2\,(\alpha+1)^{-1}\,\varrho^{-3}\,b^{-2}(\zeta) \quad [\mathrm{s}^{-1}] \tag{2.24}$$

$$R_g = \frac{v_\perp}{w_g} = \frac{m_0c^2}{eB}\sqrt{\alpha(\alpha+2)}\cdot\sin\psi = 100\sqrt{\alpha(\alpha+2)}\,\eta\varrho^3|b(\zeta)| \quad [\mathrm{km}]. \tag{2.25}$$

Along a field line, the cross section of the circle of gyration changes like $b^2(\zeta) = B_0/B(\zeta)$, i.e., the magnetic flux comprised in the gyration is a constant which is only another expression of the adiabatic invariant μ. According to Hamlin, et al, 1961 (cf. Equation 2.9), the drift frequency is

$$\nu_D = \frac{1}{2\pi}\cdot\frac{3mcv^2}{eB_0\varrho^2}\cdot G^*(\eta) \approx 0{,}175\,\frac{\alpha(\alpha+2)}{\alpha+1}\,\varrho(0{,}7+0{,}3\eta) \quad [\mathrm{s}^{-1}]. \tag{2.26}$$

2.3 - Projection of Terrestrial Magnetic Field on a Dipole Field

The usefulness of the dipole-field approximation for the terrestrial magnetic field is greatly increased if a satisfactory rule exists by which the two fields can be projected on each other point by point. The procedure for this which must start in this connection obviously from the particle motion, has already been outlined in sub-section 2.1. It consists simply in a correlation of the invariant surfaces determined respectively by μ and J. As assumed here, if the field is constant in time, the dependence on energy

can be separated from μ and J and the invariant surface can be characterized through (2.5) and (2.10) by

$$\mu \cdot \frac{2 m_0}{p^2} = \frac{\sin^2 \psi}{B} = \frac{1}{B_m} \tag{2.26}$$

$$J' = \frac{J}{2p} \int_{l_1(B_m)}^{l_2(B_m)} \cos \psi \, dl = \int_{l_1(B_m)}^{l_2(B_m)} \sqrt{1 - \frac{B}{B_m}} \, dl \tag{2.27}$$

where the integral (2.27) must be taken along a field line. B_m and J' are consequently determined purely by the magnetic field and can therefore easily be introduced as coordinates in the terrestrial field. There then correspond to each pair of numbers (B_m, J') two curves enclosing the magnetic axis which may be regarded as the connecting lines of the conjugated northern and southern reflection points. The trace of these curves by altitude, geographic latitude and longitude have been computed and tabulated by Jenssen, Murray and Welch (1965) on the basis of a multipolar representation of the terrestrial magnetic field as far as the orders n = 24 and m = 17 for a number of values of B_m and J'.

In the dipole field where dependence on length becomes trivial due to rotation symmetry, there exists a simple correlation between the coordinates ρ, ζ and B_m, J'. From (2.11) and (2.15), there follows

$$\frac{B_m R_e^3}{M} = B^* = \varrho^{-3} b^{-2}(\zeta) \tag{2.28}$$

$$\frac{J'}{2 R_e} = J^* = \varrho \, \tilde{J}(\zeta), \tag{2.29}$$

$$\tilde{J}(\zeta) = \int_0^{+\zeta} \sqrt{1 - \frac{b^2(\zeta)}{b^2(\zeta')}} \cdot \sqrt{1 + 3\zeta'^2} \, d\zeta' \approx 1{,}745 \cdot \zeta^2 - 0{,}562 |\zeta|^3 + 0{,}1925 \zeta^4.$$

In the dipole field, a family of invariant surfaces all belonging to a common surface, is characterized by constant ρ. This must be regarded as a consequence of the predominantly dipolar character of the terrestrial field and makes possible, for the projection described, the further simplification

that this is valid also in satisfactory approximation -- which is by no means a matter of course -- for the accompanying invariant surfaces (of the projection) in the terrestrial magnetic field. The appurtenance of the surface B^*, J^* to such a family is then expressed, according to McIlwain (1961), in a parameter whose correlation with B^*, J^* is exactly the same as for ρ. The latter is easily obtained from Equations (2.28) and (2.29) through elimination of ζ. Initially B^*, $J^{*3} = h(\zeta)$ is a continuous monotonous function of ζ. The inverse function $\check{h}(B^*J^{*3})$ of the latter, when introduced as argument in (2.28), leads to

$$B^*\varrho^3 = b^{-2}(\check{h}(B^*J^{*3})) = H(B^*J^{*3})$$

and thus furnishes the definition of the family parameter L from

$$L^3 = \frac{H(B^*J^{*3})}{B^*}. \qquad (2.30)$$

On the basis of the numerical computations of Jenssen, Murray and Welch, McIlwain was able to show that the largest relative deviations from L along a field line still lie below 1% for L = 3.

2.4 - Definition of Distribution Function and Correlation with Intensity of Radiation

The findings just described are of considerable importance for the intended application because they guarantee, also for a quantitative calculation of particle distribution, the quality of the dipole-field approximation in combining the individual orbits to an entirety and permit the physically correct correlation of the measured data to the image loci in the dipole field. This further justifies also the utilization of the parameters $\alpha(\triangleq E), \eta(\triangleq B_m), \varrho(\triangleq L)$ defined in (2.16) initially for the dipole field, as variables of a distribution function describing the entirety of the particles. If in the following the parameter ρ is utilized instead of L as customary in literature, this is meant to express that the formulas describing distribution are valid strictly only in the dipole field.

φ occupies a special position in the model calculations to be carried out later because an effective change of this parameter does not occur in the processes treated then. Moreover, the intensity of radiation at a locus is formed only by particles whose ϱ-values lie in a very narrow interval of the magnitude of twice the gyration radius. It will be shown further that the integral of the distribution function over this interval which should consequently be carried out in principle, can be substituted in very satisfactory approximation by the values in the center of the interval. φ therefore appears as a parameter in the calculation of the distribution function. This suggests the following definition of the distribution function:

$f(\alpha, \eta; \varrho, t)\, d\alpha\, d\eta$ = number of particles with energies between α and $\alpha + d\alpha$ with $\sin \psi_0$ between η and $\eta + d\eta$ and the guiding center in a tube of force with a cross section of 1 cm^2 and the distance ϱ in the equatorial plane. (2.31)

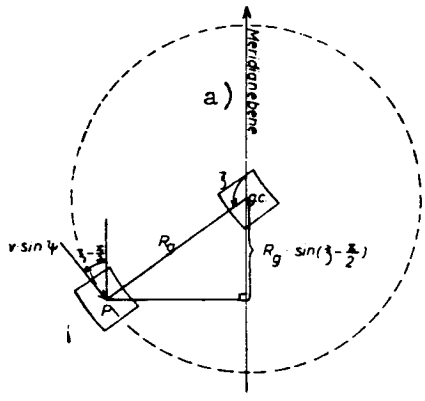

Fig. 2.2 - Interrelation between the locus of the guiding center (g.c.) and that of the true particle (P) and between the phase angle ζ and the velocity vector in a plane perpendicular to the field.
Legend: a) Meridian plane.

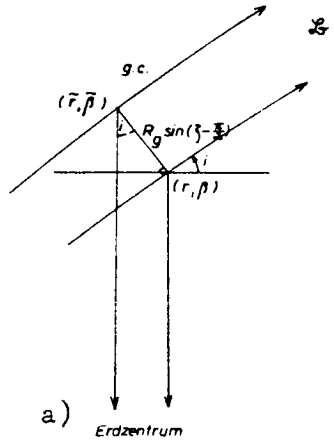

Fig. 2.3 - Same interrelation as in Fig. 2.2 seen in a meridian plane.
Legend: a) Center of earth.

Initially, the density of the guiding center of particles in the interval (α, $\alpha + d\alpha$) and (η, $\eta + d\eta$) is to be calculated from $f(\alpha, \eta; \varrho, t)$ at a point ϱ, ζ. Let a section of the tube of force with cross section of 1 cm^2 have the

length d (2.17). According to (2.24-a), the cross section of this tube of force is greater by a factor $b^{-2}(\zeta)$ in the equatorial plane so that all guiding centers characterized by $b^{-2}(\zeta)\, f(\alpha, \eta; \varrho, t)\, d\alpha\, d\eta$ transit this section in their orbit. In a stationary distribution, however, there is found here simultaneously only the fraction determined by the probability of locus $w(\eta, \zeta)\, d\zeta$. Divided by the length d of the section, the desired density of guiding center at the point ϱ, ζ reads

$$n_{g.c.}\, d\alpha\, d\eta = \frac{1}{R_e \varrho \sqrt{1 + 3\zeta^2 b^2(\zeta)}} \cdot f(\alpha, \eta; \varrho, t)\, w(\eta, \zeta)\, d\alpha\, d\eta. \tag{2.32}$$

Much less clear in contrast is the correlation between f and the intensity of radiation $I(\alpha, \varrho, \zeta, \psi, \xi)$ in which ξ = angle of orbital inclination and ψ = angle of phase around the direction of field, if we consider the finite magnitude of the gyration radii which cannot be avoided there where the intensity of radiation changes over comparable distances, i.e., precisely for protons with energies above 100 MeV in the vicinity of the earth. Fig. 2.2 shows, in a plane perpendicular to the direction of field, the relation between the direction of incidence of the radiation in a volume element around the measuring point P and the position of the appurtenant guiding center. The phase difference of 90° between these two directions has as a consequence that an increase of the density of guiding center in the vertical produces an east-west anisotropy (Lenchek, Singer 1962-c) of the radiation intensity, completely disregarding the anisotropy in the angle of orbital inclination ψ.

The locus of the guiding center $(\tilde{r}, \tilde{\beta})$ can be expressed approximately, as indicated in Fig. 2.3, by the coordinates (r, β) and the direction of incidence $(i, \xi - \pi/2)$ of the particle

$$\begin{aligned} \tilde{r} &\approx r + R_g \sin\left(\xi - \frac{\pi}{2}\right) \cos i \\ \tilde{\beta} &\approx \beta + \frac{R_g}{r} \sin\left(\xi - \frac{\pi}{2}\right) \sin i. \end{aligned} \tag{2.33}$$

With the approximation of a field homogeneous within the range of a circle of gyration, i.e., $\tilde{B} \approx B$, $\tilde{\psi} \approx \psi$, there result from this the appurtenant variables of the distribution function as

$$\tilde{\eta} = \sin\psi \cdot |\tilde{b}(\zeta)|, \quad \tilde{\zeta} = \sin\tilde{\beta}, \quad \tilde{\varrho} = \frac{\tilde{r}}{1-\tilde{\zeta}^2}. \tag{2.34}$$

Because of the constant probability of locus of the particles in the circle of gyration, there follows from the density of guiding center (2.32) with ν, $\tilde{\eta}$, $\tilde{\varrho}$ the intensity at the locus ϱ, ζ simply through multiplication with $\nu/2\pi$ in which it is necessary to state $d\tilde{\eta} = |b(\zeta)| \cos\psi \, d\psi$ and also to introduce a factor of $\frac{1}{2}$ by reason of the ambiguity of the correlation between ψ and $\tilde{\eta}$:

$$I(\alpha, \varrho, \zeta, \psi, \xi)\, d\alpha \sin\psi \, d\psi \, d\xi = \frac{\cot\psi}{4\pi R_e \tilde{\varrho} \sqrt{1+3\tilde{\zeta}^2}\,|b(\tilde{\zeta})|} \times \\ \times \nu \cdot f(\alpha, \tilde{\eta}; \tilde{\varrho}, t)\, w(\tilde{\eta}, \zeta)\, d\alpha \sin\psi \, d\psi \, d\xi. \tag{2.35}$$

In order to obtain an experimental determination of the distribution function, it would be sufficient to measure with satisfactory angular resolution the intensity of radiation in the equatorial plane which is obviously traversed by all particles. However, such measurements are not now available. The comparison between experiment and theory therefore is made most simply in the intensity averaged over the entire solid angle along a field-line shell:

$$\bar{I} = \frac{1}{4\pi} \int_0^{\pi} \int_0^{2\pi} I \sin\psi \, d\psi \, d\xi. \tag{2.36}$$

Fortunately, one of the two integrations (the one over ξ) can be carried out approximately general. In doing this, there will be substituted, except for f, the values for all expressions of the integrand (2.35) (which evidently depend only slightly on ξ at gyration radii of a few 100 km maximum) in the center of interval, i.e., in $\tilde{\varrho} = \varrho$ and $\tilde{\zeta} = \zeta$, and the remaining integral defined as

$$\bar{f}(\alpha, \eta; \varrho, t) = \frac{1}{2\pi} \int_0^{2\pi} f(\alpha, \eta; \varrho, t)\, d\xi \tag{2.37}$$

By retracting the transformation $\eta \to \psi$, $\bar{I}$ attains the form:

$$\bar{I}(\alpha, \varrho, \zeta, t)\, d\alpha = \frac{v(\alpha)\, d\alpha}{4\pi R_e \varrho \sqrt{1 + 3\zeta^2 b^2(\zeta)}} \int_{\eta_{min}(\varrho)}^{\eta_0(\zeta)} \bar{f}(\alpha, \eta; \varrho, t)\, w(\eta, \zeta)\, d\eta \qquad (2.38)$$

with the interval limits (cf. (2.13))

$$\eta_0(\zeta) = |b(\zeta)|; \quad \eta_{min}(\varrho) = \frac{\left(\frac{r_{min}}{\varrho}\right)^{3/2}}{\sqrt[4]{4 - 3\frac{r_{min}}{\varrho}}}, \qquad (2.39)$$

where the lower limit of η is determined by the altitude r_{min} below which the radiation can be regarded as vanishing.

In case the gyration radius is small in relation to the length over which particle intensity changes appreciably $\bar{f}(\alpha, \eta; \varrho, t)$ can be replaced by $f(\alpha, \eta; \varrho, t)$. However, as shown by Lenchek and Singer (1962-b) due to an error of the author (Haerendel 1962), this is possible also then when the change of radiation intensity is a pure consequence of the drop of atmospheric density, i.e., in particular if the replenishment of the particles in the range in question can be regarded as constant. This is seen most simply for the particles which are reflected in a straight line ["gerade"] at the point of measurement. Since the probability of locus is highest at the reflection point and the curve of density under the assumption is very steep, the distribution function f will be reversely proportional to the density average over the circle of radiation at the point of reflection for adjacent values of ϱ, η in the stationary case. This density differs from the density at the locus of the guiding center by the factor $I_0((R_g \cos i)/H)$ (modified Bessel function of zero order) (Haerendel 1962) if the scale height ["Skalenhoehe"] H of the atmosphere remains constant over the circle of gyration. However, the integral (2.37) does contain a corresponding mean of the radiation intensity for a circle of gyration with the point of measurement as center. Because of the reciprocity of f and of the mean density, the factor

$I_o((R_g \cos i)/H)$ is cancelled out strictly at constant scale height and approximately at slightly variable H with the result that

$$\bar{f}(\alpha, \eta; \varrho, t) = f_{inf}(\alpha, \eta, \varrho, t) \tag{2.40}$$

in which the index "inf" points to the fact that f must be calculated in the approximation of an infinitesimal radius of gyration. It is easily understood qualitatively that (2.40) is valid also for an arbitrary local angle of inclination ψ and a realistic particle replenishment which undergoes in the neutron albedo treated here (cf. sec. 6) only a geometric dilution, i.e., of 1 to 2 R_e, by a factor of about 4. This represents an essential simplification in the following.

2.5 - Changes of Distribution Function

In the changes of a given distribution f, we must distinguish between two cases: the spontaneous capture or loss of particles and the disturbance in the parameters α, η, ϱ. The capture will here be given by a stationary source function ["Quellfunction"], whose calculation is treated in sec. 6. The spontaneous particle loss, perhaps by neutralization and consequent liberation from the magnetic field or other collision processes, can be described by an effective cross section σ and the density $\bar{N}$ of the collision centers averaged over the particle orbit, in an expression of the form

$$\left(\frac{\partial f}{\partial t}\right)_r = -\sigma \bar{N} v f \tag{2.41}$$

Changes in the parameters can be caused by collisions with atmospheric particles or disturbance of the adiabatic invariants purely over the magnetic field. The former and in general also the processes falling under the second group are Markoff processes which can be determined with a Fokker-Planck equation. Their derivation (see, e.g., Chandrasekhar, 1943) is made with the aid of the probability $\varphi(\alpha, \eta; \Delta\alpha, \Delta\eta; \varrho, t)\, d(\Delta\alpha)\, d(\Delta\eta)$ for the case where the parameters α, η of a particle after a lapse of time Δt are located in the interval

$(\alpha + \Delta\alpha, \quad \alpha + \Delta\alpha + d(\Delta\alpha); \quad \eta + \Delta\eta, \quad \eta + \Delta\eta + d(\Delta\eta))$. On the assumption that the changes during this interval are predominantly small in relation to α, η, we can develop the integral expression for $f(\alpha, \eta; \varrho, t + \Delta t)$ and there results

$$\left(\frac{\partial f}{\partial t}\right)_P = -\frac{\partial}{\partial \alpha}(\langle \Delta\alpha \rangle f) - \frac{\partial}{\partial \eta}(\langle \Delta\eta \rangle f) + \frac{1}{2}\frac{\partial^2}{\partial \alpha^2}(\langle \Delta^2\alpha \rangle f) + \\ + \frac{\partial^2}{\partial \alpha\, \partial \eta}(\langle \Delta\alpha\, \Delta\eta \rangle f) + \frac{1}{2}\frac{\partial^2}{\partial \eta^2}(\langle \Delta^2\eta \rangle f) \qquad (2.42)$$

with the <u>diffusion coefficients</u>

$$\langle \Delta\alpha \rangle = \frac{1}{\Delta t}\int \Delta\alpha \cdot \varphi \cdot d(\Delta\alpha)\, d(\Delta\eta)$$

$$\langle \Delta^2\alpha \rangle = \frac{1}{\Delta t}\int (\Delta\alpha)^2 \cdot \varphi \cdot d(\Delta\alpha)\, d(\Delta\eta)$$

etc.

$$\int \varphi(\alpha, \eta; \Delta\alpha, \Delta\eta; \varrho, t)\, d(\Delta\alpha)\, d(\Delta\eta) = 1. \qquad (2.43)$$

The Fokker-Planck equation has been written within the sense of definition (2.31) for constant ϱ because it is used in this study explicitly only in this form.

3 - Collision with Atmospheric Particles

3.1 - Calculation of Diffusion Coefficients

The definition of the diffusion coefficients (2.43) was made with the aid of the probability $\varphi(\alpha, \eta; \Delta\alpha, \Delta\eta; \varrho, t)\, d(\Delta\alpha)\, d(\Delta\eta)$ for the change of the parameters α, η within the time Δt. With its neglect of all geometric details, this form of the probability function is too abstract to be applied to collision processes. It is therefore to be replaced by a new form which is the product of the local probability of collision -- possessing greater clarity -- and the probability of locus at all loci attainable under given ξ, η and in the possible orientations. $\Delta\eta$ is then to be expressed as a function of the geometric variables.

The <u>probability of locus</u> dw_a in the three phases ξ, η, ζ which remain open in the characterization of the particle orbit, can -- normalized to one -- be immediately indicated with (2.19) as

$$dw_a = w(\eta, \zeta)\, d\zeta \cdot \frac{d\lambda}{2\pi} \cdot \frac{d\xi}{2\pi}. \tag{3.1}$$

We arrive at the probability of collision by way of the differential effective cross sections of the various collision processes for which we can state here as follows

$$Q(\alpha, \Delta\alpha, \Theta)\, d(\Delta\alpha) \cdot q(\alpha, \Theta) \sin\Theta\, d\Theta\, d\Phi. \tag{3.2}$$

in which $Q(\alpha, \Delta\alpha, \Theta)$ designates the correlation between the change of energy $\Delta\alpha$ and the angle of dispersion Θ which has, under elastic collision, e.g., the character of a δ-function. Let it be considered as normalized to one so that consequently $q(\alpha, \vartheta)$ contains the actual effective cross section. Under the assumption here applicable that the collision centers in the system of the static magnetic field may be regarded as at rest in comparison to the colliding particles, Θ and ϑ can be interpreted as angles of dispersion in this system.

The multiplication of (3.2) with the velocity $v(\alpha)$ of the colliding and the density $N(\varrho, \zeta, \lambda, t)$ of the encountered particles produces the number of collisions per unit time which leads to a dispersion according to $(\Theta, \Theta + d\Theta)$, $(\Phi, \Phi + d\Phi)$ at a loss of energy between $\Delta\alpha$ and $\Delta\alpha + d(\Delta\alpha)$. Strictly speaking, the phase ξ in the circle of gyration still belongs to the arguments of N because the density over the diameter of the latter can change appreciably. However, we have just shown it to be reasonable in sub-section 2.4 that the approximation of an infinitesimal gyration radius' signifies a consistent simplification in the calculation of the mean intensity (2.38) and the mean density $\overline{N}$. With the reciprocal collision time

$$\frac{1}{\Delta t} = N(\varrho, \zeta, \lambda, t)\, v(\alpha) \int_0^{2\pi} \int_0^{\pi} q(\alpha, \Theta) \sin\Theta\, d\Theta\, d\Phi \tag{3.3}$$

we then obtain the probability of collision normalized to one

$$dw_s = \Delta t \cdot v(\alpha)\, N(\varrho, \zeta, \lambda, t)\, Q(\alpha, \Delta\alpha, \Theta)\, d(\Delta\alpha)\, q(\alpha, \Theta) \sin\Theta\, d\Theta\, d\Phi. \tag{3.4}$$

The collision time Δt here appears as the natural interval of time to which the probability $\varphi d(\Delta\alpha)\, d(\Delta\eta)$ was referenced in (2.43). Consequently, the definition of the diffusion coefficients in the description of collisions reads

$$\langle \Delta \cdots \rangle = \frac{1}{\Delta t} \int \Delta \cdots dw_s\, dw_a \tag{3.5}$$

or expanded

$$\langle \Delta \cdots \rangle = v(\alpha) \int \Delta \cdots N(\varrho, \zeta, \lambda, t)\, Q(\alpha, \Delta\alpha, \Theta)\, d(\Delta\alpha) \times$$
$$\times\, q(\alpha, \Theta) \sin\Theta\, d\Theta\, d\Phi\, w(\eta, \zeta)\, d\zeta\, \frac{d\lambda}{2\pi} \cdot \frac{d\xi}{2\pi}. \tag{3.5a}$$

Δw occurs in (3.5-a) as a variable; consequently only $\Delta\tau$ needs to be indicated as function of the other variable. From fig. 3.1, we obtain for the angle of orbital inclination ψ' subsequent to collision, in the spherical cosine theorem, the relation

$$\cos\psi' = \cos\psi\cos\Theta + \sin\psi\sin\Theta\cos\Phi. \quad (3,6) \tag{3.6}$$

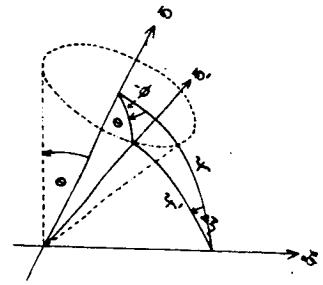

Fig. 3.1 - Collision cone with aperture Θ around the velocity v prior to collision and the change of the angle of orbital inclination ψ and the phase τ in the circle of gyration at a velocity v' subsequent to collision.

With the abbreviation

$$y = \sin\psi,\ \Delta y = \sin\psi' - \sin\psi$$

this furnishes

$$\Delta y = \sqrt{1 - \cos^2\psi'} - y.$$

With (2.13), there follows

$$\Delta\eta = |b(\zeta)| \cdot \Delta y(\eta, \zeta, \Theta, \Phi). \tag{3.7}$$

In the sense of the derivation of the Fokker-Planck equation, there are of interest above all the small-angle collisions. For this or more exactly for

$$\Delta\psi = \psi' - \psi \ll \psi$$

a more convenient form of $\Delta\eta$ can be derived from (3,6):

$$\cos\psi' - \cos\psi = -\tan\left(\psi + \frac{\Delta\psi}{2}\right) \cdot (\sin\psi' - \sin\psi) \approx -\tan\psi \cdot \Delta y$$

i.e.,

$$\Delta y \approx \cot\psi\cos\psi\,(1 - \cos\Theta) - \sin\psi\sin\Theta\cos\Phi. \qquad (3,6)\ [\text{sic}]$$

For $\Theta \approx \sin\Theta$ there results

$$\Delta\eta \approx \frac{b^2(\zeta) - \eta^2}{2\eta}\Theta^2 \mp \sqrt{b^2(\zeta) - \eta^2}\,\Theta\cos\Phi. \qquad (3,7a)$$

With the dispersion, the position of the guiding center also changes. This leads to $\Delta\varrho$ and, by way of (3,5-a), to the diffusion coefficients $\Delta\varrho$ and $\Delta^2\varrho$. However, the first vanishes by reason of the averaging over the phase ξ in the circle of gyration and the influence of the second is also very minor. This is due to the fact that, in the time in which η has changed in the mean by any appreciable amount (about $\eta/\langle\Delta\eta\rangle$ or $\eta^2/\langle\Delta^2\eta\rangle$), i.e., in which a given distribution of reflection points has become appreciably dispersed, the dispersion of the guiding centers in ϱ is only of the magnitude of one gyration radius. However, the description of such structures was explicitly excepted in subsection 2,4. By contrast, the dispersion of the reflection points has a non-evaluable effect, i.e., a diffusion of the particles into the trough represented by the denser atmosphere. Neglect of $\langle\Delta^2\varrho\rangle$ represents in relation to the collision losses the justification for the definition (2,31) of the distribution functions and for the form (2,42) of the respective Fokker-Planck equation.

3.2 - Review of the Processes Important for Protons

3.2.1. - Coulomb Dispersion

Coulomb dispersion is a process for which the derivation of the diffusion coefficients can be made in a simple manner. The classic non-relativistic

treatment is adequate for this purpose. It is convenient here to characterize the hyperbolic orbit of the collision particle (m_1, e_1, v) in the field of a particle at rest (m_2, e_2) by the collision parameter P. The latter is correlated with the angle of dispersion χ in the center-of-gravity system through

$$\cot\frac{\chi}{2} = \frac{m_2}{m_1 + m_2}\cdot\frac{p}{p_0}; \quad p_0 = \frac{e_1 e_2}{m_1 v^2} \tag{3.8}$$

The transformation of χ to the angle θ in the laboratory system reads

$$\cot\theta = \cot\chi + \frac{m_1}{m_2}\sin^{-1}\chi \tag{3.9}$$

and the energy loss ΔE of the primary particle under elastic collision reads

$$\frac{\Delta E}{E} = -4\frac{m_1 m_2}{(m_1 + m_2)^2}\cdot\sin^2\frac{\chi}{2}. \tag{3.10}$$

(3.10) corresponds to a δ-function for $Q(\alpha, \Delta\alpha, \theta)$ in the differential effective cross section (3.2) which now obtains, by using the collision parameter p, a very clear form

$$p\,dp\,d\Phi. \tag{3.2a}$$

The integration over p in the calculation of the diffusion coefficients must be carried out from a minimum value containing the limit of validity of the classic Coulomb dispersion at nuclear dimensions, to an outer limit beyond which the charge under question can be considered as screened by opposite-charge carriers. Whereas we take into account, in dispersion on atoms, screening continuously with a factor of atomic form, it has been proved to be a satisfactory method in dispersion on free charge carriers (Cohen, Spitzer and Routley, 1950), to calculate with the undistrubed two-particle collision within a Debye radius

$$h_D = \sqrt{\frac{kT}{4\pi N_e e^2}} \tag{3.11}$$

and to terminate integration at that point.

In this approximation, we intend to treat first the energy transfer $\langle \Delta E \rangle$ to the free charge carriers in the plasma. Of the six integrations in (3.5-a), five can be carried out immediately: one by way of $\Delta\lambda$ and/or ΔE by using expression (3.10) for ΔE, one by way of ϑ and ζ trivially because ΔE does not depend on them and -- if we forget for the moment that the upper limit h_D of the p-integration depends on N and consequently on ζ and λ -- one by way of ζ and λ formally by introducing the mean density

$$\bar{N}(\eta, \varrho, t) = \frac{1}{2\pi} \int_{-\zeta_m(\eta)}^{+\zeta_m(\eta)} \int_0^{2\pi} N(\varrho, \zeta, \lambda, t)\, w(\eta, \zeta)\, d\zeta\, d\lambda. \tag{3.12}$$

From

$$\sin^2 \frac{\chi}{2} = \left(1 + \cot^2 \frac{\chi}{2}\right)^{-1}$$

and (3.8), there consequently follows

$$\langle \Delta E \rangle = -2\pi \bar{N} v \cdot 4E \frac{m_1 m_2}{(m_1 + m_2)^2} \int_{p_{\min}}^{h_D} \frac{p\, dp}{1 + \left(\frac{m_2}{m_1 + m_2} \frac{p}{p_0}\right)^2}.$$

The substitution

$$x = \frac{m_2}{m_1 + m_2} \cdot \frac{p}{p_0}, \quad \Lambda = \frac{m_2}{m_1 + m_2} \cdot \frac{h_D}{p_0} \tag{3.13}$$

produces

$$\langle \Delta E \rangle = -8\pi \bar{N} v E p_0^2 \frac{m_1}{m_2} \int_{x_{\min}}^{\Lambda} \frac{x\, dx}{1 + x^2}.$$

If we substitute in (3.11) the numerical values which may be expected for the upper atmosphere, we find h_D in the order of magnitude of one cm whereas probably $p_{min} \approx 10^{-13}$ to 10^{-12} cm. The lower limit of the integration x_{min} can therefore without difficulty be stated as equal to zero. Consequently

$$\langle \Delta E \rangle = -8\pi \bar{N} v \cdot E \cdot \frac{m_1}{m_2} p_0^2 \cdot \ln \Lambda. \tag{3.14}$$

The logarithmic member contains the density and should therefore actually be contained in the averaging (3.12). Because of the slight dependence on density, however, it will constitute a satisfactory approximation if we retain the form (3.14) and substitute the mean density $\bar{N}_e$ in h_D.

The <u>calculation of</u> $\langle \Delta \vartheta \rangle$ becomes similarly simple. Let us here also neglect the near collisions and therefore select the lower integration limit p_{min} so that we can state $\sin \vartheta \approx \vartheta$. This is attained already for

$$p > p_{\min} = 10 \frac{m_1 + m_2}{m_2} \cdot p_0$$

and there follows from (3.8) and (3.9)

$$\Theta \approx \frac{m_2}{m_1 + m_2} \chi \approx 2 \frac{p_0}{p}. \tag{3.15}$$

For $\Delta \eta$, we can utilize the approximation (3.7-a) from which remains, through integration by way of λ, only the first member

$$\langle \Delta \eta \rangle = 2\pi v \int_{-\zeta_m}^{+\zeta_m} \int_0^{2\pi} \int_{p_{\min}}^{p_D} N(\varrho, \zeta, \lambda, t) \cdot \frac{b^2(\zeta) - \eta^2}{2\eta} \cdot w(\eta, \zeta) \left(2 \frac{p_0}{p}\right)^2 p \, dp \, d\zeta \, \frac{d\lambda}{2\pi} \approx$$

$$\approx 4\pi v \cdot \bar{\bar{N}}(\varrho, \eta, t) \cdot \eta \cdot \eta \cdot p_0^2 \int_{10 \frac{m_1+m_2}{m_2}}^{\Lambda} \frac{x \, dx}{x^2}$$

i.e.,

$$\langle \Delta \eta \rangle = 4\pi v \bar{\bar{N}} p_0^2 \ln \frac{\Lambda}{10} \cdot \eta \tag{3.16}$$

with

$$\bar{\bar{N}}(\varrho, \eta, t) = \frac{1}{2\pi} \int_{-\zeta_m(\eta)}^{+\zeta_m(\eta)} \int_0^{2\pi} N(\varrho, \zeta, \lambda, t) \cdot \left(\frac{b^2(\zeta)}{\eta^2} - 1 \right) w(\eta, \zeta) \, d\zeta \, d\lambda. \tag{3.17}$$

$\bar{\bar{N}}$ is distinguished from $\bar{N}$ by the fact that it is weighted with a positive factor which vanishes at the reflection point and has its maximum at the equator. The change of the reflection points in relation to dispersion around Ψ is much more sensitive at lower altitudes, i.e., at relatively small Ψ, than at $\Psi = \pi/2$.

Entirely correspondingly, we find for the second dispersion coefficient, if we neglect members with ϑ^4 in $\Delta \zeta$,

$$\langle \Delta^2 \eta \rangle = 8\pi v \bar{\bar{N}} \eta^2 p_0^2 \ln \frac{\Lambda}{10} = 2\eta \langle \Delta \eta \rangle. \tag{3.18}$$

Initially it should be noted that we can restrict ourselves to the coefficients $\langle \Delta\alpha \rangle$, $\langle \Delta\eta \rangle$, $\langle \Delta^2\eta \rangle$ in this connection. This is due to the fact that both $\langle \Delta\alpha \Delta\eta \rangle$ as well as $\langle \Delta^2\alpha \rangle$ lead to integrals over x in which the nominator is of the fourth instead of the second order in x, i.e., only the value of the integral at the lower limit plays a role. The other expressions are therefore greater by at least one factor $\ln \Lambda (\approx 30)$. This result derived for the Coulomb dispersion is valid also for other collision processes, provided the small-angle collisions possess a largely predominant probability which is a prerequisite for the usefulness of the Fokker-Planck equation. An exception is discussed in subsection 3.2.3. However, with this the Fokker-Planck equation (2.42) also becomes simplified (if $\langle \Delta x \rangle$ is again introduced for $\langle \Delta E \rangle$) to

$$\left(\frac{\partial f}{\partial t}\right)_P = -\frac{\partial}{\partial \alpha}(\langle \Delta\alpha \rangle f) - \frac{\partial}{\partial \eta}(\langle \Delta\eta \rangle f) + \frac{1}{2}\frac{\partial^2}{\partial \eta^2}(\langle \Delta^2\eta \rangle f) \tag{3.19}$$

or, specifically for the correlation (3.18),

$$\left(\frac{\partial f}{\partial t}\right)_P = -\frac{\partial}{\partial \alpha}(\langle \Delta\alpha \rangle f) + \frac{\partial}{\partial \eta}\left(\eta \frac{\partial}{\partial \eta}(\langle \Delta\eta \rangle f)\right). \tag{3.19a}$$

This derivation corresponds somewhat to that of McDonald and Walt (1961).

To turn now to the treatment of the <u>protons</u>, it will be well to compare the time scales of energy loss and dispersion. (3.14) and (3.18) produce

$$\left| \frac{E}{\langle \Delta E \rangle} \Big/ \frac{\eta^2}{\langle \Delta^2 \eta \rangle} \right| \approx \frac{\bar{\bar{N}}}{\bar{N}} \cdot \frac{m_2}{m_1}. \tag{3.20}$$

The most important difference consists in the factor m_2/m_1. It means that the primary particles transfer their energy principally to the electrons and that, especially for protons ($m_2/m_1 = m_e/m_p$), <u>dispersion can be neglected in relation to the energy loss</u>; until deceleration, the protons essentially retain their orbit. Even the factor $\bar{\bar{N}}/\bar{N}$ does not change anything in this and

it can easily be estimated for constant distribution of density, i.e., for the case in which it assumes the greatest values, with (2,20), (2,21) and (2,29):

$$\frac{\bar{\bar{N}}}{\bar{N}} \leqq \int_{-\zeta_m}^{+\zeta_m} \left(\frac{(b^2(\zeta)}{\eta^2} - 1 \right) w(\eta, \zeta)\, d\zeta = \frac{2}{\Re(\eta)\,\eta^2} \int_0^{\zeta_m} b^2(\zeta) \sqrt{1 - \eta^2 b^{-2}(\zeta)} \sqrt{1 + 3\zeta^2}\, d\zeta \leqq$$

$$\leqq \frac{2}{\Re \eta^2} \int_0^{\zeta_m} \sqrt{1 - \eta^2 b^{-2}(\zeta)} \sqrt{1 + 3\zeta^2}\, d\zeta = \frac{2\tilde{J}(\zeta_0(\eta))}{\Re(\eta)\,\eta^2}.$$

For $\beta_m = 55^\circ$, a latitude reached by the particles only with $\varrho > 3$, the right side of the inequality is approximately 39.

The collision losses of the protons are consequently described by the very simple equation

$$\left(\frac{\partial f}{\partial t}\right)_E = -\frac{\partial}{\partial \alpha} (\langle \Delta \alpha \rangle f) \tag{3,21}$$

whereas the treatment of the electrons must start from (3,19-a) which contains one order and one dimension additionally.

Finally, $\langle \Delta E \rangle$ is to be expanded relativistically.

With the definition of the deceleration cross section $\varepsilon(\alpha)$

$$\langle \Delta \alpha \rangle = -\bar{N}_e \cdot v \cdot \varepsilon(\alpha) \tag{3,22}$$

we then obtain, simply by substituting the relativistic mass and velocity, from (3,8) and (3,14)

$$\varepsilon_e(\alpha) = A \frac{(\alpha+1)^2}{\alpha(\alpha+2)} \left[\ln \frac{\alpha(\alpha+2)}{(\alpha+1)^2} + B \right]. \tag{3,23}$$

The coefficients A and B for the energy loss in free electrons read

$$A = \frac{4\pi e^4}{m_e m_p c^4} = 0{,}605 \cdot 10^{-27}\ \mathrm{cm}^2$$

$$B = \ln \left[\left(\frac{kT}{4\pi N_e e^2} \right)^{1/2} \cdot \frac{m_e c^2}{e^2} \right] = 30{,}7 + \frac{1}{2} \ln \frac{T_e}{N_e}. \tag{3,24}$$

3.2.3 - Ionization and Excitation

The collisions of the protons with electrons bound in the atom are not so essentially different from those with free electrons that the results of

the preceding subsection, especially equation (3.21), would lose any of their validity. In addition to definition (3.22), we need therefore really only the deceleration cross sections for the collisions in question. From the familiar Bethe formula (1930), there follows, for their dependence on energy, the statement corresponding to (3.23)

$$\varepsilon_a(\alpha) = A\left[\frac{(\alpha+1)^2}{\alpha(\alpha+2)}\left(\ln\alpha(\alpha+2)+B\right)-1\right], \tag{3.25}$$

whose coefficients were determined on the basis of the experimental data grouped by W. Whaling (1958) (cf. Table 3.1).

Table 3.1

	A	B
H	$0.595 \cdot 10^{-27}\,cm^2$	10.4
He	$1.09 \cdot 10^{-27}\,cm^2$	10.14
N	$3.82 \cdot 10^{-27}\,cm^2$	9.29
O	$4.36 \cdot 10^{-27}\,cm^2$	9.19

(3.25) is a satisfactory approximation down to a few 100 keV, with these values. However, this is entirely sufficient because charge exchange (cf. subsection 3.2.4) predominates by far here and at smaller energies.

3.2.3 - Nuclear Processes

For E > 100 MeV, i.e., for $\alpha > 1/10$, as will be seen from (3.24) and Table 3.1, the deceleration cross sections lie within the range of some 10 to 100 "mbarn," the magnitude of the geometric cross section of the atomic nuclei. At this point, nuclear processes therefore begin to play a role (Fraden and White, 1960) whose relative influence quickly increases in relation to the deceleration decreasing with increasing energy because of their minor dependence on energy. They can be characterized roughly by a total effective cross section which represents the sum of an absorption cross section σ_{ab} and of an approximately equally large elastic dispersion cross section

σ_{el}. Elastic dispersion is restricted even for light elements essentially to small angles ($<20^{\circ}$). Consequently, the integral of the differential cross section multiplied with the square of the angle of dispersion which leads according to (3.7-a) and (3.10) to the appurtenant diffusion coefficients $\langle \Delta\alpha \rangle$, $\langle \Delta\eta \rangle$, etc., becomes small in relation to the elastic dispersion cross section itself. The absorption cross section σ_{ab} on the other hand practically describes a particle loss and consequently enters fully into the determination of a characteristic loss time. If $\sigma_{ab} \approx \sigma_{el}$, it is consequently possible to neglect the elastic dispersion entirely.

The processes grouped under <u>absorption</u> consist in the creation of secondary particles such as n, π, D, T, α and in non-elastic dispersion. Little is as yet known on the relative shares of the individual processes. However, we can probably also add the non-elastic dispersion to the particle loss because the energy loss high on the average in a proton-source function which is at least as steep as E^{-2}, lets the secondary protons become relatively unimportant and also because the generally large angles of dispersion further lead to an appreciable loss to the lower atmosphere. Consequently, the nuclear processes can be described with the simple equation (2.41) if we utilize the absorption cross section σ_{ab}:

$$\left(\frac{\partial f}{\partial t}\right)_T = -\bar{N} \cdot v \cdot \sigma_{ab} \cdot f. \qquad (3.26)$$

Some values for σ_a according to A. Wattenberg (1957) have been grouped in Table 3.2. They are only slightly variable between 100 MeV and some GeV.

Table 3.2

	H	He	N	O
σ_{ab} (barn)	0.027 for E > 800 MeV	0.1	0.24	0.27

An exception is constituted by the absorption cross section of hydrogen which is determined by the π-meson creation beginning above 290 MeV. Only

at 300 MeV, does this reach the magnitude of the elastic dispersion cross section which, by contrast, is almost constantly equal to 0.025 "barn" between 70 and 600 MeV. Moreover, the differential cross section in the center-of-gravity system is independent from the angle of dispersion χ (Hess 1958). The final circumstance, the relative frequency of large angular collisions, prevents the applicability of the Fokker-Planck equation which was derived (cf. sec. 2.5) under the assumption that the changes of α, η within the time Δt are primarily small in relation to the magnitudes themselves. Formally, the invalidity is shown by the fact that the coefficients formed according to (3.5-a) become only slowly smaller with increasing order.

However, it is still very instructive to calculate the mean velocity of variation $\langle \Delta\alpha \rangle$ of the energy. Let $q^* \sin\chi \, d\chi \, d\Phi$ be the differential elastic effective cross section in the center-of-gravity system. For the energy loss in elastic collision of equal masses, there is valid $\Delta\alpha = -(\alpha/2)(1-\cos\chi)$. Because of the impossibility of distinguishing between primary and secondary particles, we integrate by way of χ only as far as $\pi/2$:

$$\langle \Delta\alpha \rangle = -2\pi q^* v \bar{N} \frac{\alpha}{2} \int_0^{\pi/2} (1-\cos\chi) \sin\chi \, d\chi = -\alpha \frac{\pi}{2} q^* v \bar{N} = -\alpha v \bar{N} \frac{\sigma_{el}}{4}.$$

After the time $\alpha / |\langle \Delta\alpha \rangle| = 4/v\bar{N}\sigma_{el}$, a particle has in the mean transferred its energy, except for a small fraction, to its environment. It can thus be regarded as lost. Accordingly, we will have an entirely useful approximation if the loss of energy and very roughly the effect of dispersion is combined as of equal magnitude in an actual effective cross section σ_{eff}, i.e., define

$$\sigma_{eff} \approx \frac{\sigma_{el}}{2}$$

and describe this case of elastic dispersion which actually should find its expression in a Boltzmann collision term, with the simple equation (3.26). The doubtful character of this procedure is of little importance in this connection

because the elastic p-p dispersion which should be effective in the energy range between 200 and 700 MeV according to fig. 3.2, is largely blanketed by other processes as will be shown in secs. 4 and 7.

3.2.4 - Charge Exchange

Stuart (1959) was the first to point out that, below 1 MeV, it is possible to liberate the protons by charge exchange with slow neutral particles from their bond to the magnetic field and thus become spontaneously lost to the radiation belt. The effective cross section of this process drops with decreasing energy so steeply that the proton spectrum should be practically cut off at a few 100 keV. The data for the cross section of charge exchange were derived from a synopsis by S. K. Allison (1958). They can be satisfactorily described between 150 keV and 1 MeV by

$$\sigma_{Uml} = a \cdot \alpha^{-b} \tag{3.27}$$

with the values of the constants a, b grouped in Table 3.3.

Table 3.3

	a	b
H	$1.52 \cdot 10^{-37}\,cm^2$	5.1
He	$2.75 \cdot 10^{-34}\,cm^2$	4.4
O, N	$8.83 \cdot 10^{-31}\,cm^2$	3.5

3.3 - Life Span

Before we compare the effectiveness of the collision processes described above, we shall specify the concept of life span. With an equation of type (3.26), this makes no difficulty;

$$\tau = \frac{1}{\bar{N} v \sigma} \tag{3.28}$$

here designates the time after which a given distribution has attenuated to 1/e. In order to define a similar time for Equation (3.21), let us examine the behavior in time of an initial distribution $f_0(\alpha) = f(\alpha, t = 0)$. With the statement -- certainly useful in part -- $\langle \Delta\alpha \rangle = -A \cdot \alpha^{-n} (A > 0)$ and $g = \langle \Delta\alpha^2 \rangle \cdot f$, (3.21) is written as

$$\frac{\partial g}{\partial t} - A\alpha^{-n}\frac{\partial g}{\partial \alpha} = 0.$$

The solution of this equation is obtained by substituting

$$\varphi(\alpha, t) = [\alpha^{n+1} + (n+1)\,A\,t]^{(1/n+1)}$$

in $g_0(\alpha)$; expressed in f

$$f(\alpha, t) = \left(\frac{\varphi}{\alpha}\right)^{-n} \cdot f_0(\varphi(\alpha, t)).$$

If we further make the statement $f_0 = C\alpha^{-m}$ for f_0, we can see clearly how the change of distribution is dependent on the spectrum:

$$\frac{f(\alpha, t)}{f(\alpha, 0)} = \left(\frac{\varphi}{\alpha}\right)^{-(n+m)}.$$

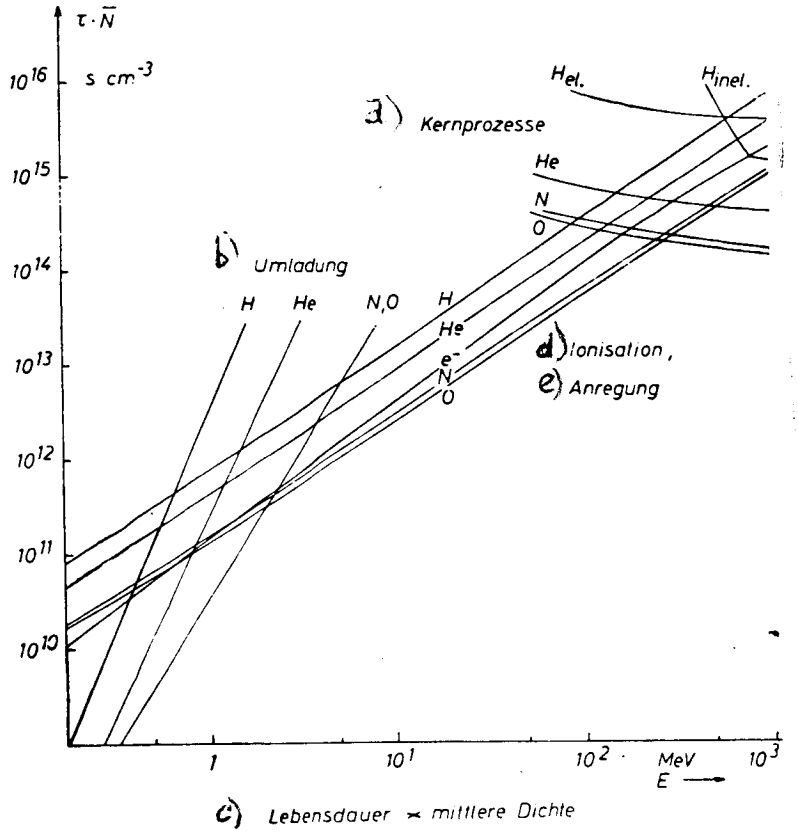

Fig. 3.2 - Life span of protons multiplied by mean density of collision centers in hydrogen, helium, nitrogen, oxygen and in relation to three electrons (e^-).
Legend: a = nuclear processes; b = charge conversion; c = life span x mean density; d = ionisation; e = excitation.

The characteristic loss time $\tau_{\frac{1}{2}}$ shall now be defined so that

$$\varphi(\alpha, \tau_{1/2}) = 2\alpha \qquad (3.29)$$

i.e., $f = 2^{-(n+m)} \cdot f_o$ after its lapse. In the collision processes effective here, n lies between 0 and 0.5 in the range of interest here. The albedo neutrons investigated in sec. 7 furnish a proton spectrum which can here be largely represented by m = 1.5, i.e., the times 3.28 and $\tau_{\frac{1}{2}}$ are approximately comparable. Written out, definition (3.29) then reads

$$\tau_{1/2} = \frac{2^{n+1} - 1}{n+1} \cdot \frac{\alpha}{|(\Delta\alpha)|}. \qquad (3.29a)$$

With (3.28) and (3.29-a), the magnitudes $\bar{N} \cdot \tau$ and/or $\bar{N} \cdot \tau_{\frac{1}{2}}$ are plotted in fig. 3.2 for the most important processes; division by $\bar{N}$ consequently furnishes the life span in seconds.

4 - Impairment of Adiabatic Invariants in the absence of collision

In addition to collisions, we may also imagine losses through the disturbance of the adiabatic invariants which are what provides capture in the terrestrial magnetic field (cf. subsec. 2.1). Singer (1959) was the first to point out the impairment of μ when the radii of gyration are so large that the inhomogeneity of the magnetic field becomes sensible in the range of the circle of gyration. Welch and Whitaker (1959) directed attention to the disturbances in time of the field which were investigated in greater detail by a number of authors, by Dragt (1961) and Wentzel (1961, 1962) in regard to μ, by Parker (1961) in regard to J and by Parker (1960) and Davis and Chang (1962) in regard to Φ on hand of special models. There is no intention at this point to undertake an evaluation of their work but an attempt is made, starting from the simplest conceivable example, to segregate the general behavior of the adiabatic invariants and to obtain, in the absence of a general theory, indications on the order of magnitude and the qualitative progress of the effects through conclusions by analogy. Even though it signifies a reinforcement of confidence

in this procedure that the findings of the special investigations quoted above fit into this frame, it still remains affected with extremely high factors of uncertainty. On the other hand, the intention is only to constitute in this manner a base on which the requirements for other loss processes which must necessarily be postulated by reason of the failure of a model taking into account only collisions (cf. subsec. 7.4), can be interpreted somewhat further.

4.1 - Disturbance in Time in the Homogeneous Magnetic Field

The development of the equation of motion of a charged particle according to the magnitude

$$d = \frac{1}{\omega_g B} \left| \frac{d\mathfrak{B}}{dt} \right|_{\max}, \qquad (4.1)$$

assumed as small from which follows as a first approximation (Alfven, 1950) the constancy of the magnetic moment, furnishes even in the higher orders no indication on an impairment of the invariance; μ results as constant in every order (Hellwig 1955; Schlueter, Hertweck, 1957; Kruskal, 1957). This finding signifies primarily that such a development does not converge and that we must follow other paths in order to obtain usable estimates of the change of μ. This has so far been done only for a few special cases in which the simplest, the disturbance in time of a homogeneous magnetic field, shall now be briefly considered in the hope that it already contains the essential features.

Hertweck and Schlueter (1957) integrated the equation of motion of a charged particle on the assumption that the homogeneous magnetic field, assumed to be created by a long, extended coil, increases in the interval of time Δt from B_0 to B_1 and is constant outside of the latter. The change of the magnetic moment μ is then well defined and given generally by

$$\frac{\Delta \mu}{\mu_0} = 2\varepsilon \cos(\xi + \chi_0) |P| + (1 + \varepsilon^2) |P|^2 + o(|P|^3) \qquad (4.2)$$

in which ξ = the phase in the circle of gyration; ϱR_g = distance of guiding center from coil axis (both at start of interference) and $P = |P|\, e^{i\chi_0}$ = a function dependent on the trace of disturbance whose form is, in the case of a very rapid change of field,

$$|P| = \frac{B_1 - B_0}{2\sqrt{B_1 B_0}} \quad \text{for} \quad \Delta t \ll \frac{2\pi}{\omega_g} \tag{4.3}$$

and, in the case of a slow change of field, is of the type

$$|P| \sim \exp\left(-K\,\frac{\omega_{g0}}{\lambda}\right) \quad \text{for} \quad \lambda \ll \omega_{g0} \tag{4.4}$$

λ^{-1} here measures the time during which the change basically takes place. In a specific example of the authors quoted as well as in an entire class of field changes encompassing this example (Backus, Lenard, Kulsrud, 1960), the value of the constants K in (4.4) results as $\pi/2$. The factor before the e-function depends on the example; particularly important is the steepness of the decrease of $\Delta\mu/\mu_0$ if the disturbances is slow in relation to the characteristic frequency. In the following, the interest is on small disturbances of a magnetic field constant in the mean. Consequently, in the configuration considered by Hertweck and Schlueter, the effect of a cosinoid individual disturbance of the duration $(\omega/2\pi)^{-1}$ has been treated. The result is communicated without demonstration:

$$|P|^2 = \frac{1}{8}\left(\frac{\Delta B_{\max}}{B_0}\right)^2 \frac{1 - \cos 2\pi\,\frac{\omega_{g0}}{\omega}}{\left(1 - \left(\frac{\omega_{g0}}{\omega}\right)^2\right)^2}. \tag{4.5}$$

The trace of the frequency-dependent term in (4.5) is plotted in fig. 4.1. The deviation from Equation 4.4 at $\omega_{g0}/\omega > 1$ has its reason in the unsteadiness of the higher derivations of time at the start and the end of the selected disturbance.

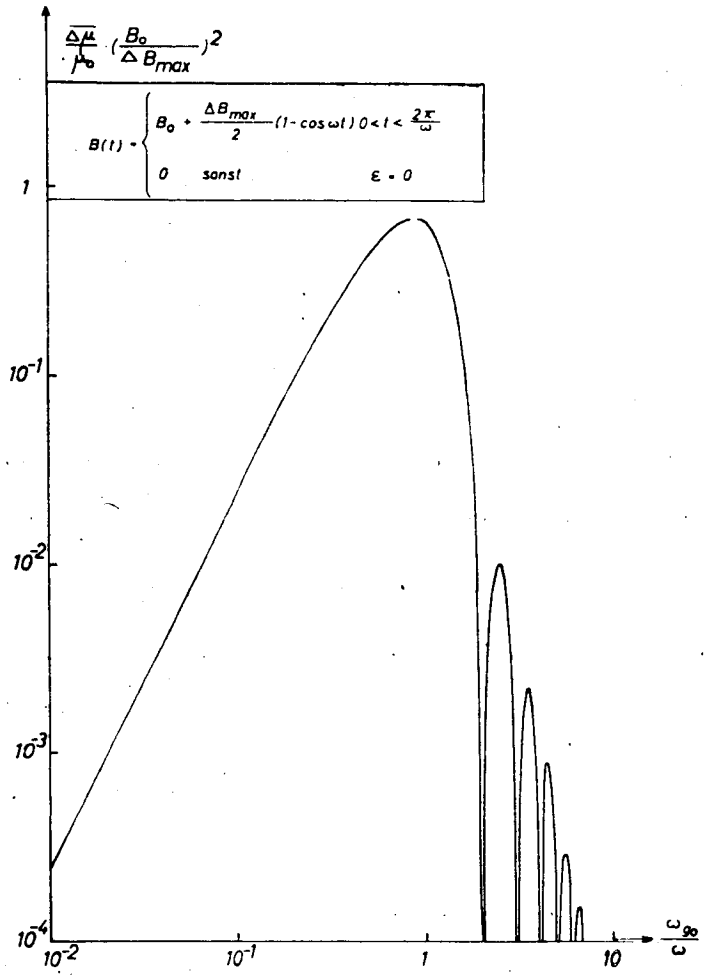

Fig. 4.1 - Variation of magnetic moment μ in a homogeneous magnetic field at a cosinoid disturbance of the field of duration $2\pi/\omega$ and the amplitude ΔB_{max} as a function of the ratio of non-disturbed gyration frequency ω_{go} to the interfering frequency ω.

4.2 - Disturbances in Time of the Terrestrial Magnetic Field

Kruskal (1962) has been able to expand the result found for μ to a very general system with multiple almost periodic solutions, i.e., that the adiabatic variant appertaining to the respective periods (given through the correlated action integral) are constant in all orders of an asymptotic development according to a magnitude of disturbance defined according to (4.1). This includes in particular also the free invariants μ, J, Φ in the terrestrial magnetic field which can be derived in analogous manner from the equation of motion of a charged particle as phase integral by successively

eliminating the periodicities of motion. The equivalence with which they appear from this point of view gives rise to the conjecture that the situation is similar also in their actual change under small disturbances of the field. Let us therefore make the attempt to describe them, in adaptation of (4.2), quite generally through the statement

$$\frac{\Delta\mu}{\mu},\quad \frac{\Delta J}{J},\quad \frac{\Delta\Phi}{\Phi} = K_{i1}\cos\chi_0\,|P| + K_{i2}\,|P|^2 + \cdots \qquad (4.6)$$

and $|P|^2$ of the type of (4.5) and to place all difficulties of the specific process in the constants K_{ij} which are evidently dependent on the model but -- if the wave type is actually effective for the disturbance -- should not be too far distant from 1. The index i (= g, Osz, D) refers to the three characteristic frequencies. In fact, the findings of the investigations of special cases of this problematic quoted above concord with (4.6) whose indeterminacy is initially not greatly important because it is exceeded even more by the lack of knowledge of the kind and distribution of the magnetic-field disturbances.

The picture imagined by a number of authors, and in particular Parker, of the occurrence and propagation of these disturbances shall here be briefly sketched: Through the interaction of the interplanetary plasma with the terrestrial magnetic field, numerous disturbances and hydromagnetic waves are excited in these border areas where the energy density of the field and of the plasma are comparable (Parker, 1958). We may conjecture that strong excitation no longer takes place further inward. However, since the frequencies in the range of the local frequency of ion gyration are strongly attenuated through phase mixture (Stix, 1958) and still higher frequencies through interaction with the electrons (Luest, 1959), the spectrum of the waves travelling inward in the vicinity of the earth should be almost cut off approximately at the frequency of ion gyration at the inner edge of each excitation region.

The inner border of this region was estimated, e.g., by Parker (1961) as $5\ R_e$ ($\triangleq \omega_{max} = 24\ s^{-1}$) and by Wentzel (1962) as $8\ R_e$ ($\triangleq \omega_{max} = 6\ s^{-1}$). (These indications are always understood as in the equatorial plane; all frequencies are expressed as angular velocities ($\omega = 2\pi\nu$.) Kato and Tamao (1962) also derived a minimum frequency $\omega_{min} \approx 2 \cdot 10^{-2} s^{-1}$ from the finite expansion of the region of excitation.

The propagation of these waves inward is a difficult problem because of the geometry of the field and the variable density of the gas. The finiteness of the length of the field lines results in characteristic frequencies which should partially or totally reflect waves entering from the outside, depending on the respective type of wave (Kato, Tamao, 1962).

Without consideration of geometry and dispersion, Parker (1961) merely demands the conservation of density of the energy flux of the hydromagnetic waves and finds the relation

$$\Delta^2 B \cdot v_A = \text{const.} \tag{4.7}$$

between the square of the wave amplitude $\Delta^2 B$ and the velocity of propagation which is here approximately equal to the Alfven velocity ν_A. From the joint action of the trace of density and magnetic field, there results at an altitude of 3,000 km a maximum of ν_A which amounts to $\approx 5 \cdot 10^8$ cm s^{-1} according to Parker who estimates the drop outward as $\sim r^{-2}$.

The dissipation of the waves in the ionosphere and the phenomena here added make it difficult to conclude on the circumstances at high altitudes from observations from the ground. However, the so-called continuous geomagnetic pulsations (pc) according to Obayashi and Jacobs (1958) show a frequency distribution whose maximum has a considerable dependence on latitude which corresponds to the trace of the characteristic frequency with the distance of the field lines. The dispersion of frequency is, however, very

large, even after low values which are weakened by reflection.

Of more importance for the present problematics are the measurements in the exosphere of which there are unfortunately still very few. Sonett and associates (1960) determined with Pioneer I and Coleman et al (1960) determined with Pioneer V strong fluctuations of the magnetic field of the magnitude of its mean value between 10 and 14 R_e which fit very well into Parker's concept of the excitation of hydromagnetic waves at the limit of the terrestrial magnetic field. The spectrum of the amplitude square on a geomagnetically quiet day on the side toward the sun is, according to Sonett et al (1960), roughly $\sim\omega^{-1}$ between $\omega = 0.1$ and $\omega = 3 s^{-1}$. An analysis of the Pioneer I data at lesser altitude (3.7 - 7 R_e) (Sonett et al, 1962) resulted on the whole in similar findings, except that some "spectrum lines" are superposed to the continuum which we shall here neglect, however. The continuum can be represented at $\varrho = 4.5$ between $\omega = 0.2$ and 6 s^{-1} (again as a rough approximation) by $\Delta^2 B(\omega) \approx 15\,\gamma^2/\omega$. The experimentally found limit frequency of $\omega_{max} \approx 6\ s^{-1}$ allows us to localize the inner border of the excitation region at $\approx 8\ R_e$. The magnetic vector of the observed fluctuations lay predominantly parallel to the static field.

Let us now abstract from this material a model which is regarded as characteristic for magnetically quiet days, i.e., for the mean behavior of the terrestrial fields. The indicated approximation of the frequency spectrum at $\varrho = 4.5$ shall serve as a basis and shall be extrapolated inward through equation 4.7:

$$\frac{\widetilde{\Delta^2 B}}{B_0^2} \approx \begin{cases} \dfrac{10^{-4}}{\omega}\left(\dfrac{\varrho}{4{,}5}\right)^8 & \text{for } 0{,}2 \leqq \omega \leqq 6\ s^{-1} \\ 0 & \omega > 6\ s^{-1}. \end{cases} \qquad (4.8)$$

As expressed in (4.8), the conservation of the form of the frequency spectrum in wave propagation inward, a consequence of neglecting refraction, is rather questionable. This further uncertainty in the conclusions to be

drawn below is to be stressed here emphatically. By order of magnitude, (4.8) furnishes the same values as were measured under continuous pulsation in low altitudes (Kato, Saito, 1962).

From the existence of a maximum disturbing frequency and the requirement that the characteristic frequency must be smaller than the former (4.6) in order to produce any appreciable change of the adiabatic invariants, there result limits of the energy ranges at any distance in which a disturbance of the adiabatic invariants is possible. According to Welch and Whitaker (1959) and Dragt (1961), there exists a possibility, although we always have $\omega_g \gg \omega_{max}$, also for the impairment of μ, provided that

$$\omega_g \leqq \omega \cdot \frac{v \cos \psi}{v_A} \tag{4.9}$$

i.e., if the disturbance in the system at rest of the oscillating guiding centers appears Doppler-displaced as far as the gyration frequency or beyond.

At $\varrho = 1.5$, the proton energies at which J is no longer a satisfactory invariant, lie below 6 MeV; an impairment of Φ may therefore be already expected below 2.5 GeV. By contrast, the range defined here by (4.9) extends above about 4 GeV where we state $\cos \psi = 0{,}5$ ($\triangleq \beta_m = 15°$) and $v_A = 5 \cdot 10^8$ cm s^{-1}. Fig. 4.2 represents the characteristic energy ranges for higher altitudes (with small $v_A \sim \varrho^{-2}$); an extension downward is avoided because of the uncertainty of the behavior of the hydromagnetic waves. Of great importance for the existence of protons in the radiation belt is the steep drop of the minimum energy resulting from (4.9) (Dragt, 1961) as well as the fourth limit curve contained in fig. 4.2 which shall be explained in the next section.

In reference to (4.5), let us now estimate in the ranges so characterized the time scale of a perceptible change of μ, J, Φ. Initially we take the mean over the phase angle χ_o in (4.6) because the disturbances are considered to be statistically distributed. Only frequencies in the vicinity of the characteristic

frequency ω furnish an appreciable contribution, i.e., the effective range according to fig. 4.1 is of the magnitude ω_i. At a given Fourier spectrum of the amplitudes square $\widetilde{\Delta^2 B}(\omega)$, let us therefore set $\widetilde{\Delta^2 B}(\omega_i)\omega_i$ in place of $\Delta^2 B_{max}$ in (4.5). Through multiplication with the number of disturbances per unit time $\omega_i/2\pi$, we then obtain for the variation of Φ as far as factors of the magnitude 1:

$$\frac{\langle \Delta\Phi \rangle}{\Phi} \approx \frac{\langle \Delta^2\Phi \rangle}{\Phi^2} \approx \frac{\widetilde{\Delta^2 B}(\omega_D)\,\omega_D}{B_0^2} \cdot \frac{\omega_D}{2\pi}.$$

If $\omega_D < \omega_{max}$, there follows from (4.8)

$$\frac{1}{\tau_\Phi} = \frac{\langle \Delta^2\Phi \rangle}{\Phi^2} \approx 2{,}4 \cdot 10^{-9} \left(\frac{\varrho}{1{,}5}\right)^8 \omega_D \qquad (4.10)$$

and correspondingly for J

$$\omega_{osz} < \omega_{max}: \frac{1}{\tau_J} = \frac{\langle \Delta^2 J \rangle}{J^2} \approx 2{,}4 \cdot 10^{-9} \left(\frac{\varrho}{1{,}5}\right)^8 \omega_{osz}. \qquad (4.11)$$

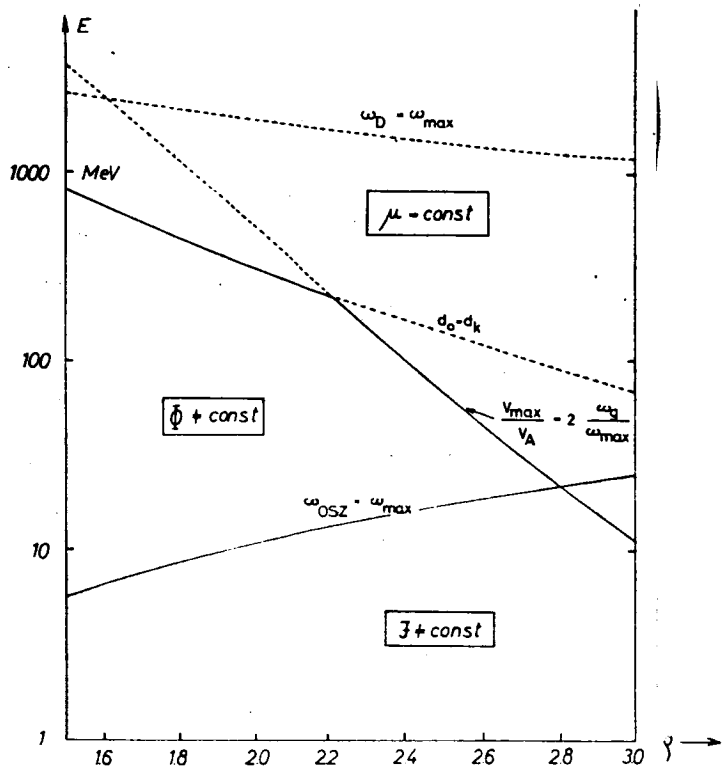

Fig. 4.2 - Limits of the ranges in which the three adiabatic invariants μ, J, Φ are subject to interference if the maximum frequency of the fluctuations of the magnetic field $\omega_{max} = 6\ s^{-1}$. The curve $d_o - d_k = 0{,}165$ limits the vulnerability of μ by reason of the large gyration radius in the pure dipole field.

(4.11) also approximately indicates the time scale of the impairment of μ because only few disturbances of relatively large amplitude (vicinity of Equator!) are encountered during one oscillation. However, ω_{osz} must be substituted in an entirely different energy range (cf. fig. 4.2). An important assumption made without further discussion is that the disturbances of the terrestrial magnetic field are of equal effectiveness in regard to a variation of the three invariants. However, this is by no means a matter of course.

The effect of a statistical variation of Φ and/or μ and J is essentially (cf. below) a radial diffusion and/or one following the field lines of the reflection points. It leads to losses to the interplanetary space or the denser atmosphere; τ_Φ and τ_J can therefore be interpreted as life spans. In Table 4.1, they have been calculated for $\rho = 1.5$ and some energy values from (4.10) and (4.11) have been compared with the oxygen density $\bar{N}_{equiv}$ which leads under pure collision losses on the basis of fig. 3.2 to the same life span. If the mean atmospheric density becomes $\bar{N}(\eta, \varrho) \lesssim \bar{N}_{equiv}$, the finite duration of the adiabatic invariance can no longer be neglected.

Table 4.1 ($\varrho = 1.5$)

E [MeV]	ω_{osz} [s^{-1}]	ω_D [s^{-1}]	τ_J bzw. τ_μ [s]	τ_Φ [s]	$\bar{N}_{equiv}$ [cm^{-3}]
0,3	1,04		$4,0 \cdot 10^8$		$2,5 \cdot 10^9$
1	1,90		$2,2 \cdot 10^8$		$1,6 \cdot 10^9$
3	3,28		$1,27 \cdot 10^8$		$4,0 \cdot 10^8$
10		$3,5 \cdot 10^{-2}$		$> 1,2 \cdot 10^{10}$	$\lesssim 2 \cdot 10^2$
30		$1,05 \cdot 10^{-1}$		$> 4,0 \cdot 10^9$	$\lesssim 2,3 \cdot 10^3$
100		$3,4 \cdot 10^{-1}$		$1,2 \cdot 10^9$	$4,0 \cdot 10^4$
300		$9,4 \cdot 10^{-1}$		$4,4 \cdot 10^8$	$2,2 \cdot 10^5$
1000		$2,6 \cdot 10^0$		$1,6 \cdot 10^8$	$8,5 \cdot 10^5$
4000	$1,6 \cdot 10^2$		$\approx 10^8$		$\approx 10^8$

(The signs of equality at $\omega_D \lesssim 0{,}1\,s^{-1}$ recall the increased unreliability of approximation (4.8) at these frequencies.)

In the estimate of the life span for $\varrho = 1.5$, it should be kept in mind that the time scales (4.10) and (4.11) were derived for reflection points in

the vicinity of the Equator. As will be seen directly from expression (2.27), the ratio of disturbing amplitude to magnetic-field intensity at the reflection point is controlling for the impairment of J. Since the losses here take place by diffusion along the field into the denser atmosphere, there enters into the effective loss time not the field intensity at lower latitudes as in (4.11) but at constant altitude. From this and from $\omega_{osz} \sim \rho^{-1}$ and from (4.7), there consequently results an only slight dependence of the loss time on ρ under disturbance by J. An entirely different behavior of the impairment of J will be found from the expression (2.9) for the velocity of drift v_D. It furnishes the main contribution to ω_D for the smallest magnetic-field intensities where the disturbances in a radial direction also become most effective through $\partial B/\partial t \neq 0$. The decrease of the probability of locus in this range with increasing latitude of reflection point is compensated by the factor cos ψ before $\partial B/\partial t$. The loss time under disturbance of Φ is therefore probably only slightly dependent on η and therefore on ρ about as in (4.10).

In contrast to the investigations of Parker (1962) and Davis and Chang (1962), this entire consideration is oriented on <u>normal magnetic conditions</u>. During magnetic storms, there will probably occur briefly considerable reductions of the derived time scale which may be in the mean of the same importance for the particle distribution as the continuous disturbances. This question will be raised once more in sub-section 7.7 in regard to observation.

Let us repeat at this point that no decisive importance must be ascribed to the details of the picture sketched -- the numerical values have been written only for the sake of more precise definition of the statement -- and that the picture shall serve rather as a qualitative guide in the interpretation of findings which were obtained by neglecting all of the effects here mentioned. Depending on the validity and reliability of these findings, there may then of

course result retroactively indications on the soundness of one or the other concept.

- - - - - - - - - - - - -

Whereas the vulnerability of the adiabatic invariant μ, as already mentioned, should lead in the inner belt practically to the complete elimination of the captured radiation and these processes can therefore be treated as a pure interception of the spectrum, it is important in the disturbance of J or Φ -- only one process is of importance respectively -- to study the behavior of the motion parameters. From (2.26), (2.27), (2.39) and the definition of ϱ, there follows

$$\begin{aligned} \mu &\sim p^2 \eta^2 \varrho^3 \\ J &\sim p \varrho \tilde{J}(\zeta_m(\eta),) \\ \Phi &\sim \varrho^{-1} \end{aligned} \tag{4.12}$$

in which $(\zeta_m(\eta)$ is given by (2.22) and (2.15)). From this, we derive the following relation:

for	$J \neq$ const.,	$\mu =$ const, $\Phi =$ const.	
there is		$\eta^{-1} \tilde{J}(\zeta_m(\eta)) \sim J$	
		$p \sim \eta^{-1}$	
		$\varrho =$ const.	(4.13)
and for	$\Phi \neq$ const., $\mu =$ const.,	$J =$ const.	
		$\varrho \sim \Phi^{-1}$	
		$p \sim \varrho^{-n(\eta)}$	
		$\eta^{-1} \tilde{J}(\zeta_m(\eta)) \sim \varrho^{+1/2}$	(4.14)

with a monotonously increasing function $n(\eta)$ which lies between 1 and 3/2.

The diffusion along the field lines at $J \neq$ const. and that in ϱ at $\varrho \neq$ const. takes place under acceleration of the particles. However, due to the spatial delimitation of the region in which these correlations exist, by the atmosphere and the regions, $\mu \neq$ const. (cf. fig. 4.2) which represent troughs for the particles, the maximum gain of energy upon decrease of ϱ (4.14) or J (4.13) is restricted; the limit lies between a factor of 10 and 100. The

particle loss due to diffusion counteracts this possible acceleration so highly, however, that there is no point in attempting to understand the origin of high-energy protons through the acceleration of any low-energy protons (see also Parker, 1961). An effective acceleration would therefore be possible only under impairment of μ which would then condition, however, such a drastic shortening of all time scales that they would be completely incompatible with the life spans resulting from the interaction with the atmosphere (see subsec. 7.4). This is valid for the protons in the inner Van-Allen belt; for electrons in the outer belt, local acceleration processes cannot be excluded.

The mathematical treatment of diffusion requires a change of definition (2.31) of the distribution function; this is now referenced preferably directly to μ, J, Φ because two of these variables remain comparably constant respectively. The disturbance of J and/or Φ can then be described by a Fokker-Planck Equation in only one variable with a diffusion coefficient (4.11) and/or (4.10). The transition to the magnitudes p and η, physically more easily interpreted, can then be carried out easily through (4.13) and (4.14). The most difficult point here will be the conjunction with another region where the collision losses predominate and (4.13) or (4.14) are no longer valid.

4.3 - Impairment of μ in the Static Dipole Field

If the discriminant (4.1) in the static dipole field

$$d = \frac{|(\mathfrak{v}\ \mathrm{grad})\ \mathfrak{B}|}{\omega_g B} \tag{4.15}$$

is no longer small in relation to one, the Alfven approximation breaks down; μ is no longer a satisfactory invariant. Singer (1959) has thus explained the absence of high-energy protons in the outer Van Allen belt. The problem of how the absent homogeneity of the field over a circle of gyration as measured by (4.15), exactly affects the impairment of μ has unfortunately not yet been

solved satisfactorily. The comparison with numerical integrations of the complete equations of motion becomes difficult by the fact that the changes of interest here, are so small that they become perceptible only after 10^3 and more gyration periods. Moreover, it is not always easy to conclude from one geometric configuration to another.

If we now come back again, with the aid of analogy, to the case of the disturbance in time of a homogeneous magnetic field as represented in subsec. 4.1, this will have to be done with great care because of the profound difference existing in the fact that there the change of μ takes place with the absorption or transfer of energy whereas the energy remains constant in the static magnetic field.

The finding of Kruskal (1957, 1962) that μ is constant in every order of the development of the equation of motion according to d, makes it obvious to describe the relative change $\Delta\mu/\mu$ through a similar expression as in the border case of a slow change of a homogeneous field (4.4):

$$\frac{\Delta\mu}{\mu} \sim e^{-\frac{\text{const}}{d}}. \qquad (4.16)$$

It should be pointed out that this function cannot be developed around $d = 0$. Garren et al (1958) have confirmed the correlation resulting from this between $\Delta\mu/\mu$ and the velocity through the numerical integration of the equation of motion of particles in a reciprocal computer ["Spiegelmaschine"?] over several powers of 10. This steep dependence on μ leads to the fact that the entire change of μ during one oscillation between the reflection points is almost completely determined through the change in the equatorial plane where d reaches its maximum. The critical value d_0 will therefore be the maximum of d over all phases in the equatorial plane. In the dipole field,

$$d_0 = \frac{3vB_0}{\omega_{g0} B_0 \varrho R_e} = 3\frac{R_g}{\varrho R_e} = 4{,}69 \cdot 10^{-2}\sqrt{\alpha(\alpha+2)}\,\varrho^2. \qquad (4.17)$$

is independent of η. However, this does not mean that the constant occurring in the exponent of (4.16) is independent of τ. In analogy with (4.2) let us therefore make the following formulation

$$\frac{\Delta\mu}{\mu} = F_1(\eta)\, G(\xi)\, e^{-\frac{F_3(\eta)}{2d_0}} + F_3(\eta)\, e^{-\frac{F_3(\eta)}{d_0}} . \tag{4.18}$$

The function $G(\xi)$ can be assumed as an approximately sinoid function according to the calculations of Garret et al (1958) and Grad and Van Norton (1962). Nothing further can here be said on the functions $F_1(\tau)$ than that their asymptotic behavior for $\eta \to 1$ must be so that $\Delta\mu/\mu \to 0$ because a particle completely captured in the equatorial plane cannot again leave the latter. For mean values of η, it is again assumed that $F_1(\tau)$ and $F_3(\tau)$, as in (4.4), lies in the vicinity of π.

For the calculation of the cumulative effect of many oscillations, it is of importance that the change of phase difference $\xi_1 - \xi_0 = {}^1/_2 \oint \omega_\varrho / v_{||}\, dl$, traversed during one-half oscillation is a relatively large number at a small change of $\eta: \Delta\eta\, d/d\eta\, (\xi_1 - \xi_0)$. This signified (Grad, Van Norton, 1962) that $\Delta\mu/\mu$ is a function of the initial phase ξ_0 oscillating so greatly after a large number of oscillations that $\Delta\mu/\mu$ can be regarded practically as noncorrelated with ξ_0. It is then permissible to take the mean simply over ξ_0. On the assumption $|F_1(\eta)\, \overline{G(\xi)}| \ll F_3(\eta)$ and from $\mu \sim \eta^2$, there follows from this

$$\begin{aligned} \frac{\langle\Delta\mu\rangle}{2\mu} &= \frac{\langle\Delta\eta\rangle}{\eta} \approx \frac{\omega_{osz}}{2\pi}\, F_3(\eta)\, e^{-\frac{F_3(\eta)}{d_0}} \\ \frac{\langle\Delta^2\mu\rangle}{4\mu^2} &= \frac{\langle\Delta^2\eta\rangle}{\eta^2} \approx \frac{\omega_{osz}}{4\pi}\, F_1^2(\eta)\, \overline{G^2(\xi)}\, e^{-\frac{F_3(\eta)}{d_0}} . \end{aligned} \tag{4.19}$$

because $p = \text{const.}$ and $\varrho = \text{const}$ (theorem of energy and angular momentum!).

In order to find which time scale results for the impairment of μ from (4.19), let us state ${}^1/_2 F_1^2(\eta)\, \overline{G^2(\xi)} \approx F_3(\eta) \approx 1$ and $F_0(\tau) = \tau$. At $\varrho = 1.5$, we then obtain the times and densities of oxygen equivalent recorded in Table 4.2 (cf. Table 4.1). The time scale is so sharply dependent on energy that

even a considerable error in the estimate of the functions F_1 and F_2 is not greatly significant whereas the times are critically dependent on $F_2(\eta)$.

Table 4.2

E [MeV]	$\frac{\eta^2}{\langle \Delta^2 \eta \rangle}$ [s]	$\bar{N}_{equiv}$ [cm^{-3}]
300	10^{15}	1
600	10^{9}	10^{5}
800	10^{7}	10^{7}
1000	10^{6}	10^{8}
1500	10^{4}	10^{10}

In order to make a comparison with the other non-adiabatic effects discussed in the preceding section, let us consider an equivalent density of 10^7 cm^{-3} as critical value and define a <u>critical discriminant</u> where the spectrum of the captured protons is approximately intercepted upon reaching the former. According to (4.17) and Table 4.2, this is $d_K = 0.165$. The curve $d_0(\alpha, \xi) = d_K$ is plotted in Fig. 4.2. Its trace over ξ is much flatter than the one defined by (4.9). This should make it possible to distinguish the two effects.

It is of interest to compare this determination of d_K with an entirely different determination, i.e, from numerical integrations in the dipole field. R. Gall (1962) very roughly differentiates such orbits whose reflection points still lie there where they are localized by the Alfven approximation, from those orbits which <u>clearly</u> deviate from this and do not have any fixed reflection points. The author here finds a high dependency on η but differentiates only very roughly between large and small η and indicates $d_K = 0.19$ and/or 0.12 as the limits at which the Alfven approximation is still valid. This still does not say anything on the behavior under many oscillations, i.e., a migration of the reflection points, but it should be noted as an important result that the critical discriminant apparently becomes appreciably smaller with increasing latitude of the reflection points, i.e., with smaller η.

We shall enter on the empirical determinations of d_K by Singer during the discussion of the observations in Subsection 7.6.

5 - Calculation of Mean Density

In order to be able to utilize the accuracy with which the loss cross sections are known also in their absolute value for calculation of particle distribution, a procedure is required which guarantees without too great an expenditure a usable mean of the atmospheric density over the orbit of the guiding center. Numerical indications on these orbits exist in the Tables of Jenssen, Murray and Welch (1960) described in Subsection 2.3. What is involved here is to approximate this numerical material in such manner that the occurring deviations are small in relation to the scale height of the atmosphere at least in the regions contributing appreciably to the mean value, and also to take into consideration to a reasonable extent the capacity of the available computer and the time of computation required.

Let us start with the assumption that the density of number of each atmospheric component can be represented for these purposes as a pure function of the distance s from the center of the earth and the time t:

$$N = N(s, t). \tag{5.1}$$

This requires a justification because, beyond 300 km, the density is subject to an increasing extent to considerable diurnal variations as we know from the deceleration of the satellites (see, e.g., King-Hele, Walker, 1961). However, since the drift period of the protons to be investigated amounts at the most to a few hours and is in general much shorter than their life span, they experience several times the diurnal cycle so that it is permissible to conceive of the mean over the diurnal cycle as fully executed and to measure with the time t only intervals which are large in relation to one day. The addition of the so far negative result in the determination of a dependence on latitude of the density at a few 100 km of altitude (King-Hele, Walker, 1961) lets the formulation (5.1) appear as reasonable.

In the following, we basically utilize the possibility of projecting the terrestrial magnetic field on a dipole field as discussed in Subsection 2.3. Here, in contrast to reality, the orbits of particles are conceived in a pure dipole field and the spherical shells (s = const.) concentric with the center of the earth are bent in such manner into the dipole field that the correlation of the spatial points to the dipole coordinates defined through the representation (2.28) and (2.29) is maintained. This procedure essentially facilitates computation without leading to any notable errors.

From (2.28) and (2.29), there result the coordinates B^*, J^* to ϱ, ζ from which the distance s is tabulated as a function of geographic latitude and longitude in the Tables of Jenssen (1960). In fact, however, s is desired as a function of a parameter λ which is inversely proportional to the local drift velocity. Strictly speaking, this is a difficult demand. However, within the frame of the desired accuracy, it is sufficient to approximately identify the length defined in the customary geomagnetic coordinate system with λ. In moderate latitudes, this is already true for the geographic longitude. We can therefore regard $s(\varrho,\zeta,\lambda)$ in principle as known. The mean density thus becomes

$$\bar{N}(\varrho,\eta,t)=\frac{1}{2\pi}\int_{-\zeta_m(\eta)}^{\zeta_m(\eta)}\int_{0}^{2\pi}N(s(\varrho,\zeta,\lambda),t)\cdot w(\eta,\zeta)\,d\zeta\,d\lambda. \qquad (5.2)$$

The search for a favorable representation $s(\varrho,\zeta,\lambda)$ will logically be guided by the actual form of the invariant surfaces of which figures 5.1 to 5.3 are intended to give an impression. The first shows the projection of some corresponding curves of constant B^*, J^* on the surface of the earth with altitudes indicated in km. They were selected so that they have approximately the same altitude at longitude 120°. The most notable characteristic is that they reach their lowest altitude above the Southern Atlantic Ocean, i.e., the difference in relation to other longitudes and especially in relation to the

conjugated northern points is so great that, at a scale height of magnitude 100 km as it is found in the vicinity of the earth, the collision losses predominately take place here. With increasing scale height, the share of the other regions in the mean density increases; however, we are then no longer much concerned with the details of the orbital trace. This suggests a division in two of the manner of description: within the range of the Atlantic anomaly as far as possible with an accuracy of ± (10-20) km and, outside of this, a simple overall representation which does not take account of occasional deviations of ± (200-300) km because, even at a scale height of about the same magnitude, the influence of the Atlantic anomaly is still large enough to keep the error in density here below 20%.

A typical example for the trace of altitude of curves with constant B^*, J^* above the Atlantic anomaly is given in Fig. 5.2. It is shown that the calculated orbital points can be approximated with great accuracy in part linear in any surface $J^* = \text{const.}$, i.e., the selection of the salient points $i = 1, \ldots, 5$ can be made so that their differences of longitude for J_k^* and all B^* are respectively constant. Beyond this, we find that the distances s_{ik} of the salient points belonging to fixed i and J_k^* change approximately in accordance with a power law with two individual constants:

$$s_{ik}(B^*) = \frac{C_{ik}}{B^{*b_{ik}}}. \tag{5.3}$$

The mean quadratic deviation here lies below 10 km.

The data so far available are restricted to some discrete values J_k^* which still correspond to rather large differences of latitude. The consequently necessary interpolation method is to be selected so that it will lead to trivial results in the concentric dipole field. For this, we attempt first to find the latitude which is defined through the section of the spherical

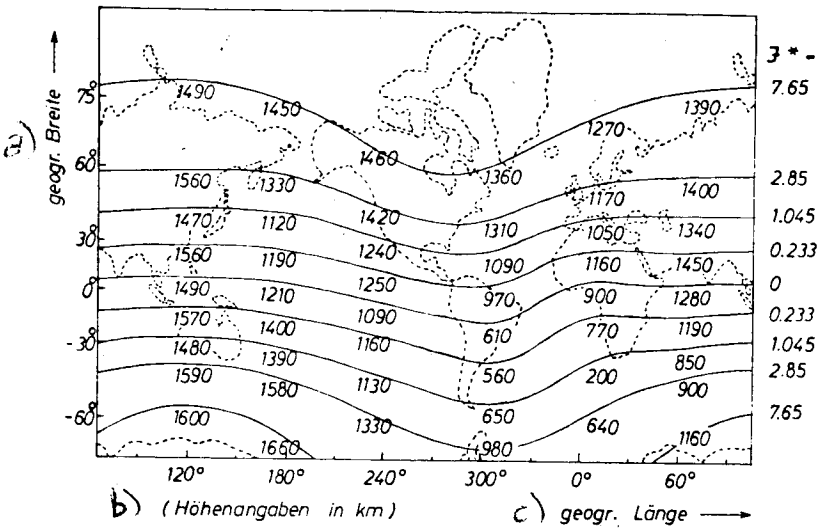

Fig. 5.1 - Traces of the reflection points projected on the surfaces of the earth at some values of J^* (cf. (2.29)) and an approximate altitude of 1,500 km at geographic longitude 120° (according to Dessler, Satellite Environment Handbook, 1961).
Legend: a = geographic latitude; b = altitude in km; c = geographic longitude.

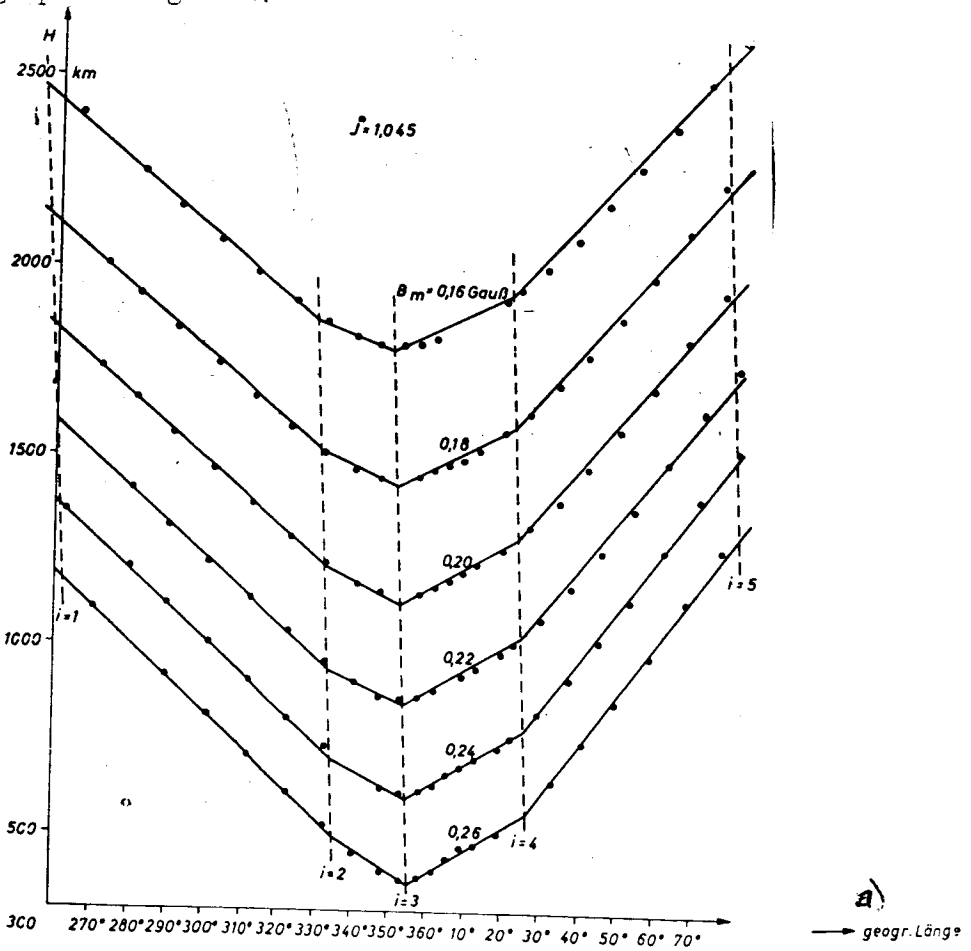

Fig. 5.2 - Particle-orbit points calculated by Jensson, Murray, Vette (1960) in the terrestrial magnetic field for $J^* = 1.045$ and some magnetic-field values; the straight lines represent the approximation of the data here utilized.
Legend: a = geographic latitude.

shell $r = \varrho(1 - \zeta^2) = \text{const.}$, around the dipole with a surface $J^* = \text{const.}$ (2.29):

$$J^* = \varrho \tilde{J}(\zeta) = r \frac{\tilde{J}(\zeta)}{1-\zeta^2}$$

i.e.

$$\zeta^2 = G\left(\frac{J^*}{r}\right) \approx \begin{cases} 0{,}601 \dfrac{J^*}{r} - 0{,}1938 \left(\dfrac{J^*}{r}\right)^2 & \text{for} \quad \dfrac{J^*}{r} \leqq 0{,}3 \\ 1 - \left(0{,}978 + 0{,}706 \dfrac{J^*}{r}\right)^{-1} & \text{for} \quad \dfrac{J^*}{r} > 0{,}3. \end{cases} \tag{5.4}$$

Let now $J_k^* \leqq J^*(\varrho, \zeta) < J_{k+1}^*$. The instruction then reads: determine B^* at the points

$$r, \zeta_k = \left[G\left(\frac{J_k^*}{r}\right)\right]^{1/2} \quad \text{or} \quad r, \zeta_{k+1} = \left[G\left(\frac{J_{k+1}^*}{r}\right)\right]^{1/2}$$

and in the dipole field consequently

$$B_k^* = \frac{\sqrt{1+3\zeta_k^2}}{r^3}, \tag{5.5}$$

calculate the distances $s_{ik}(B_k^*)$ and $s_{ik+1}(B_{k+1}^*)$ belonging to fixed i and interpolate, in proportion to the difference of latitude $\zeta - \zeta_k$

$$s_i(\varrho, \zeta) = \frac{s_{ik+1} - s_{ik}}{\zeta_{k+1} - \zeta_k} (\zeta - \zeta_k) + s_{ik}, \tag{5.6}$$

and correspondingly for $\Delta\lambda$;

$$\Delta\lambda_i(\varrho, \zeta) = \frac{\Delta\lambda_{ik+1} - \Delta\lambda_i}{\zeta_{k+1} - \zeta_k} (\zeta - \zeta_k) + \Delta\lambda_{ik}. \tag{5.7}$$

The quality of this procedure can be approximately estimated from fig. 5.3 in which the altitudes of the salient point i = 3 over ζ, i.e., over the latitude, are plotted for three levels r = const. In the concentric dipole field, they would lie on horizontals. It may be assumed that no deviations appreciably greater than 20 km occur in the linear interpolation (5.6) along the broken line.

The trace in λ between the points i = 1 and i = 5 is then obtained from (5.6) and (5.7), as intimated in fig. 5.2, also by linear interpolation:

$$s^A(\varrho, \zeta, \lambda) = \frac{s_{i+1}(\varrho, \zeta) - s_i(\varrho, \zeta)}{\Delta\lambda_i(\varrho, \zeta)} (\lambda - \lambda_i) + s_i(\varrho, \zeta). \tag{5.8}$$

The <u>representation of the resulting orbital trace</u>, starts from the fact that the terrestrial magnetic field can be approximated rather well by the

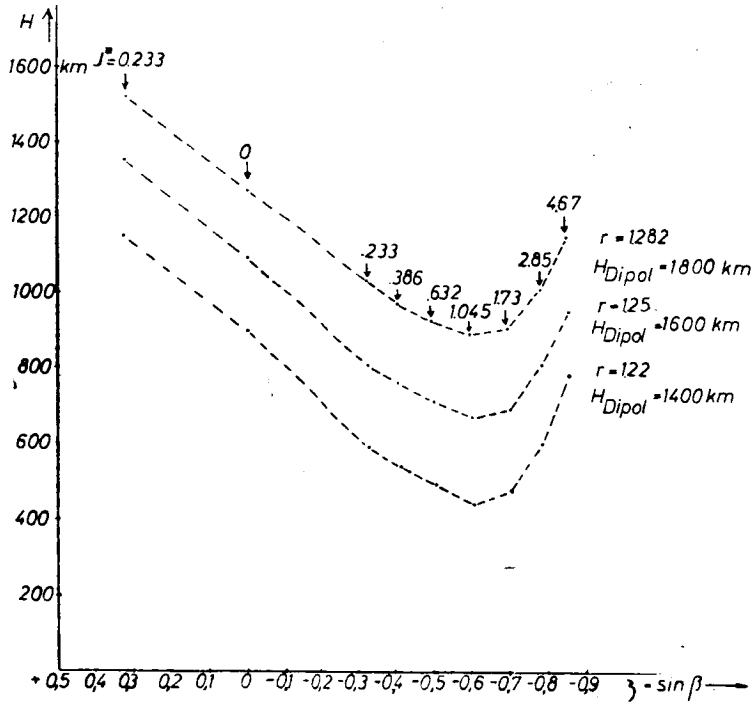

Fig. 5.3 - Demonstration of the interpolation method utilized between the particle-orbit data at various values of J^* by maintaining the distance $r = \varrho(1 - \zeta^2)$ in the dipole field belonging to J^*, B^*.

field of an eccentric dipole (Parkinson, Cleary, 1958). With an eccentricity e at a length of λ_e, s results, provided the center of the earth lies in the equatorial plane, from

$$s^2 = r^2 + e^2 + 2er\cos\beta\cos(\lambda - \lambda_e)$$

or if $e \ll r$:

$$s \approx r + e\cos\beta\cos(\lambda - \lambda_e).$$

Correspondingly, let us here make the somewhat enlarged formulation $\left(\cos\beta = \sqrt{1-\zeta^2}\right)$:

$$s(\varrho, \zeta, \lambda) = \varrho\cdot(1-\zeta^2) + \sqrt{1-\zeta^2}\,(e\cos(\lambda - \lambda) + \Delta e). \qquad (5.9)$$

By comparison with the data of Jensen et al., we find with eR_e = 280 km, $\Delta e \cdot R_e$ = 130 km and $\lambda = \lambda_e$ for geographic longitude 125°, a rather satisfactory representation which contains, however, outside of the Atlantic anomaly, also both positive and negative deviations of 300 km maximum.

With the expressions (5.8) and (5.9), integration over λ (Equation 5.7) is to be carried out still in general. Let us here make for each component of

the atmosphere the simple isothermal formulation

$$N(S) = N_0 e^{-\frac{s-s_0}{h}} \tag{5.10}$$

That this formulation concords with simple theories of the exosphere -- the layer of the neutral atmosphere beginning at about an altitude of 550 km in which the collisions can be neglected -- as shown by Herring and Kyle (1961) or as also follows from the numerical integration of the equations propounded by Johnson and Fish (1960), should here not be too highly evaluated because the basic models are certainly too simple, especially by reason of neglecting diurnal variations. (5.10) is to be rather an approximation formula valid in part which has primarily the advantage of reducing the determination of density to be made in Subsection 7.4 from the distribution of equilibrium to a mere variation of the parameters N_0 and h (which may be moreover slowly variable functions of time).

The contribution to mean density furnished by the Atlantic anomaly south ($-\zeta$) of the magnetic equator $J^* = 0$ between the points i = 1 and i = 5 is, according to (5.8) and (5.10),

$$\frac{\Delta\lambda}{2\pi} \cdot N^{\Delta}(\varrho, -\zeta, t) = \frac{1}{2\pi} \sum_{i=1}^{4} \int_{\lambda_i}^{\lambda_{i+1}} N_0(t)\, e^{\frac{s^{\Delta}(\varrho,\zeta,\lambda)-s_0}{h(t)}} = \tag{5.11}$$

$$= \frac{1}{2\pi} \sum_{i=1}^{4} \Delta\lambda_i \cdot h(t) \cdot \frac{N(s_i, t) - N(s_{i+1}, t)}{s_{i+1} - s_i}$$

with

$$\Delta\lambda = \sum_{i=1}^{4} \Delta\lambda_i .$$

The northern hemisphere ($+\zeta$) is described by (5.9),

$$\frac{1}{2\pi} \int_0^{2\pi} e^{-\frac{\sqrt{1-\zeta^2}}{h} e \cos(\lambda-\lambda_e)}\, d\lambda = I_0\left(\frac{\sqrt{1-\zeta^2}\, e}{h}\right)$$

with the modified Bessel function of zero order now is I_0 and the whole expression for the mean density is

$$N^N(\varrho, +\zeta, t) = N(\varrho(1-\zeta^2) + \sqrt{1-\zeta^2}\, \Delta e, t) \cdot I_0\left(\frac{e}{h(t)} \sqrt{1-\zeta^2}\right). \tag{5.12}$$

In order also to include the remainder of the orbit in the southern hemisphere,

let us simply multiply (5.12) with $(2 - \Delta\lambda/2\pi)$. This is inaccurate in general but the error which may amount to about 50% of (5.12) for large values of $\sqrt{1-\zeta^2}\,e h^{-1}$ carries little weight because the influence of (5.11) then largely predominates. In the opposite border case e/h → 0, on the other hand, this procedure becomes just accurate. Thus there finally results from (5.2), (5.11) and (5.12):

$$\bar{N}(\varrho, \eta, t) = \int_0^{\zeta_m(\eta)} \left[\frac{\Delta\lambda}{2\pi} N^A(\varrho, -\zeta, t) + \left(2 - \frac{\Delta\lambda}{2\pi}\right) N^N(\varrho, \zeta, t)\right] w(\eta, \zeta)\, d\zeta. \qquad (5.13)$$

The division in two parts of the description of the particle orbits suffers from a further deficiency. At reflection points in the vicinity of the Equatorial plane over which the Atlantic anomaly (as will be seen from fig. 5.3) actually extends still further north, which has been neglected in (5.12), it leads to an error of one factor which lies between 1 and $\frac{1}{2}$ depending on scale height. This must be taken into account in the calculation of the distribution of equilibrium but is not really critical because, for $\beta_m \approx 5$, the error already lies below the accuracy limit of the total calculations at a scale height of 70 km. It is difficult to estimate the final error under this approximation method because all results are obtained by integration over many spatial points. It is estimated that it does not essentially exceed the inaccuracy in the calculations of orbit which amounts to about ± 10 km so that, at any scale height of more than 60 km, the calculated values of $\bar{N}(\eta, \varrho)$ should be reliable within 30% or less.

6 - Proton Capture in the Terrestrial Magnetic Field Through Decay of Albedo Neutrons

A prolonged validity of the three adiabatic invariants (cf. subsec. 2.2) must be regarded as a fundamental condition for the existence of the radiation belt. The reverse of this demand is the impossibility to capture here in a

simple manner charged particles penetrating directly from the outside. In order to explain how the observed radiation is continually maintained, three suggestions have been basically made: penetration impossible to the single particle might be provided in the wake of a whole cloud of solar plasma by the ability of the latter of shielding itself against the terrestrial field, or through the changed conditions due to the hydromagnetic waves produced, or else these disturbances of the magnetic field lead only within the range of the radiation belt to an acceleration of unspecified low-energy particles (existing in a sufficient quantity) to the energies observed. The concrete formulation of these two concepts is obviously a difficult task. Correspondingly, we can say very little as yet on their significance for the captured corpuscles. In any event, there exists a number of serious objections; in the first case primarily on the part of observation (Dessler and Karplus, 1960) and, in the second case, through the impairment, necessarily always accompanying an appreciable acceleration, of at least one of the adiabatic invariants which would tend to lead, however, rather to increased losses by diffusion than to a prolonged increase of the radiation intensity (cf. subsec. 4.2).

Initially, only the third suggestion which utilizes the detour over neutral particles, is open to quantitive investigation. This involves the albedo neutrons escaping into space as products of the interaction between cosmic radiation and atmosphere which constitute a promising and repeatedly investigated source of captured particles (cf. sec. 1). It has not yet been clarified whether other neutral particles may not also lead to a similarly effective production at least in certain ranges.

This study bases itself only on the albedo neutrons. It presupposes moreover knowledge of the intensity of the neutron flux at a level r_0 above the layer of its origin (10-30 km). In this chapter, specifically, only the

geometric circumstances of proton capture are to be clarified. That this is possible independently of the energy distribution of the neutrons is conditioned by two characteristics of their decay. Through their long life span of about 1,000 s, an interval of time in which they can cover far greater distances at the velocities considered, than the dimensions of the radiation belt and by the fact that the proton absorbs the entire impulse of the neutron with a relative error of the magnitude of the ratio of mass of electron/proton. Moreover the energies (> 100 keV) are large enough so that the influence of the gravitational field can be neglected.

For neutron intensity at the altitude r_o, let us make the formulation $I_n = I_n(\varkappa, \vartheta', \zeta', t)$ in which ϑ' is the distance of the zenith at the locus $P'(r_o, \zeta')$. The distribution of orientation is taken into account as rotation-symmetrical around the vertical and the spatial variation from the geomagnetic latitude ($\zeta' = \sin \vartheta'$) is taken into account. This is reasonable because the active cosmic radiation is influenced by the terrestrial magnetic field and, in particular, the lower limit of energy of the particles still reaching the surface of the earth is a function of magnetic latitude.

The task now consists in deriving from I_n a source function $Q(\alpha, \eta; \varrho, t)\, d\alpha\, d\eta$ which indicates the protons captured per second in a tube of force of the equatorial cross section 1 cm^{-2} with the distance ϱ in the interval $(\alpha, \alpha + d\alpha;$ $\eta, \eta + d\eta)$. For this we need first the correlation between I_n and the neutron intensity at an arbitray locus P in space, expressed in coordinates which are oriented in the magnetic field. With fixed ϑ and φ, the rate of decay is then indicated over an invariant surface, i.e., over the three phases ξ, ζ, λ. In contrast to atmospheric density, the neutron flux attenuates so slowly with decreasing distance that the magnetic field may be considered, in an extremely rough approximation, as a central dipole, without running the risk of appreciable deviations from reality. The circumstances then become independent of

the length λ.

The number dN of the neutrons which infiltrate a surface element $d\sigma'$ at the locus $P'(r_0, \zeta')$ and a second surface element $d\sigma$ in P per unit time is

$$dN = I_n(\alpha, \vartheta', \zeta', t)\, d\alpha \cos\vartheta'\, d\sigma'\, d\Omega'$$

with

$$d\Omega' = d^{-2}\, d\sigma \cos d.$$

ϑ' and ϑ are the angles of the respective surface normals n' and n and d is the distance $\overline{P'P}$ (fig. 6.1). However, regarded from P, $d\sigma'$ forms the solid-angle interval

$$d\Omega = d^{-2}\, d\sigma' \cos\vartheta',$$

and we obtain

$$dN = I_n(\alpha, \vartheta', \zeta', t)\, d\alpha \cos\vartheta\, d\sigma\, d\Omega. \qquad (6.1)$$

If ϑ' and ζ' are determined as functions of the coordinates selected in P, (6.1) furnishes the neutron flux through $d\sigma$ in P.

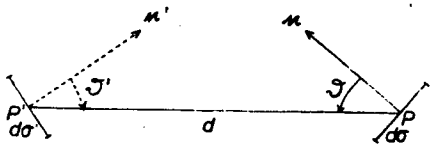

Fig. 6.1 - Explanation of the interrelation between neutron intensity at two points P and P'.

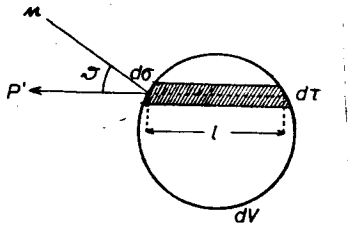

Fig. 6.2 - Derivation of the decay rate in the volume element dV.

We now consider a volume element dV -- convex for the sake of simplicity -- around P (fig. 6.2). The neutron beam (6.1) here occupies the part $d\zeta' \cos\vartheta \cdot l$. ($l$ = length of beam in dV). The number of the neutrons from this beam decaying in dV per unit time is given by the probability of decay: $l \cdot (\gamma v L_n)^{-1}$ (L_n = life span of neutrons $\approx 10^3$ s, $\gamma = (1 - v^2/c^2)^{-1/2}$ = dilation of time) and fig. 6.2:

$$\frac{l}{\gamma v L_n} dN = \frac{I_n(\alpha, \vartheta', \zeta', t)\, d\alpha}{\gamma L_n v} \cdot l\, d\sigma \cos\vartheta\, d\Omega = \frac{I_n(\alpha, \vartheta', \zeta', t)\, d\alpha}{\gamma v L_n} d\tau\, d\Omega.$$

There follows from this then the entire number of the protons captured in dV per unit time from the direction P'P by integration over $d\Upsilon$:

$$\frac{I_n(\alpha, \vartheta', \zeta', t)\, d\alpha}{\gamma v L_n} \cdot dV\, d\Omega. \tag{6.2}$$

As already discussed in subsec. 2.4, the locus of the particle can here also be replaced by that of the guiding center because the neutron flux scarcely changes during one radius of gyration. It then becomes easy to write the summation of all contributions (6.2) to the source function $Q(\eta, \zeta; \varrho, t)$. We must first integrate, at a fixed value of the corresponding angles of orbital inclination $\psi(\eta, \zeta)$ and $\pi - \psi$, over all values of ξ which furnish a direction leading from P to the spherical shell $r = r_0$ and then over all ζ between $-\zeta_m(\eta)$ and $+\zeta_m(\eta)$ (cf. 2.22) by taking into account the variability of the cross-section of the tube of force. With (2.17) and (2.24-a), we obtain

$$dV = dl \cdot b^2(\zeta) \cdot 1\ \mathrm{cm}^2 = R_e \varrho \sqrt{1 + 3\zeta^2}\, d\zeta\, b^2(\zeta) \cdot 1\ \mathrm{cm}^2$$

and, with (2.18),

$$d\Omega = \sin\psi\, d\psi\, d\xi = \frac{b^{-2}(\zeta)\, \eta\, d\eta}{\sqrt{1 - \eta^2 b^{-2}(\zeta)}}\, d\xi.$$

From (6.2), there then follows the source function

$$Q(\alpha, \eta; \varrho, t)\, d\alpha\, d\eta = \frac{2 R_e \varrho \eta}{\gamma v L_n}\, d\alpha\, d\eta \times$$

$$\times \int_{-\zeta_m(\eta)}^{+\zeta_m(\eta)} d\zeta \int_0^{\xi_{max}} d\xi\, [I_n(\alpha, \vartheta'_+, \zeta'_+, t) + I_n(\alpha, \vartheta'_-, \zeta'_-, t)] \frac{\sqrt{1 + 3\zeta^2}}{\sqrt{1 - \eta^2 b^{-2}(\zeta)}} \tag{6.3}$$

with

$$\vartheta'_+ = \vartheta'(\psi, \xi, \varrho, \zeta); \qquad \beta'_+ = \beta'(\psi, \xi, \varrho, \zeta)$$
$$\vartheta'_- = \vartheta'(\pi - \psi, \zeta, \varrho, \xi); \qquad \beta'_- = \beta'(\pi - \psi, \zeta, \varrho, \zeta). \tag{6.4}$$

Let $\xi = 0$ always designate that direction on the double cone defined by $\psi(\eta, \zeta)$ and $\pi - \psi$ which is closest to the center of the earth -- it necessarily lies in a meridian plane -- and ξ_{max} the tangent to the surface $r = r_0$, inasmuch as the latter actually exists. The factor 2 contains the symmetry to the meridian plane.

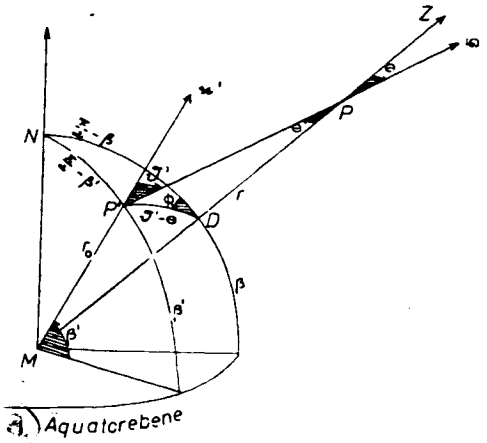

Fig. 6.3 - Interrelation between direction of emission ϑ' of a neutron from the atmosphere at P'(r, β') and the direction Θ at P(r, β).
Legend: ä = equatorial plane.

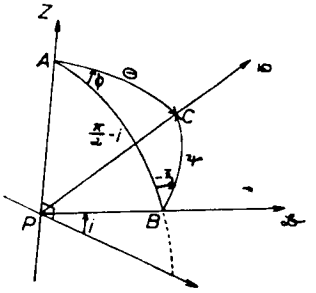

Fig. 6.4 - Interrelation between the angles of direction of proton velocity at P in relation to the verticals (Θ, Φ) and in relation to the magnetic field (ψ, ξ) at inclination i of the field.

We now need merely constitute the trigonometric relations symbolized by (6.4). Let us initially introduce (fig. 6.3), at the test point P, a spherical coordinate system (Θ, Φ) in which Θ is the angle of zenith and/or of the direction from the center of the earth M to P.

a) Fig. 6.3 -- triangle P'PM (law of sine):

$$\sin \vartheta' = \frac{r}{r_0} \sin \Theta \tag{6.5}$$

triangle N P'D (spherical cosine law):

$$\sin \beta' = \sin \beta \cos (\vartheta' - \Theta) + \cos \beta \sin (\vartheta' - \Theta) \cos \Phi. \tag{6.6}$$

Since we always have $\vartheta' \leqq \pi/2$ and $r > r_0$, there follows from (6.5): $\Theta \leqq \vartheta' \leqq \pi/2$, i.e., the angles in (6.5) and (6.6) are determined uniquely.

There now follows the transition $\Theta, \Phi \rightarrow \psi, \xi$, which depends only on the inclination i of the field, i.e., according to (6.12), only on magnetic latitude.

b) Fig. 6.4 -- triangle ABC (spherical cosine law):

$$\cos \Theta = \cos \psi \sin i + \sin \psi \cos i \cos \xi \tag{6.7}$$

$$\cos\psi = \cos\Theta \sin i + \sin\Theta \cos i \cos\Phi \qquad (6.6)$$

(2.13):
$$\cos i = \pm \sqrt{\frac{1-\zeta^2}{1+3\zeta^2}}.$$

The four equations (6.5 to 6.8), form together with (2.13) the relations (6.4). The limit ξ_{max} is determined by the facts that the direction defined by ψ, ξ, i in the point (ϱ, ζ) just touches the spherical shell $r = r_o$, i.e., $\vartheta' = \pi/2$.

From (6.5), $\vartheta' = \frac{\pi}{2}$ follows $\sin\Theta_m = \frac{r_0}{r}$ and $\cos\Theta_m = \sqrt{1-\left(\frac{r_0}{r}\right)^2}$

and

(6.7)
$$\cos\xi_m = \frac{\sqrt{1-\left(\frac{r_0}{r}\right)^2} - \cos\psi \sin i}{\sin\psi \cos i} \qquad (6.9)$$

Although the denominator of (6.9) is always not equal to zero because 0 and π are values of ψ of no concern, the entire right side is not necessarily smaller or equal to 1 in amount. However, then

$$\sin(i \pm \psi) \geqq \sqrt{1-\left(\frac{r_0}{r}\right)^2}$$

i.e., there is no intersection with the surface $r = r_o$.

7 - Protons in the Inner Radiation Belt

7.1 - The Model

The discriminating viewpoint for the model calculations consists in the fact that only collision losses and, as proton supplier, only the decay of the albedo neutrons of cosmic radiation is taken into account in an appropriate manner. As a further simplification, all time derivations are stated as equal to zero.

Only the first of these assumptions can be justified a priori at least for a certain range: the steep increase of radiation at altitudes of several hundred km is quite evidently an expression of the decrease of atmospheric density; both scale heights concur roughly. However, the extent of the

extent of this range in which collisions determine life span consequently is not yet quite clear and is one of the essential questions to which this study is devoted. That the albedo neutrons of the (galactic) cosmic radiation create at these altitudes sufficient protons for the maintenance of the distribution of equilibrium has been made probable by the work of various authors (cf. introduction) but requires more detailed examination. The neglect of the time-dependence of replenishment is consistent with the constancy in time of cosmic radiation in moderate magnetic latitudes but also implies a restriction to small values of ϱ because primary particles of low energy showing a greater variation in time (McDonald, Webber, 1962) with increasing latitude and, in particular, also solar protons reach the atmosphere of the earth (Ogilvie et al., 1962; Davis et al., 1962; Winkler, 1962) and can create albedo neutrons in their turn. Because of the umbral effect of the earth, these encounter, however, mostly only field lines with $\varrho \geq 1.7$ (Naugle, Kniffen, 1961; Lenchek, Singer, 1962-a; Lenchek, 1962). Finally, atmospheric density is subject to various variations in time. The diurnal variation which probably has the greatest amplitude, is averaged during the particle drift around the earth (see sec. 5); all life spans are in general long in relation to the drift period. The amplitude of the semiannual period (Paetzold, Zschoerner, 1961) and the variations correlated with the geomagnetic disturbances are sufficiently small so that neglect does not carry too much weight whereas the 11-year variation correlated with solar activity (Harris, Priester, 1962) must be taken into account. However, if the life span is very much shorter than this period, we can count at any time with a stationary density. This is initially asserted here and will later be examined in subsec. 7.7 in regard to its justification.

In order to make the model outlined more concrete, we lack two data which are the intensity of the albedo neutrons and the density distribution of the atmosphere. We shall proceed so that we make the formulation $N_i(s) = N_{io}\, e^{-s-s_o/h_i}$ explained in sec. 5, for the various components i of the atmosphere, and the open parameters N_{io}, h_i are determined so that optimum concordance between the theoretical and the measured proton distribution exists at a given neutron flux (cf. subsec. 7.2). The model of the atmosphere so obtained can then be compared with other determinations. Any possible deviations in the absolute amount of the densities will have to be interpreted as indications of the intensity of the proton source whereas deviations in the relative trace should give indications on the quality of all of the models, specifically the consideration of the loss processes.

7.2 - Albedo Neutrons of Cosmic Radiation

The spatial and energetic distribution of the albedo neutrons of cosmic radiation has been investigated theoretically by Hess, Canfield and Lingenfelder (1961). The base of their calculations is represented by measurement of the distribution of equilibrium of neutrons in the atmosphere to an altitude of 200 g/cm^{-2} at geomagnetic latitude 44^{o} N from 1957 (Hess et al., 1959) which were obtained with counters of very different spectral sensitivity. Below 10 MeV, the authors obtain from the flux of the neutrons escaping upward from the atmosphere through a diffusion theory. At higher energies, application of the diffusion equation is no longer possible because of the anisotropy of the emission of secondary particles in nuclear processes. The authors here derive a spectrum of the secondary neutrons from measurements of the protons generated by cosmic radiation in nuclear-emulsion plates (Camerini et al., 1950) -- on the argument that neutrons and protons behave similarly at high energies --, calculate the percentage of the particles decelerated through

collisions in the diffusion range which permits them determination of absolute intensity from comparison with the measured data in this range, and find intensity and angular distribution of the albedo neutrons from geometrical considerations of the range of action of the primary particles and of the angle of aperture of the emission of secondary particles which becomes increasingly smaller at higher energies.

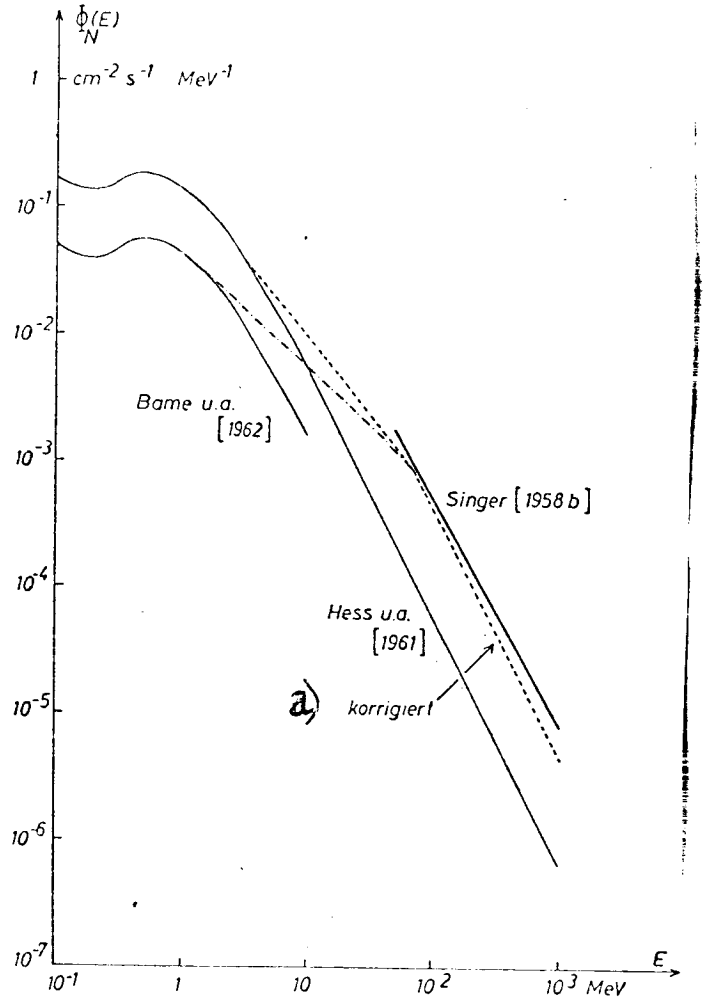

Fig. 7.1 - Theoretical spectra of the albedo neutrons of cosmic radiation according to Hess and Singer and to measurements by Bame. Broken-line curves show, above 30 MeV, the requirements on the part of the model calculations carried out in subsec. 7.4 and, below 30 MeV, a schematic continuation to the curves of Hess and Bame.
Legend: a = corrected.

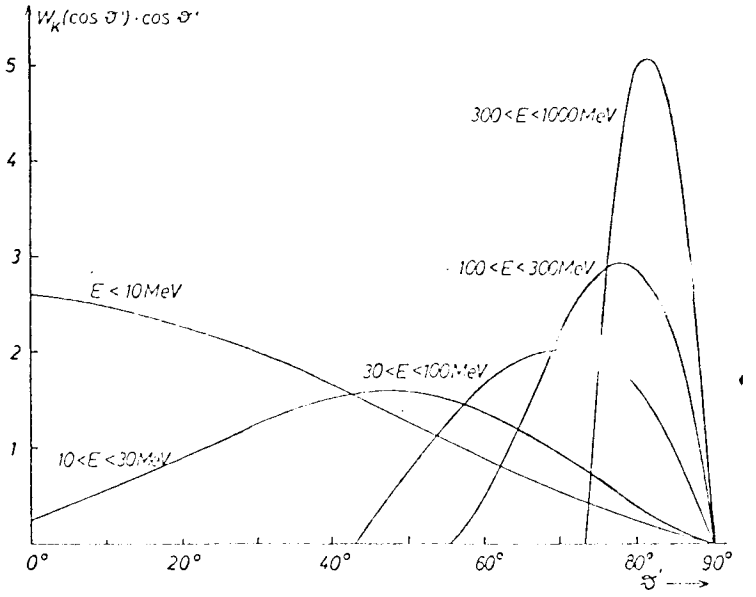

Fig. 7.2 - Angular distribution of albedo neutrons above the atmosphere for various energy ranges (normalized to 1) (according to Hess et al., 1961).

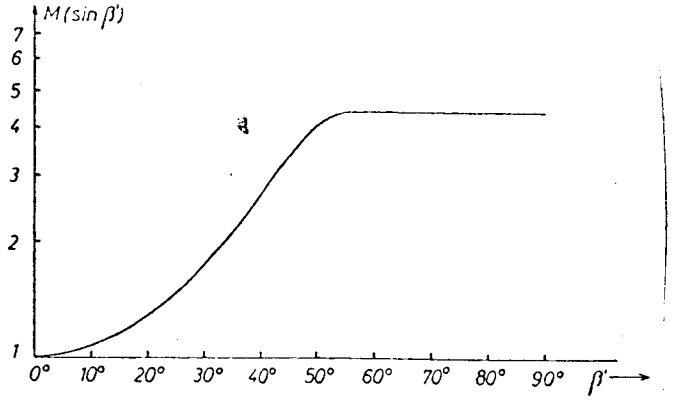

Fig. 7.3 - Dependence on latitude of neutron flux according to Hess et al., (1961).

The method has inherent considerable factors of uncertainty which lead us to consider the findings above 1 MeV with caution. Fig. 7.1 contains the spectrum determined for the vicinity of the Equator, and Fig. 7.2 the distribution of direction normalized to 1 for various ranges of energy. The conclusions from the initial data at $\beta = 44^{\circ}$ to other latitudes is made by the authors through simple multiplication with the variation of latitude measured by Simpson (1951) of the total neutron flux at low altitude ($\simeq$ 300 g/cm^{-2}, fig. 7.3). From the measurement of the dependence on latitude

of ionization (Neher, 1962), it may be conjectured that it is more pronounced also for the neutrons in higher atmospheric layers than is shown in Fig. 7.3. However, in the low altitudes under consideration here this does not play a great role.

The idealization contained in the product formulation is initially unavoidable. Wentworth and Singer (1955) have derived an albedo-proton spectrum from the already quoted nuclear-emulsion data of Camerini (1950) which Singer (1958-b) regards as valid also for neutrons between 50 and 400 MeV and which does not vary too greatly ($\sim E^{-1.8}$) from that of Hess ($\sim E^{-2}$). The absolute amount of the albedo neutrons alone is estimated by Singer at about one order of magnitude greater than by Hess and associates (cf. Fig. 7.1).

The best information on the albedo neutrons may be expected from direct measurements above the atmosphere. Here also findings are already available but differ greatly from each other. For example, Hess and Starnes (1960) and Albert, Gilbert and Hess (1962) found with B^{10} F_3-counters imbedded in a hydrogen moderator, a total neutron flux which agrees with the theoretical expectations of Hess et al., (1961). However, Reidy et al., (1962) registered (without moderator) the five-fold amount whereas Bame et al., (1962) again using a moderator, found only one-third. These last measurements most probably regarded as the most reliable because $Li^6I(Eu)$-scintillation counters permit differentiation both of the neutrons from charged particles by the intensity of impulse and, moreover, in contrast to other experiments, the generation of secondary neutrons in the material of the surroundings was kept appreciably lower through the separation of the counters from the rocket. On the basis of the form of the neutron spectrum theoretically obtained by Hess and associates, Bame et al., were successful in reducing the count rate of the counters with very different sensitivities in the energy range from 100 keV to 10 MeV

(which furnishes the main contribution to the total flux) to the same true intensity. Above 10 MeV where counter sensitivity and neutron intensity strongly decline, the validity of these measurements is only small. They are therefore plotted in Fig. 7.1 through displacement of the Hess spectrum < 10 MeV by a factor of 1/3.

If in the following our calculations are based on the findings of Hess, Canfield, and Lingenfelder, this is done in order to be able to completely formulate initially the model for the protons captured in the vicinity of the earth. The uncertainties of this basis should be kept in mind and subjected to discussion where they are of importance (cf. subsec. 7.5).

For the neutron intensity I_n above the atmosphere (altitude $\approx$ 100 km), let us make, according to Hess, a product formulation from the energy distribution $\Phi_n(\alpha)$, the angular distribution $W_k(\cos\vartheta')$ for different ranges of energy K and the modulation of latitude $M(\zeta')$:

$$I_n(\alpha, \vartheta', \zeta') = \frac{1}{2\pi} \Phi_n(\alpha) \cdot W_k(\cos\vartheta') \cdot M(\zeta') \quad \text{for} \quad \alpha_k \leqq \alpha < \alpha_{k+1}. \tag{7.1}$$

The angular distributions were approximated from the curves indicated by the authors through the development

$$W_k(\cos\vartheta') = \begin{cases} a_k + b_k \cos\vartheta' + c_k \cos^2\vartheta' & \text{for} \quad \vartheta' > \vartheta_{k,gr} \\ 0 & \text{and/or otherwise} \end{cases}$$

with

$$\int_0^1 W_k(\cos\vartheta') \cos\vartheta' \, d(\cos\vartheta') = 1 \tag{7.2}$$

and plotted in Fig. 7.2. From the simple diffusion theory, there results $a_0 = 1, b_0 = 3/2, c_0 = 0$. No great importance needs to be ascribed to the accurate form of the curves and only the qualitative influence of anisotropy on the rate of capture should be examined from them. With (7.1), the general expression (6.3) assumes the following form for the source function

$$Q(\alpha, \eta; \varrho) = \frac{\Phi_n(\alpha)}{\sqrt{\alpha(\alpha+2)}} G_k(\eta, \varrho) \tag{7.3}$$

with

$$G_k(\eta,\varrho)=\frac{R_e\varrho\eta}{\pi L_n c}\int_{-\zeta_m}^{+\zeta_m}\int_{0}^{\xi_{max}}\left[W_k(\cos\vartheta'_+)M(\zeta'_+)+W_k(\cos\vartheta')M(\zeta'_-)\right]d\xi\,\frac{\sqrt{1+3\xi^2}\,d\zeta}{\sqrt{1-\eta^2b^{-2}(\zeta)}}. \qquad (7.4)$$

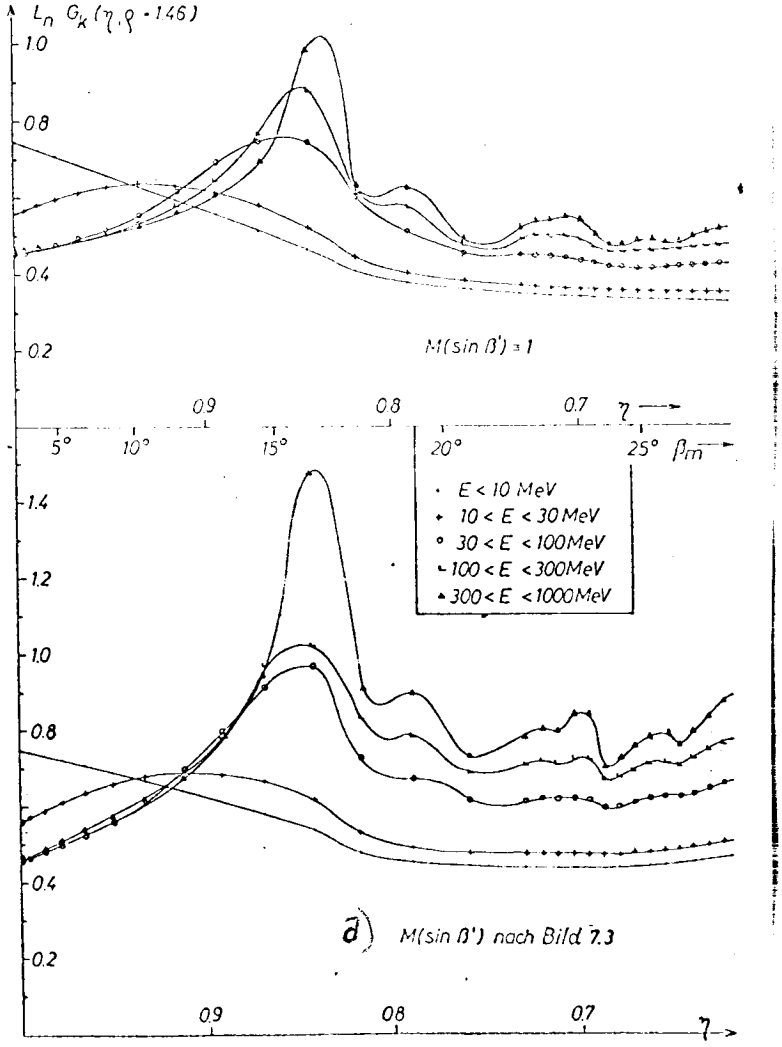

Fig. 7.4 - Geometric component of rate of capture (7.4) of protons at $\varrho = 1.46$ for the angular distribution in Fig. 7.2 when neglecting dependence on latitude, and when taking the latter into account according to Fig. 7.3. The points indicated were calculated numerically.
Legend: a = $M(\sin\beta')$ from fig. 7.3.

The functions (7.4) for $\varrho = 1.46$ are plotted in Fig. 7.4-a with $M(\zeta') = 1$ and with $M(\zeta')$ from Fig. 7.3. It will be seen from the formalism of sec. 6 that a considerable effort is contained in the calculation of $G_k(\eta, \varrho)$. In

order not to let the time required for calculation increase too greatly, accuracy was selected not better than 10 % which is, however, entirely sufficient for the overall calculation. The individual maxima of $G_k(\eta, \varrho)$ for higher energies are difficult to grasp intuitively because the contributions originate from regions which are intersected by a double cone with aperture $\vartheta(\eta)$ travelling along the field lines. However, the qualitative trend, specifically the relative increase of the rate of capture with increasing anisotropy and latitude of reflection point can be easily understood: if the reflection point lies close to the equatorial plane, the (very truncated) double cone intersects the atmosphere so that almost all zenith angles ϑ' between 0 and 90° occur in the connecting straight lines. Only W_0 and W_1 are not equal to zero for all ϑ'. However, if the reflection point lies at a higher latitude, then there are here increasingly preferred, because of the steeper inclination of the field line, the large zenith angles in which lies the predominant probability of emission of the high energies but only a small part of the low energies (normalized to 1!). This behavior is in direct contrast to the findings of Lenchek and Singer (1962-b; fig. 5) who obtain a decrease of the rate of capture with increasing anisotropy which is only little dependent on latitude, and based on this a greater steepness of the proton spectrum (cf. subsec. 7.6). Unfortunately, it cannot be determined from the paper quoted just how the rates of capture were obtained.

In order to smooth out the non-steady energy spectrum (7.3), we recommend interpolation linear in the logarithm of energy between G_k and consequently the following definitive definition of the proton source function:

$$Q(\alpha, \eta, \varrho) = \frac{\Phi_n(\alpha)}{\sqrt{\alpha(\alpha+2)}} \cdot G(\alpha, \eta; \varrho) \qquad (7.5)$$

with

$$G(\alpha, \eta; \varrho) = \frac{G_{k+1} - G_k}{\ln \alpha_{k+1} - \ln \alpha_k} (\ln \alpha - \ln \alpha_k) + G_k \text{ for } \alpha_k \leq \alpha < \alpha_{k+1}, \qquad (7.6)$$

in which α_k is the geometric mean of the interval limits indicated in Fig. 7.2 and 7.4.

7.3 - Solution of the Time-Independent Problem for Pure Collision losses

The equilibrium model described in subsec. 7.1 finds its expression, with the collision losses (3.21) and (3.26) and the source function (7.5), in the customary linear inhomogeneous differential equation of the first order

$$\frac{d}{d\alpha}\left(\bar{N}(\eta,\varrho)\cdot\bar{\varepsilon}(\alpha,\eta,\varrho)\cdot v(\alpha) f\right)-\bar{N}(\eta,\varrho)\,\bar{\sigma}(\alpha,\eta,\varrho)\cdot v(\alpha) f+Q(\alpha,\eta;\varrho)=0. \tag{7.7}$$

$\bar{\varepsilon}$ and $\bar{\sigma}$ originate through summation of the contributions of the various constituents i of the atmosphere to the effective cross sections

$$\begin{aligned}\bar{N}(\eta,\varrho)\cdot\bar{\varepsilon}(\alpha,\eta,\varrho)&=\sum_i \bar{N}(\eta,\varrho)\,\varepsilon_i(\alpha)\\ \bar{N}(\eta,\varrho)\cdot\bar{\sigma}(\alpha,\eta,\varrho)&=\sum_i \bar{N}_i(\eta,\varrho)\,\sigma_i(\alpha)\\ \bar{N}(\eta,\varrho)&=\sum_i \bar{N}_i(\eta,\varrho).\end{aligned} \tag{7.8}$$

In those regions where the particle loss greatly predominates (Fig. 3.2) over the energy loss, (7.7) has as solution

$$vf=\frac{Q}{\bar{N}\cdot\bar{\sigma}} \quad \text{for} \quad -\frac{d}{d\alpha}\left(\frac{\bar{\varepsilon}}{\bar{\sigma}}Q\right)\ll Q. \tag{7.9}$$

In general, (7.7) can be reduced to quadratures. The obvious limit condition is that f vanishes at sufficiently high energies. Actually, however, this limit may already lie at relatively low energies if the discriminant (4.1) of the Alfven approximation becomes so large that the particles are no longer held effectively captive. This is possible already in the static dipole field. Subsec. 4.3 furnished an estimate of the time scale $\tau_\mu=\eta^2/\langle\Delta^2\eta\rangle$ (4.19) for this effect. With this, the upper limit of vf, in accordance with (7.9), is to be represented by

$$vf=\tau_\mu v Q \quad \text{for} \quad -\frac{d}{d\alpha}\left(\bar{N}\bar{\varepsilon}\tau_\mu v Q\right)\ll Q \tag{7.10}$$

Although this is a very rough method where it would actually be necessary to solve a Fokker-Planck equation, there is so much uncertainty inherent in the coefficients on the one hand and on the other hand they are such steep functions of energy that a correct solution would change only very little in the energy spectrum. Not far below the energies at which the spectrum is interrupted by means of (7.10), the spectrum is no longer influenced by this (cf. subsec. 7.5).

If we assume that the inequality in (7.10) is no longer satisfied with a given accuracy, then the further solution is represented by

$$v f = e^{\int^{x_0} p\,dx'} \cdot \left(\tau_\mu v Q|_{x_0} + \frac{1}{\bar{N}\bar{\varepsilon}} \int_{\alpha}^{x_0} Q e^{-\int^{x_0}_{x'} p\,dx''} dx' \right) \qquad (7.11)$$

with

$$p(\alpha, \eta, \varrho) = \frac{\bar{N}\bar{\sigma} + \frac{1}{\tau_\mu v}}{\bar{N}\bar{\varepsilon}} \qquad (7.12)$$

The proton flux $F_p(\alpha_z, \varrho, \zeta)$ above the energy threshold α_z of the counter with whose rate of count the comparison is to be carried out, reads, according to (2.38),

$$F_p(\alpha_z, \varrho, \zeta) = 4\pi \int_{\alpha_z}^{\infty} \bar{I}(\alpha, \varrho, \zeta)\, d\alpha =$$

$$= \frac{1}{R_e \varrho \sqrt{1 + 3\zeta^2 b^2(\zeta)}} \int_{\eta_{min}(\varrho)}^{\eta_0(\zeta)} \mathscr{F}(\alpha_z, \eta; \varrho)\, w(\eta, \zeta)\, d\eta, \qquad (7.13)$$

with the expression

$$\mathscr{F}(\alpha_z, \eta; \varrho) = \int_{\alpha_z}^{\infty} v(\alpha)\, \bar{I}(\alpha, \eta; \varrho)\, d\alpha, \qquad (7.14)$$

which is intended to show the sequence in which numerical calculation continues [illegible] appropriately, (cf. flow diagram below).

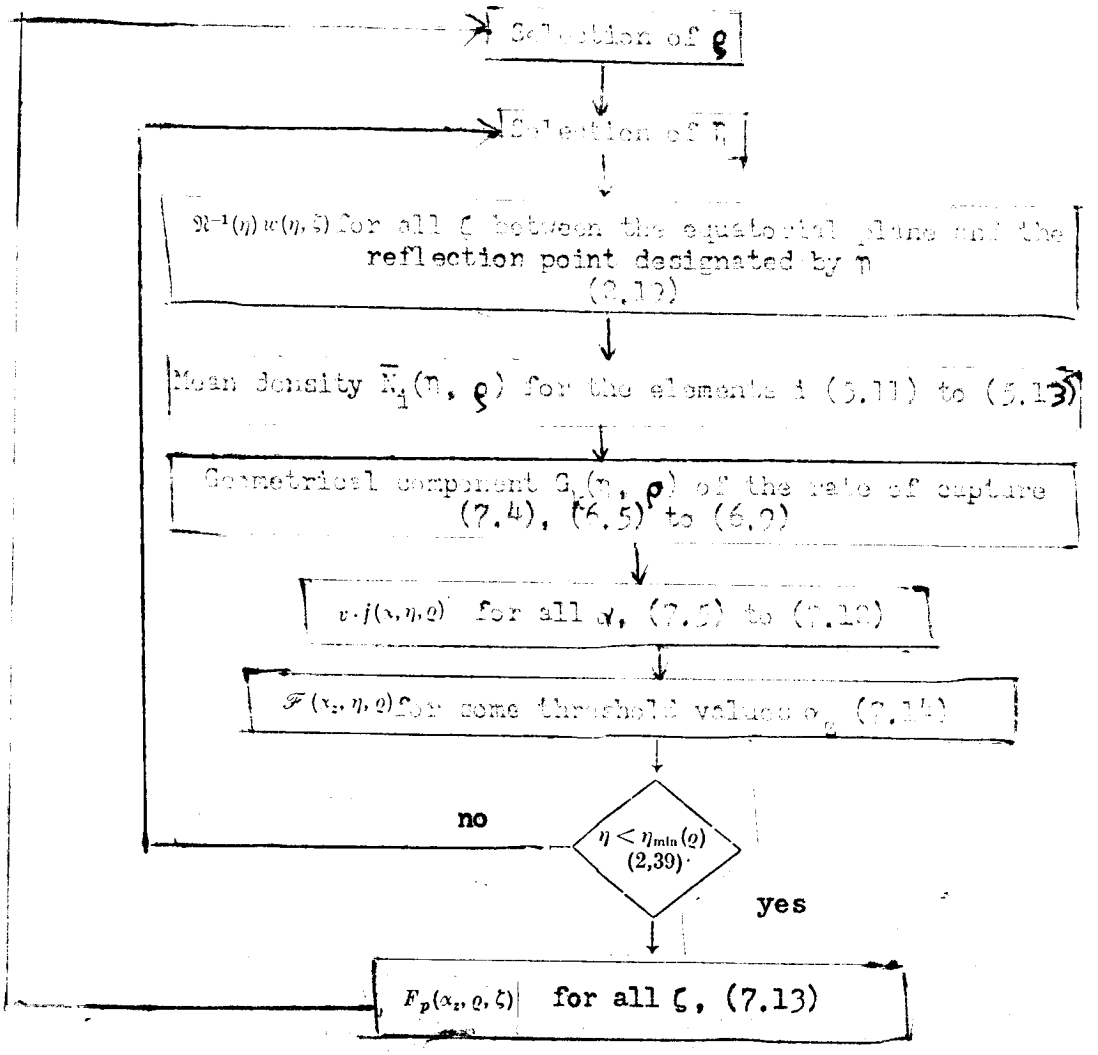

All quadratures were carried out with the Simpson Rule in regard to energy and with the introduction of log α as variable. The step interval was adapted to the increase of density of the atmosphere so that the difference of adjacent values of (7.14) was sufficiently small to permit linear interpretation with a maximum error of about 10 %. Here as in the calculation of the geometric component of the rate of capture where maximum errors also lie around 10 %, we neglected in most cases a shortening of the step interval in consideration of the required time of calculation. All other numerical errors lie far below 10 % so that the maximum error of numerical calculation can be estimated as about 20 %. The main contribution to the inaccuracy of the results lies in deficiencies of the orbital approximation (cf. sec. 5) which leads to the values of $\bar{N}(\eta, \varrho)$.

Calculation was carried out on the electronic computer G-2 of the Max-Planck Institute for Physics and Astrophysics. The construction of the program is outlined roughly in the above Flux diagram.

2.4 - Proton Distribution and Atmosphere

Prerequisite for the comparison of theoretical proton distribution with the measured data is the certainty that the latter can actually be ascribed to the protons. Since the Geiger counters utilized respond, in addition to protons, also to electrons and, with a sensitivity reduced by a factor of $< 10^5$, to their radiative deceleration, this question must be answered by the analysis of measurements independent of the latter two. Pizzella, McIlwain and Van Allen (1962-a), arrive, in regard to the Geiger counter of type Anton-302 in Explorer VII (very similar to those of Explorer I and IV and Pioneer III) in this manner at the conclusion that for $\rho \leq 1.8$ -- the range initially investigated here -- the radiative deceleration of electrons below a threshold value (1.1 MeV) for direct penetration does not furnish any appreciable contribution to the count rate. Nothing very certain is known of the electrons above 1 MeV. The measurements of Holly and Johnson (1961) do indicate a steep decrease of the electron spectrum above 450 keV but the measurements are not reliable enough to furnish a decision on the absolute values at a few MeV. That an origin from neutron decay cannot be expected to furnish any appreciable intensities with E > 780 keV, also does not lead to a decision as long as there is no greater certainty in regard to this point than at the present. However, we may enter on the positive side that the identification of the particles measured by Geiger counters in the vicinity of the earth is consistent both with the indications of a triple-coincidence counter of Fair et al., (1961) for protons > 75 MeV and in ionization chambers (Van Allen et al., 1959; Huffman et al., 1960) as well as with the protons definitely demonstrated in

nuclear emulsions (Freden, White, 1959; Armstrong et al., 1961; Naugle, Kniffen, 1961). The proton flux which cannot be entirely accurately derived from the nuclear-plate data because of the integration in time over the orbit, concords with a factor of two with the Geiger-counter data. Moreover, it is possible to indicate upper limits for the electron flux from the particle tracks; Freden and White (1959) find an upper limit of 1% of the proton flux for electrons with $E > 12$ MeV. On the basis of all the foregoing, there can be no objections to regarding the count rate of the Geiger counters as an indication of the proton flux.

The calculation of proton distribution is essentially based on the measurements with Explorer IV (Van Allen et al., 1959) which were plotted by McIlwain (1961) in the natural coordinates B, $L(\hat{=} \rho)$. They were obtained at an altitude of 2,200 km in the summer of 1959. The conversion of the count rate to proton flux is made by division with the geometrical factor 0.54 cm^2 and the energy threshold is about 30 MeV.

Of the knowledge of the atmosphere, we utilize only that initially N_2, then O($\approx$ 250 km) (see, e.g., Johnson, 1961), and beyond this He ($\approx$ 1,000 km) (Nicolet, 1961) predominates above the homosphere. Hydrogen should not begin to dominate until about 3,000 km and is probably already strongly ionized (Hanson, 1962). The effective cross-sections of N, O, He for energy loss in nuclear processes differ from each other only by a constant factor nearly equal for both processes (Fig. 3.2)

$$\varkappa_N = \frac{\varepsilon_N}{\varepsilon_0} \approx \frac{\sigma_N}{\sigma_0} \approx 0{,}88; \quad \varkappa_{He} = \frac{\varepsilon_{He}}{\varepsilon_0} \approx \frac{\sigma_{He}}{\sigma_0} \approx 0{,}28. \tag{7.15}$$

This simplifies (7.8); the energy spectrum becomes independent of composition and we can calculate with the single effective density

$$\bar{N}_{eff} = \sum_i \varkappa_i N_i \tag{7.16}$$

by referencing ourselves, for example, to the effective cross-section of oxygen.

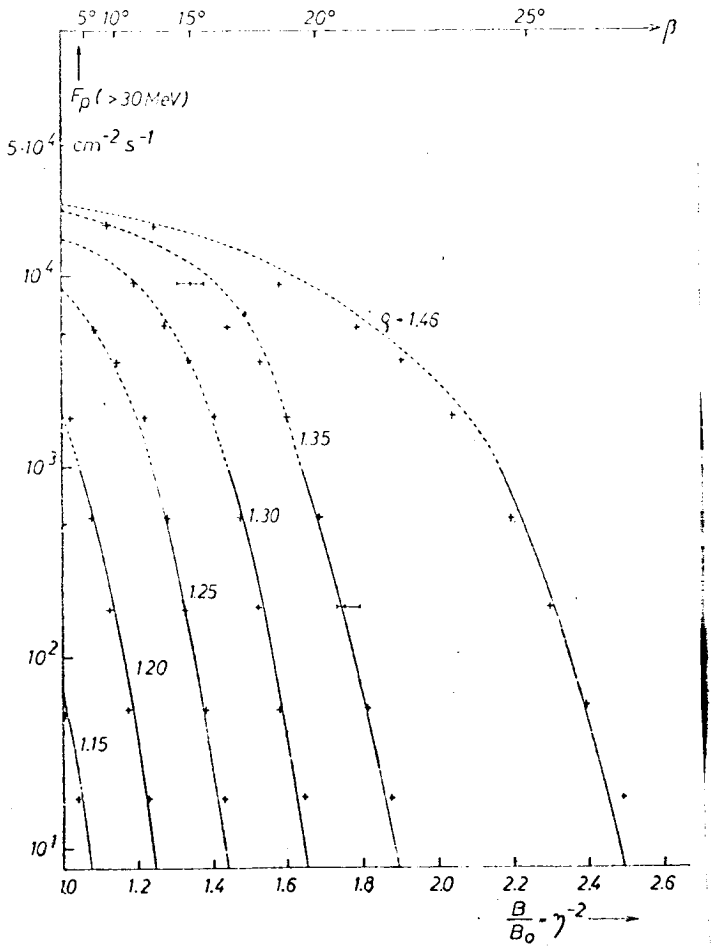

Fig. 7.5 - Proton distribution along fixed values of ϱ on the basis of Geiger-counter data (E > 31 MeV) of Explorer IV (McIlwain, 1961); at ϱ = 1.35, the scatter range of the data is indicated in two cases. The solid curves are approximations from the model calculations with a density profile ① of the atmosphere in Fig. 7.6 and the neutron flux according to Hess (fig. 7.1) and/or the density profile ② and the neutron intensity designated as "corrected" in Fig. 7.1. The broken-line curve also comprises the continuation of the density profile ② and the non-adiabatic losses in Table 7.1.

The formulation (5.13) for the trace of altitude of density is independent of latitude in agreement with observation. Consequently, if the model outlined so far is realistic and, in particular, if the method of calculation of the neutron density and the magnetic field data on which it is based are sufficiently

an atmospheric model determined exclusively through adaptation of theoretical and measured proton distribution approximately along $\rho = 1.5$, should provide concordance also on all invariant surfaces lying farther inward. This is true only for the first steep increase of radiation which shall therefore be considered initially by itself.

The approximation of the measured data $F_p(> 30\ \text{MeV}) < 10^3\ \text{cm}^{-2}\text{s}^{-1}$ through the calculated stationary distribution (solid-line curves) represented in fig. 7.5 was obtained with the following model of density:

$$\begin{aligned} N_{N_2} &= 3{,}4 \cdot 10^8 \cdot e^{-\frac{s-s_0}{0{,}0053}}\ \text{cm}^{-3} \\ N_O &= 3{,}6 \cdot 10^8 \cdot e^{-\frac{s-s_0}{0{,}012}}\ \text{cm}^{-3} \\ s_0 &= 1{,}0385 \triangleq 245\ \text{km height.} \end{aligned} \tag{7.17}$$

Only three of the four constants in (7.17) were actually determined through adaptation to the measured data (within about $\pm$ 10%). The scale height of the N_2-distribution cannot be determined with equal certainty because satisfactory measuring points no longer exist (the background given by cosmic radiation already lies too close) in the range of intensity $F_p(>30\ \text{MeV}) < 10\ \text{cm}^{-2}\,\text{s}^{-1}$, which suffers its losses primarily in the N_2-layer and because, moreover, the scale height is so low that the deficiencies in the orbital representation utilized no longer permit a very reliable calculation of the orbital mean of density. It has therefore been taken from the atmospheric model with which (7.17) will be compared below.

Three conclusions may be drawn from the calculations at this point: the satisfactory consistency of the curves for different values of ρ testifies to the usability of the data and of the method for taking the mean atmospheric density over the particle motion and for the fact that the collisions with the atmosphere determine the lower limit of the radiation belt in the manner imagined. The theoretical curves all lie within the range of scatter of the measured data (the latter is indicated in fig. 7.5 for two cases). The

statement on the significance of the collisions is reinforced if we compare the trace of density (7.17) with that determined by Kallmann-Bijl (1963) from many satellite and rocket data which is approximately characteristic for 1959. Although (7.17) (curve (1) in fig. 7.6) lies appreciably below these density values, the correlation of (7.17) with the values between 200 and 300 km, i.e., a multiplication with a factor of 6.5, brings the model derived here exactly to the point where the mean over the diurnal cycle of density should lie (curve (2)). Consequently, the third and most important result reads: <u>the proton replenishment in the energy range > 30 MeV must be a total greater by a factor of about 6.5 than corresponds to the intensity of the flux of albedo neutrons derived by Hess and associates (1961).</u>

Let us accept this finding initially without discussion and investigate the results which can be derived in regard to the losses at higher altitude after the determination of the proton-source intensity so made, provided that it varies as little with altitude as in the decay of the albedo neutrons. It is now shown that the assumption of pure collision losses, i.e., a loss rate dependent only on s, does not lead to consistent models above $F_p(> 30\ \text{MeV}) = 10^3\ \text{cm}^{-2}\text{s}^{-1}$. A distribution of density obtained perhaps through adaptation along $\varrho = 1.5$, always furnishes excessive losses at lower values of ϱ. The further we progress in ρ, the more pronounced is this behavior. The explanation for this is seen in the fact that other losses, i.e., <u>loss processes</u> increasing with ρ, become superposed on the collision losses in the altitude range above about 1,000 km. This apparently concerns processes in the magnetic field.

In order to investigate the ratio of the two loss mechanisms in the zone of transition somewhat more in detail, let us select here the following simple procedure. To the atm. density $\bar{N}(\rho, \varrho)$ which results from model (7.17) multiplied by 6.5, let us add an imaginary density $\bar{N}_{\text{imag}}(\rho)$ so that the measured

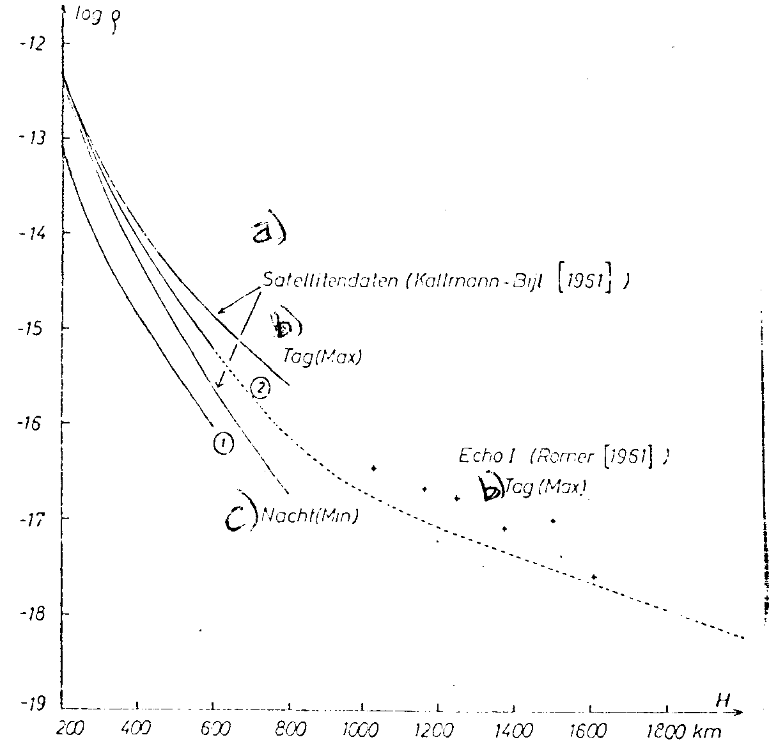

Fig. 7.6 - Derived density profiles (cf. Fig. 7.5) and measured data from the deceleration of artificial satellites.
Legend: a = satellite data ...; b = day (maximum); c = night (minimum).

intensity of distribution is represented as satisfactorily as possible with an albedo neutron flux also multiplied by 6.5. $\overline{N}_{equiv}(\rho)$ represents the non-adiabatic losses without consideration of their probably totally different dependence on energy and their different action on distribution. If we add to this procedure the requirement (which is reasonable according to sec. 4) that $\overline{N}_{equiv}$ can only be a function monotonely increasingly with ρ, we then obtain for $1.2 < \rho < 1.4$ appreciably higher particle fluxes in the vicinity of the Equator than those measured. This result is interpreted as an indication of the presence of a lighter component of the atmosphere, i.e., helium, occurring at altitude 1,000 km (Nicolet, 19[illegible]). Hydrogen is eliminated because the required density is greater by two powers of 10 than is compatible with the [illegible] measurements of absorption of [illegible] (19[illegible]). [illegible] model (7.17) [illegible] provided ([illegible] by 6.5 [illegible]

assumption of approximately constant exospheric temperature) with a third component with the quadruple scale height of oxygen (T = const., i.e., $h_{He}/h_0 \approx m_0/m_{He} = 4$) and the absolute values of the latter determined by the procedure just outlined, i.e., under inclusion of the non-adiabatic losses. This complements the curves in fig. 7.5 and 7.6 by the broken-line parts. The whole atmospheric model now reads:

$$\begin{aligned} N_{N_2} &= 2{,}2 \cdot 10^9 \, e^{-\frac{s-s_0}{0{,}0053}} \text{ cm}^{-3} \\ N_O &= 2{,}35 \cdot 10^9 \, e^{-\frac{s-s_0}{0{,}012}} \text{ cm}^{-3} \\ N_{He} &= 2{,}9 \cdot 10^7 \, e^{-\frac{s-s_0}{0{,}018}} \text{ cm}^{-3} \\ s_0 &= 1{,}0385. \end{aligned} \tag{7.18}$$

The ratio of the collision losses in the vicinity of the Equator ($\eta \approx 1$) to the non-adiabatic losses measured by the equivalent oxygen density in the range > 30 MeV, can be derived from Table 7.1.

Table 7.1

ϱ	$\bar{N}_{\varrho\,\text{äquiv}}(\varrho)[\text{cm}^{-3}]$	$\varkappa_{He} \cdot \bar{N}_{He}(\eta, \varrho)[\text{cm}^{-3}]$
1,25	$< 10^4$	$8{,}0 \cdot 10^4$
1,30	$2{,}5 \cdot 10^4$	$2{,}8 \cdot 10^4$
1,35	$3{,}8 \cdot 10^4$	$1{,}0 \cdot 10^4$
1,46	$7{,}4 \cdot 10^4$	$1{,}25 \cdot 10^3$

The procedure described which leads to this division of the two loss processes in the area of transition, is obviously not very credible because it is oriented only on the differential equation which describes the collision losses. In the absence of better information on the complex processes with which the disturbances of the magnetic field act on distribution, however, it is not possible at the moment and within this energy range to arrive at a better interpretation of the measured data. However, we can state that, between $\varrho = 1.25$ and 1.4 in the vicinity of the Equator and energies > 30 MeV, the non-adiabatic losses substitute themselves for the collisions in the determination of distribution and can regard the time scale contained in Table 7.1 as

approximately characteristic. (It is of minor importance that we here calculate with an albedo neutron flux increased by a factor of 6,5 although this manner of replenishment is by no means confirmed (cf. subsec. 7.5). It is supported merely by the assumption that the proton-source intensity determined in the foregoing changes only very little between ρ = 1.25 and 1.5.)

The helium density in (7.18) must consequently be regarded as rather uncertain. Interesting is a comparison with the density determinations from the orbital data of Echo I (Roemer, 1961) which are valid for the diurnal maximum (Crosses in fig. 7.6). If we assume a range of variation with a factor of 5 to 7 for the day-night variation at these altitudes in agreement with the model calculations of Harris and Priester (1962), the density (7.18) then has the trace to be expected from the diurnal mean. However, there is still some disagreement in the interpretation of the data from Echo I so that no reliable conclusions can be drawn from this concordance.

7.5 - Albedo Neutrons and Proton Spectrum

The model calculations carried out permit a relatively accurate determination of the proton-source intensity at the lower limit of the inner radiation belt in the energy range above 30 MeV. The knowledge of the atmosphere and of the particle orbits in the terrestrial magnetic field is sufficiently satisfactory to enable a credible calculation of the loss rate by collisions. The satisfactory qualitative consistency of theoretical and measured distribution was regarded in the last Section as confirmation for the usability in principle of the model which calculates with the temporarily constant and spatially little variable proton replenishment and pure collision losses in the vicinity of the earth. The identification of the measured particles with protons is a logical necessity at least within a factor of 2.

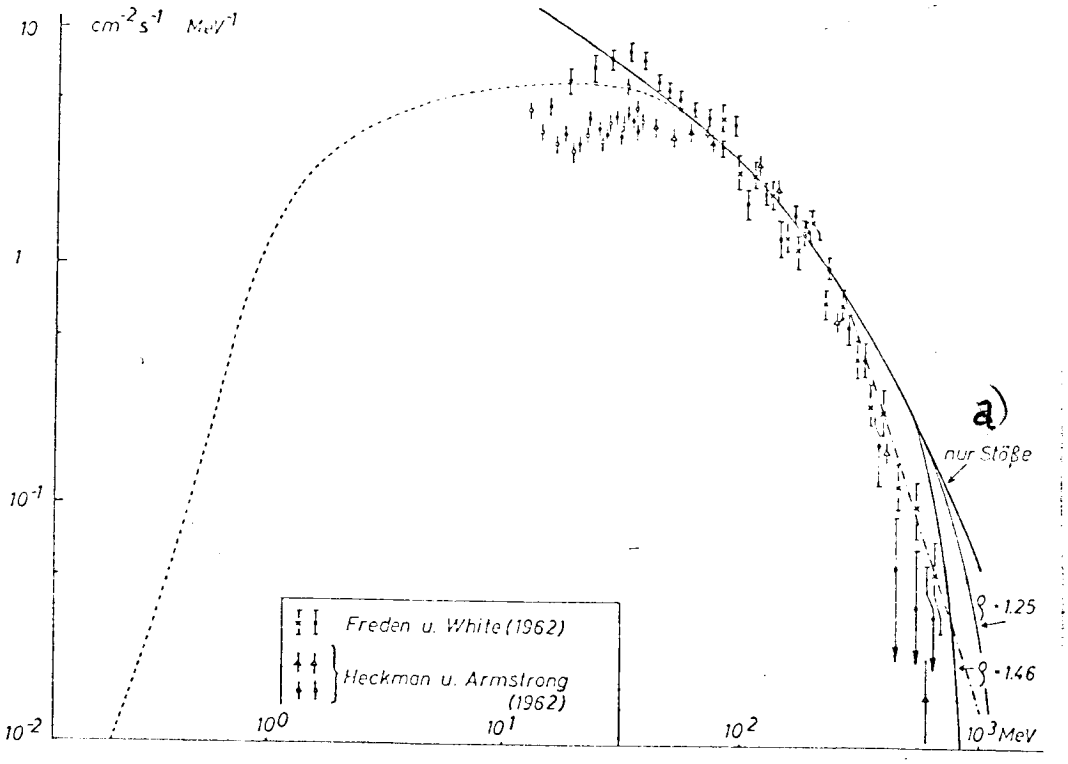

Fig. 7.7 - Proton spectrum obtained with nuclear-emulsion plates at different but very similar rocket orbits between $\varrho = 1.25$ and 1.5 and connected to each other at 100 MeV. The solid-line curves show the theoretical spectrum for a neutron spectrum according to Hess (Fig. 7.1) under exclusive consideration of the collisions and/or inclusion of the impairment of μ in the static dipole field at high energies (curves $\varrho = 1.46$, 1.25). The broken-line spectrum is based on the broken-line spectrum of Fig. 7.1 and shows the effect of charge conversion below 1 MeV. The dotted line indicates the impairment of the adiabatic invariant Φ.
Legend: a = only collisions.

If the protons are furnished primarily by the decay of the albedo neutrons, then their density of flux in the energy range E > MeV must be, in accordance with subsection 7.4, greater by a factor of about 6.5 than was determined by Hess et al., (1961) theoretically, i.e., lie in the neighborhood of the estimates of Singer (1958, b). The measurements of Bame, et al., (1962) furnished; however, at lower energies (10 MeV and less) only a third of the flux density according to Hess so that, by retaining the form of the theoretical neutron-energy spectrum at high energies, a discrepancy with a

factor of 20 would occur.

There are two issues from this situation. One lies in the possibility which cannot be excluded, of a further still unknown replenishment mechanism which far exceeds the neutron decay in effectiveness, and the other lies in the change of the form of the energy spectrum of the albedo neutrons which would then have to have a trace between 1 and 30 MeV appreciably flatter than that calculated by Hess. Since we lack at the present time an acceptable concept in regard to the first possibility, let us here draw merely the consequences from the second.

The energy spectrum of the protons in the region investigated so far is rather well known between 15 and 600 MeV through the nuclear-emulsion experiments of Freden and White (1962) and Heckman and Armstrong (1962). The measured points combined in fig. 7.7 of the two groups of authors were obtained in part from the same and in part from very similar rocket orbits (apogee: $\varrho = 1.46$; $\zeta = 0.413$). They were conjoined in the neighborhood of 100 MeV.

For the question here discussed, only the data below 100 MeV are of significance. The solid-line curve in fig. 7.7 -- conjoined to the measuring points without consideration of the absolute amount (!) at 100 MeV -- shows the theoretical proton spectrum which results on the basis of the Hess albedo-neutron spectrum (fig. 7.1) and pure collision losses. Between 40 and 200 MeV, it can be brought satisfactorily into agreement with the measurements; however, with decreasing energy, it deviates perceptibly from the measured data which are here unfortunately not very consistent. In any event, it becomes clear that it is less steep below 30 MeV than it should be in accordance with the second interpretation of the higher proton-source intensity. If we increase the neutrons spectrum of Hess above 20 MeV by a factor of 7 and conjoin it below this amount completely schematically (as shown in the broken-line curve

of fig. 7.1) to the original spectrum at about 3 MeV, we then obtain as spectrum of proton equilibrium the broken-line curve in fig. 7.7. (The steep drop below 1 MeV is a consequence of the reversal of charge; cf. fig. 3.2). Since according to the description of the experiments, there is no choice between the data of Freden and White (1962) and of Heckman and Armstrong (1962) within the energy range of 15 to 40 MeV, an even greater flattening of the spectrum such as should be required in conjunction with the neutron measurements of Bame, is entirely within the range of possibility.

Does the increase of the total neutron flux which would follow from the changes of form of the energy spectrum discussed, still concord with the measured data? Since the high energies furnish a relatively small contribution to the total flux, we find, for example, the change of the Hess spectrum indicated by the broken-line curve in fig. 7.1, especially in view of the counter sensitivity highly decreasing with increasing energy, still within the limit of measurement accuracy of the experiment of Hess and Starnes (1960). This is different for the measurements of Bame, et al., which -- as demonstrated in subsec. 7.2 -- must be regarded as the most reliable neutron measurements outside of the dense atmosphere. A combination of these data at 1 MeV with the required neutron flux at 70 MeV by an exponential function (broken line in fig. 7.1) produces an increase of the total flux by a factor of 2.2. Such a change should have been observed in the rather different dimensioning of the neutron counters.

Consequently, there results here a serious objection against an increase of the neutron flux at high energies which is, however, not as yet compelling. It is entirely possible to conceive of forms of the energy spectrum between 1 and 70 MeV which will appreciably reduce this discrepancy and still can be brought into concordance with the proton spectrum. A minimum in the neutron

spectrum at 20 MeV, as discussed by Freden and White (1962), belongs among these possibilities. For the definite clarification of this question so very important for the understanding of the inner radiation belt, an extension of the proton spectrum down to 1 MeV, in addition to further reliable neutron measurements, will be of considerable benefit. From this, we could then derive the requirements for an appurtenant neutron spectrum and subject the consistency of the latter with the count rates of the various neutron counters of Bame to detailed examination.

7.6 - Non-Adiabatic Losses

Pointers to the action of non-adiabatic effects involve the two factors of spatial distribution of the integral proton intensity (cf. subsec. 7.4) and of the form of their energy spectrum. The cancellation of the adiabatic invariance of μ cuts off ["Abschneiden"] the spectrum (cf. Table 4.1 and 4.2). The theoretical expectations of this effect occurring in the static dipole field according to subsec. 4.3 in the consideration (7.10) illustrate the two parts designated by $\varrho = 1.25$ and $\varrho = 1.46$ of the theoretical proton spectrum (fig. 7.7) which otherwise calculates only with collision losses. (Between $\varrho = 1.46$ and $\varrho = 1.25$, the rockets moved approximately on lines of equal proton intensity.) Only slightly below this curve, the experimental data also show a steep drop of intensity. In view of the uncertainties of the theory and the crudity of the method (7.10), the concordance is rather satisfactory but far removed from a compelling confirmation. We can only conclude this much: the critical discriminant defined in subsec. 4.3 which was then determined as $d_k = 0.165$, is $(|\beta| < 25°) \gtrsim 0{,}13$ at these latitudes.

It is of interest to make the comparison with the values of d_k which are obtained if we regard -- as was done by Singer -- as a consequence of this effect the repeatedly measured drop of the penetrating component in the

neighborhood of $\rho = 2$ which is apparently a function of the energy threshold of the measuring instrument (and of time). By correlation with the Pioneer III data ($E > 30$ MeV), Singer (1959) found $d_k = 0.05$ and, with the Explorer VI data ($E > 100$ MeV) found $d_k = 0.09$ (Lenchek, Singer, 1962-b). The first value is incompatible with the energy spectrum of fig. 7.7; however, the second, determined in contrast to the first at mean latitudes ($|\beta| > 30°$), would be compatible with the estimate found here if we assume a decrease of the critical discriminant beyond higher reflection-point latitudes in accordance with the findings of Gall (1962).

We might also see in the cut-off of the spectrum at 700 MeV an expression of the impairment of μ through time-dependent disturbances of the magnetic field. Their frequency spectrum should then extend to at least $\omega_{max} \approx 19 s^{-1}$ according to (4.9). This would have as further consequence that the upper limit of energy of the possibility of impairment of J at $\rho = 1.4$ would be displaced as far as about 35 MeV. The equivalent density of the loss-time scale to be expected in accordance with sub-section 4.2 amounts to about $2 \cdot 10^5$ cm^{-3} at this energy so that these processes could be perfectly well expressed in the energy spectrum of fig. 7.7. It is therefore not impossible that the flattening of the spectrum below 30 MeV has its reason in this. The interpretation of this phenomenon discussed in the preceding subsection which was to serve for an alleviation of the difficulties with the albedo hypothesis, thus loses some of its force of conviction. However, since it is not possible to arrive at a decision in favor of one of the possibilities of explanation discussed in regard to this point of the cut-off at 700 MeV from the presently available observational material, further measurements of the energy spectrum as a function of altitude are urgently necessary.

However, we may conclude from these considerations in any event that the protons, at low values of ρ, are not threatened at least between 30 and 700

MeV by an appreciable disturbance of J or μ. On the other hand, however, the interpretation of the proton distribution with E > 30 MeV compelled us to assume non-adiabatic loss processes already at $\varsigma \approx 1.3$. Consequently, there remains here only an <u>insufficient invariance</u> of $\frac{1}{2}$ which was actually to be expected for these energies according to fig. 4.2 and whose estimated time scale entirely corresponds -- on the basis of the equivalent densities in Table 4.1 ($E \gtrsim 100$ MeV) -- to the requirements on the part of observation (Table 7.1).

The vulnerability of $\frac{1}{2}$ increases, according to subsec. 4.2, with the drift frequency, i.e., with energy; a predominance of this process over the collision losses should therefore be linked to a <u>steep rise ["Aufsteilen"] of the energy spectrum</u> of the protons. This can be demonstrated already from the measurements discussed so far. If we compare the indications of the two Geiger counters of Explorer IV with the energy thresholds at 31 and 43 MeV with the help of the simple formulation

$$F_p(>E) \sim E^{-\gamma}$$

we obtain, at equal flux densities, i.e., approximately equal life span, and increasing ϱ, higher values of γ (Table 7.2).

Table 7.2

ϱ	B [Gauss]	$F_p(>30$ MeV) (cm^{-2} s^{-1}]	γ
1,2	0,184	$1{,}8 \cdot 10^3$	1,4
1,6	0,19	$2{,}4 \cdot 10^3$	2,2
1,7	0,16	$3{,}0 \cdot 10^3$	2,8
1,8	0,183	$1{,}16 \cdot 10^3$	3,6

Outside of $\varrho \approx 1.7$, we must see in this, however, primarily an expression of an appreciably steeper proton-source spectrum because the primary particles observed after large flares on the sun above $|\beta| \approx 55°$ ($\cos^{-1} 55° = 1{,}82$) had a much steeper spectrum than the galactic cosmic radiation (see, e.g., B. Winkler, 1962). This should be correspondingly true for their albedo neutrons which

probably have an appreciable share in the proton replenishment at $\varrho > 1.7$ (Lenchek, 1962). (The Polar-Cap absorptions which are a consequence of the incidence of high-energetic protons in the atmosphere, are generally restricted to $|\beta| > 62°$ (Rose, Ziauddin, 1962).) The limit at $\varrho = 1.7$ can further be seen very clearly in the proton spectra of Naugle and Kniffen (1962). Within this limit and at greater altitude, i.e., specifically in the center of the inner radiation belt ($\varrho \approx 1.5$ $\beta \approx 0°$), the steep rise of the spectrum should be most purely pronounced by reason of the non-adiabatic processes. This makes measurements in this region extraordinarily desirable.

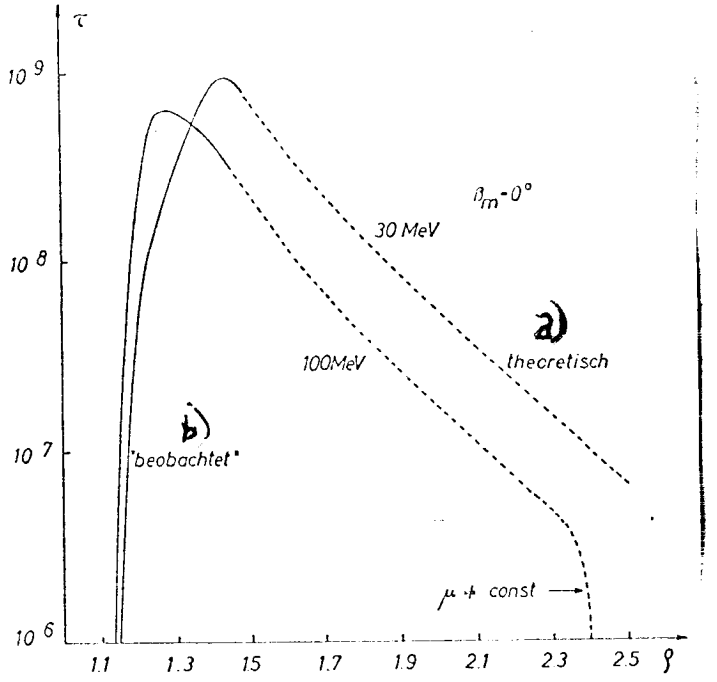

Fig. 7.8 - Life span of protons with E = 30 and 100 MeV in the vicinity of the Equator. The solid-line curves are derived from the approximation of the measured data in Fig. 7.5 and the broken-line curves are extrapolations on the basis of the theory in subsec. 4.2. The maxima designate the equality of collision losses and the impairment of τ.
Legend: a = theoretical; b = observed.

Even at the small values of ϱ ($1.25 < \varrho < 1.46$) where the proton spectrum of fig. 7.7 was obtained, this effect seems to be hinted. According to Table 7.1, the equivalent density of the non-adiabatic losses found empirically is smaller by 1 power of 10 in the energy range E > 30 MeV than the mean

atmospheric density of $4 \cdot 10^5 cm^{-3}$ belonging to the particle orbits encompassed. Since the time scale of the impairment of Φ decreases, however, with energy in contrast to the collision times, we may expect, according to Table 4.1, an equal effectiveness of the two processes at about 300 MeV and, beyond this, a steeper drop of the spectrum in exact concordance with the measurements. If we calculate, in spite of the doubts which have appeared in the preceding subsection, with the replenishment through the albedo neutrons of cosmic radiation whose energy spectrum must be approximately E^{-2} according to subsection 7.2, and take into account the life-span in relation to disturbances of Φ according to (4.10), there results an approximate equilibrium spectrum E^{-3} which is indicated in the dotted line in fig. 7.7. This part of the spectrum thus finds a new explanation (Freden, White, 1962; Haerendel, 1962; Lenchek, Singer, 1962-b) which, moreover, makes it appear entirely compatible with the albedo hypothesis.

In order to convert the equivalent density of the non-adiabatic losses (derived in subsection 7.4 with the aid of model calculations integrally for energies > 30 MeV) into life spans, we must take into account the increasing steepness of the spectrum with altitude. The assumption of the validity of the albedo hypothesis then leads from Table 7.1 to the life spans in the vicinity of the Equatorial plane designated in fig. 7.8 by "observed" ["beobachtet"]. The values at $\rho = 1.46$ have been extrapolated with the formulation (4.10), i.e., $\tau_\Phi \sim \rho^{-9}$, to higher values of ρ and, in addition, there has been indicated the attainment of the region of $\omega \neq$ const., at $\rho = 2.4$ in accordance with fig. 4.2. The ρ-dependence of τ_Φ was derived in subsec. 4.2 under highly simplifying assumptions; it may well be appreciably different from (4.10). It should be kept in mind specifically that the introduction of τ_Φ avoids the solution of a differential equation of the second order of the type of the Fokker-Planck Equation.

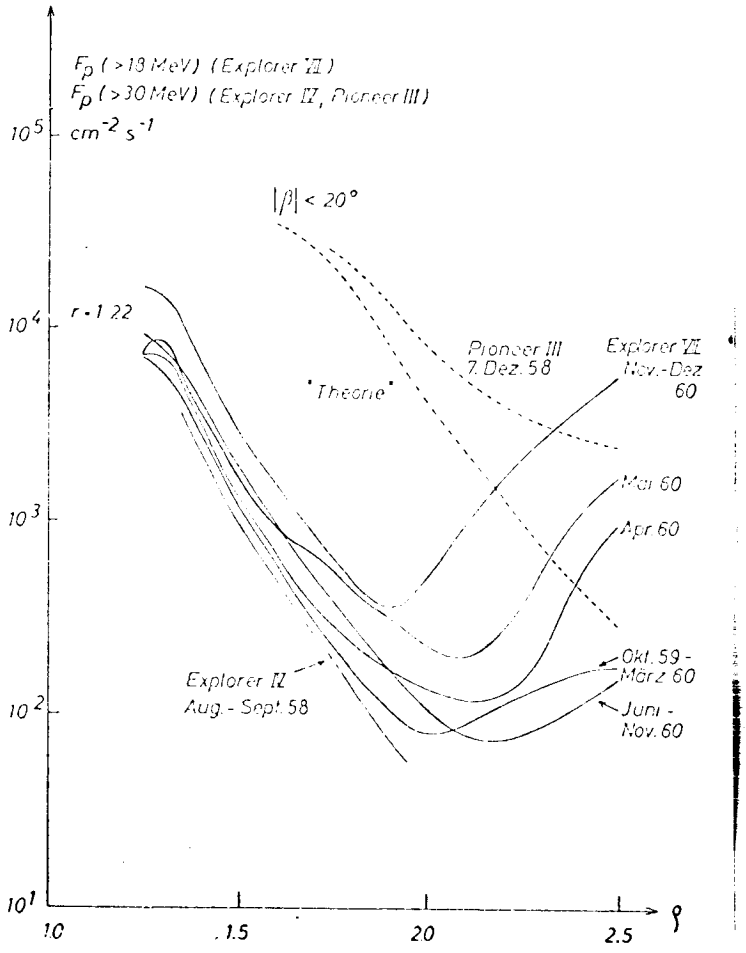

Fig. 7.9 - **Observed flux densities above 18 and/or 30 MeV; Explorer IV and VII for $r = \varrho(1 - \zeta^2) = 1.22$ (Pizzela et al., 1962-a); Pioneer III in the vicinity of the Equator (Van Allen, Frank, 1959-a) in comparison with the theoretical expectations of the broken-line albedo-neutron flux in Fig. 7.1 and the life spans from Fig. 7.8.**

Fig. 7.9 indicates the distribution of equilibrium obtained in the vicinity of the Equator at $\varrho > 1.5$ if we continue to calculate with the proton-source intensity Q determined in subsec. 7.4 from fig. 7.8 and the simple formulation $f \approx \tau_p \cdot Q$. The result, designated by "theory", lies as far as $\varrho \approx 2$ very close to the Pioneer III measurements which were obtained at low altitudes. The deviation at $\varrho > 2$ can be understood by either an increased proton replenishment through solar corpuscular radiation or through the superposition of the electrons in the count rate; it is difficult here to make a decision. The same is true for the Explorer IV and VII data which are plotted, in contrast

to the foregoing, not at constant altitudes but for

$$r = \varrho \cos^2\beta = 1{,}22$$

(in the sense of the projection of the terrestrial magnetic field on a dipole field discussed in subsec. 2.3 and sec. 5) and show the same dependence on ϱ as the theoretical curve (the deviation from intensity is explained by the low altitude).

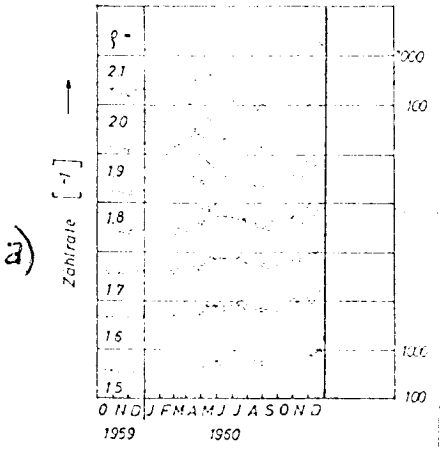

Fig. 7.10 - Counting rate of Geiger counter (E > 18 MeV) in Explorer VII between October 1959 and December 1962 according to Pizzela et al., 1962-a for r = 1.22 and a few values of ϱ.
Legend: a = counting rate.

Above ϱ = 1.9, the Explorer VII data show a strong dependence on time which is plotted in a different manner in fig. 7.10. It is here possible, from the decrease of intensity of the abrupt rise during the solar proton phenomena in May 1960, to read off a life span of about two months at ϱ = 2. This value is only very little smaller than the life span of a 100-MeV proton extrapolated in fig. 7.8, which is moreover true for the vicinity of the Equator, i.e., for a larger distance from the dense atmosphere. In view of the definition of the life spans and the uncertainties in their derivation which can be understood only as order of magnitude, we can speak of a rather satisfactory concordance so that nothing opposes the assumption to see in these measured data the decrease in time of the protons above 18 MeV after a reinforced injection by albedo neutrons of the solar corpuscular radiation. Since the total number of particles incident in such a proton phenomenon corresponds to the integral of the stationary cosmic radiation extending over several months to several years, the increases of radiation measured would then become entirely understandable as a consequence of the greatly increased

albedo-neutron flux in connection with this. Later investigations will have to show whether the measured data of fig. 7.10 may justifiably be ascribed to protons or whether this concerns, as is believed by the authors of these measurements (Pizzela et al., 1962-b), electrons for which, however, no compelling argument exists on the basis of the experiment.

7.7 - Variations in Time

The analysis of the observations carried out in the foregoing took place on a model independent of time for the conservation of the proton belt. However, such a manner of description is possible only if the life span of the particles is either very large or very small in relation to the periods occurring in replenishment and loss. Since this prerequisite is not satisfied, throughout we must consequently investigate to what extent the findings of the earlier sections are affected by this. Beyond this, an enlargement of the conception employed so far will be shown to be necessary.

Three groups of variations in time are of importance for the proton belt -- as far as we can see now --:

1. In replenishment,
   a) The eleven-year variation of cosmic radiation, and
   b) The occasional irruption of solar particles at high magnetic latitudes;
2. In the collision losses,
   a) The diurnal variation of atmospheric density, and
   b) Its 11-year variation

(To this should be added the semi-annual period and the aperiodic variations correlated to geomagnetic disturbances which are neglected because of their relatively small amplitude);

3. In the non-adiabatic effects,
   the geomagnetic storms.

Following here also the restriction expressed in the title of this paper, let us initially disregard 1 - (b), i.e., consider the region $\rho < 1.7$. Here again a division into two parts must be made depending on whether collisions or non-adiabatic effects determine the losses. Only the first case is comprised in the model calculations of subsec. 7.4 and it shall be the start of our critique.

A comparison of (2.25) with fig. 3.2 shows that a density $\bar{N}_{eff} > 10^{8}\ cm^{-3}$ is still necessary at 1 MeV in order to make the life span perceptibly shorter than the drift period during which we take the mean over the diurnal course of atmospheric density. However, here the proton-flux densities on the one hand and the amplitude of the diurnal variation are already so small that there is no hope for a measurable diurnal effect. There consequently remains in the vicinity of the earth only the 11-year variation which amounts, both on the part of the losses and of the replenishment, to an increase of proton intensity in relation to the sun-spot minimum. Concerning the latter, conditions are not uniform because not all life-spans are small in relation to 11 years. In one range, approximately characterized by $F_p(> 30\ MeV) < 10^{3} cm^{-2} s^{-1}$ in which the life span of a 30-MeV proton is less than six months, we obtain a description of the instantaneous distribution in a usable approximation when utilizing the stationary model. The correlation of the proton measures of 1958 carried out in subsec. 7.4, with the density measurements of 1958/59 for the determination of the proton-source intensity which rests precisely on flux-density values $F_p(> 30\ MeV) < 10^{3} cm^{-2} s^{-1}$ is consequently permissible. However, if we then derive, starting from the assumption that the source intensity does not vary greatly with altitude as in the case of the albedo neutrons, life spans and a distribution of atmospheric density for greater altitudes, we must then keep in mind that the findings approach the mean over the 11-year period. It is

therefore possible that the density in 1958 above about 600 km was greater than appears from fig. 7.6. According to the calculations of Harris and Priester (1962) and the findings of King-Hele and Walker (1961), no more than a factor of 4 needs to be expected for this deviation.

Even if we keep in mind the correction just discussed when interpreting the density profile in fig. 7.6, the stationary model with a density dependent only on distances obviously still remains unsuitable for the description of the real distribution because the density value lying between the instantaneous value and the temporal mean which enters at a point s into the life span, depends precisely on the latter and consequently on the energy and the probability of locus at this altitude. The consequently resulting deviation of a distribution calculated with a stationary model as against the real distribution should consist in the fact that the calculated values in the area of transition from short life span to one comparable to 11 years, lie below the measured values with increasing ϱ and increasing energy.

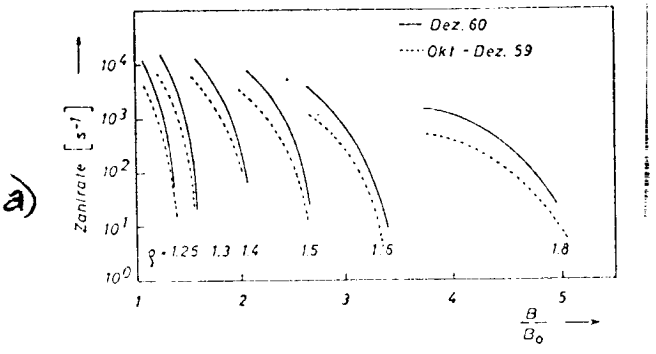

Fig. 7.11 - Counting rate (E > 13 MeV) of Explorer VII along some invariant surfaces from the end of 1958 and from December 1960 according to Pizzella et al., 1962-a.
Legend: a - counting rate.

Actually, the contrary was noted in both cases and interpreted as the consequence of a superposition of a non-linkable effect appreciably increasing with ϱ and with energy. The result of this consideration is therefore that the

neglect of time-dependence does not in any way undercut the conclusions drawn in the foregoing but is actually justified because of its vanishing under stronger effects and the related uncertainty of all quantitive indications.

If the circumstances were thus fully described, we should expect a measurable increase of intensity subsequent to 1958 in the proton flux above 30 MeV consequently only in the range of about 10^2 to $10^3 cm^{-2} s^{-1}$. Let us select two points for a more accurate estimate: B = 0.22 Gauss, $\varphi = 1.25$ and $\varphi = 1.5$. The appurtenant mean densities in 1958 are: $1.8 \cdot 10^7 cm^{-3}$ and/or $5 \cdot 10^5 cm^{-3}$; on the orbital path, primarily the altitudes immediately below 300 and/or 520 km contribute to them. According to King-Hele and Walker (1961), the density here changed between 1958 and 1960 by less than 1.3 in the first case and about 2 to 3 in the second case. According to Lin (cf. Pizzela et al., 1962-a, -b), cosmic radiation remained constant within 20 % during 1960.

The actually observed variations of proton-flux density above 18 MeV (Pizzela et al., 1962-a) cannot be brought into agreement with these expectations because, in the entire range $\varphi \leq 1.7$ and $10 < F_p(> 18 \text{ MeV}) < 10^4 cm^{-2} s^{-1}$, it increased by only a factor of 2 to 3 in 1960 (fig. 7.11, cf. discussion between Hess, 1962 and Pizzela et al., 1962-b). However, upon closer examination of the measured data (fig. 7.10), we find the following difference: the proton intensity does not decrease proportionally with time but in stages, correlated with intense magnetic storms, whereas it agrees approximately with the derived life spans between these events.

At $\varphi \leq 1.7$, only the third group of the initially enumerated effects can be made responsible for these phenomena. Let us make the following suggestion as an explanation: at the time of intense magnetic storms during which the mean field intensity varies on the surface of the earth within 1 to 2 days by more than tenfold from the normal value (cf. Ap-index in Bartels, 1962), the

amplitude of the short-period disturbances in the magnetosphere also increases. If we assume that it exceeds the mean value thirty times such an interval of time, then the time scale for non-adiabatic effects is briefly reduced by 3 powers of ten (cf. sec. 4), i.e., at 100 MeV and $\varrho = 1.5$, from 6 years to 2 days according to fig. 7.8. The migration of the reflection points linked to them could lead to an increase of intensity in given areas.

The considerations in sec. 4 made the impairment of the invariant Φ as the process most probable in the energy range from 10 to 10^3 MeV in the vicinity of the earth. An important indication exists that the impairment of μ or J is eliminated also in this connection. Its effect would be primarily a diffusion of the reflection points along the field lines which should lead as a whole to increased losses to the denser atmosphere. Instead of this, we observe an increase of intensity in 1960 (cf. fig. 7.11) along an entire shell ϱ = const. However, if only Φ is disturbed, the situation is entirely different. From (4.14), there follows for the variation in η, i.e., in the latitude of the reflection point

$$\frac{\Delta\eta}{\eta} = \frac{-1}{2(1+\nabla(\eta))} \cdot \frac{\Delta\varrho}{\varrho} \tag{7.19}$$

with $$\nabla(\eta) = -\frac{d \log \tilde{J}(\zeta_m(\eta))}{d \log \eta}$$ (see (2.29) and (2.22)

$$\nabla(\eta) > 0 \quad \text{for} \quad \eta > 0, \quad \lim_{\eta \to 1} \nabla(\eta) = \infty.$$

Diffusion inward ($\Delta\varrho < 0$) takes place with an increase of η, i.e., under decrease of the latitude of reflection point. For example, the two points $\varrho = 1.5$, $\eta = 0.786$ and $\varrho = 1.25$, $\eta = 0.800$ lie on a path characterized by (7.19) and are points where the proton intensity above 30 MeV has a ratio of 100 : 1 according to the Explorer IV data. Since any diffusion tends toward decreasing differences of concentration, there exists consequently the

possibility that a diffusion flux directed inward starts in this range during a magnetic storm.

Any quantitive statement in regard to this must await better knowledge of the diffusion coefficients (4.10) -- a preliminary formulation will be found in the work of Davis and Chang, (1962) -- and solution of the appurtenant Fokker-Planck Equation with the correct initial conditions. However, qualitatively some other aspects result: as the cause of a magnetic storm must be regarded the arrival of an increased plasma flow from the sun to the outer parts of the terrestrial magnetic field. The phenomena on the sun responsible for this are not always correlated; however, with the creation of a large number of high-energy particles ($E > 10$ MeV); on the contrary, there appears to be a correlation in an inverse direction. Accordingly, two different situations are encountered during a magnetic storm; proton intensity is greatly increased first through albedo neutrons of solar corpuscular radiation outside of $\rho = 1.7$, and is also appreciably reduced since the last such occurrence due to the here already relatively short life span (fig. 7.8). In the first case, we should find further inward ($\rho < 1.7$) an increase and, in the second case, a decrease of intensity. However, this is entirely different at $\rho < 1.5$, i.e., within the maximum of distribution of equilibrium. In this case, any intense magnetic storm should cause an increase of intensity approximately proportional to the prevailing distribution, provided the time scale of these manifestations does not change too much spatially.

Figures 4-6 in the study of Pizzela et al., (1962-a) actually permit us to recognize these tendencies. Whereas proton intensity increased everywhere as a sequel of the May and November flares, it perceptively dropped during the magnetic storm in July at $\rho = 1.6$ to 1.8; at $\rho < 1.5$, however, we find increases of almost the same magnitude as in May. However, the divergence of the data

is so high that this statement cannot be regarded as reliably confirmed.

When examining the temporal sequence of proton-flux density between magnetic storms, we must keep in mind the increase of life span with energy there where the collision losses predominate. This may be the reason that the intensity, e.g., after the increase in May 1960 at $\rho < 1.5$ does not return to the starting point with the time scale to be expected at the counter threshold, especially since its increase during magnetically disturbed conditions should be more intense precisely at the higher energies according to the considerations in subsec. 4.2.

In an extensive temporal and energetic range in the center of the inner proton belt, however, the life spans at a normal magnetic field are throughout longer than the mean interval between two solar proton phenomena and magnetic storms. The brief diffusion of protons directed inward during a strong injection at $\rho > 1.7$ may on the whole lead to an increase of replenishment also at $\rho < 1.7$. However, a more exact evaluation of the significance of these processes is not possible at the moment. We must point out, however, that, in the light of these concepts, the loss rates at higher altitudes derived in subsec. 7.4 and based precisely on the assumption of a uniform and little variable proton source, are affected with an increased uncertainty and are possibly higher by an appreciable factor.

It seems scarcely possible that replenishment also at low altitudes is increased so much through the diffusion of protons by magnetic storms that the reason for the relatively high source intensity required in subsec. 7.4 can be found in it. In that case, the proton-source intensity should appreciably decrease with decreasing proton-flux density, i.e., with decreasing life span (especially where it is short as against the interval of the magnetic storms) and it should not be possible to achieve any consistency between the scale

height of proton distribution and the atmosphere with the model utilized in subsec. 7.4.

Especially the questions raised last may make clear the factors of uncertainty with which the understanding of even the relatively easily analyzed proton belt is affected so that we may expect still many surprises from future extensive measurements and detailed analyses.

8. - Concluding Summary

We shall now briefly review the most important findings of this study and point out some measurements desirable for further clarification.

The model calculations for the intensity distribution of the protons at the lower limit of the inner radiation belt where collisions determine life span, have shown that a stationary spatially slightly variable proton replenishment as represented by the decay of the albedo neutrons of cosmic radiation, is suitable for explaining the observations also in detail. The relative density curve of the atmosphere required for this agrees well with our knowledge from satellite deceleration. Only the absolute intensity of replenishment is higher by an appreciable factor (≈ 7) than the theory of the albedo neutrons by Hess et al., (1961) is able to furnish. The discrepancy from the measurements of Bame et al., (1962) is still greater. However, since all relatively reliable statements on neutrons are referenced to energies below 10 MeV whereas the requirements here posed are basically references to energies above 30 MeV, no real ambuity exists. In order to maintain the albedo hypothesis, there results very strict requirements for the form of the proton spectrum which must then be very flat between 1 and 50 MeV and indications for this actually exist. More accurate measurements in this range of energy are of great importance, however, for a final confirmation of this hypothesis which is very reliable in many respects.

Outside of $\rho \approx 1.7$, an intense flux of albedo neutrons which may lead to an appreciable proton injection and a general steep energy spectrum, becomes occasionally superposed to the normal proton source during the intrusion of high-energy solar particles into the atmosphere at high latitudes ($|\beta| \gtrsim 55°$). Since life spans in this range are already very much shorter than the mean interval of such proton occurrences, high temporal variations occur here.

This spatially rather abrupt entry of a further proton source in conjunction with the steep decrease of life span beyond $\rho = 1.3$ to 1.6, leads to the occurrence of a maximum of the proton flux at $\rho \approx 1.5$ and of a minimum at $\rho \approx 1.8$ to 2.0 and a renewed increase outward now greatly dependent on time which, taken as a whole, produced the impression of two belts.

The energy range of the proton belt is limited upward by the cancellation of the first adiabatic invariant (μ) of particle motion; at low values of ρ, to the inhomogeneity of the non-disturbed field perceptible already during the circle of gyration at these energies and, further outward, due to variations in time. Where the second process prevails over the former cannot yet be decided. In any event, the upper limit of energy at $\rho = 3$ should have dropped to at least 10 MeV. The lower limit is produced by charge exchange with the neutral particles of the atmosphere and lies at a few hundred keV and varies only little with decreasing neutral-gas density because the charge-conversion cross sections increase steeply after low energies.

Within the range so defined, the life span of the protons is determined by non-elastic collisions, provided the mean atmospheric density over their path is large enough. At greater altitudes, the impairment of the other two adiabatic invariants becomes the predominating loss process. A steeper drop of the energy spectrum than with pure collision losses and the decrease of the life span beyond $\rho = 1.5$ at a high power of ρ must be evaluated as

definite indications of the impairment of Φ. The longest life spans (about 30 years) are attained, under this concept, by protons with energies between 10 and 100 MeV at low altitudes and $1.2 < \rho < 1.6$. The significance of the impairment of J is as yet very little clarified. The relation of the loss processes to each other will probably be determined best from energy spectra of various altitude ranges, especially from the center of the inner radiation belt where injection from the polar caps does not take place as yet.

In connection with magnetic storms, the time scale of the impairment of Φ is probably drastically shortened and thus produces an appreciable intermixture of the stationary distribution within $\rho \approx 1.7$. To what extent these processes influence the distribution in the inner part of the proton belt as a whole is difficult to delimit at the moment and is one of the most important questions for the future.

Once we have gained greater certainty on the composition of the radiation belt, we might then think of analyzing proton distribution from another viewpoint (which has always existed in the background during the preparation of this study), i.e., whether it can be used as an indication on the distribution of atmospheric density at high altitudes. Here the energy range below a few MeV promises to reach farthest because the disturbances of the adiabatic invariants in it should be by far the smallest (cf. Table 4.1).

The importance of extensive observations of the behavior in time of proton distribution at various energies for the determination of life span and the processes on which they are based, is obvious. From the point of view of theory, we must above all investigate further the problem of the impairment of the three adiabatic invariants and, with the resultant findings, subject the dynamics of proton distribution, especially also during magnetic storms, to a more exact analysis through solution of the appurtenant Fokker-Planck

Equation (cf. subsec. 4.2).

Since the investigations here embodied were terminated in the winter of 1962/63, no later measurements have been included after final review.

Grateful acknowledgement for their aid, assistance and interest is due to the following: Dr. A. Schlueter; Dr. R. Luest; Dr. L. Bierman (who permitted me to prepare this communication at the Max-Planck Institute for Physics and Astrophysics and to use the G-3 Computer at the Institute); Dr. R. S. White; Mrs. U. Banik and the members of the Institute for Astrophysics.

2. - Appendix

Frequently Used Symbols

$\mathfrak{B}$ = magnetic field intensity
B = $|\mathfrak{B}|$, B^* non-dimensional (2.22)
ΔB = Amplitude of variations of field intensity
$L^2(\zeta) = \frac{B_o}{B(\zeta)}$
B_o = $B(\zeta = 0)$
B_m = B for $\zeta = \frac{\pi}{2}$

c = velocity of light
d = discriminant of the Alfven approximation (4.1)
E = Energy
e = elementary charge
F_p = proton-flux density above energy E
f = distribution function (2.31)
G = geometric component of Q (7.5)
g.c. = guiding center
h = scale height
h_D = Debye length (3.11)

I = proton intensity
I_n = neutron intensity at altitude 100 km
J = second adiabatic invariant (2.10)
J^* = J non-dimensional (2.29)
$\mathcal{J}$ = component of J* dependent on latitude
i = magnetic inclination
ι = $\triangleq \varphi$
L_n = decay time of neutron

l = arc length along field lines
M = magnetic moment of terrestrial field
$M(\zeta)$ = component of I_n (7.1) dependent on latitude
m = (indices: e,p,1,2) particle mass
m_o = mass at rest
$\mathfrak{N}$ = normalization function in $W(\tau, \zeta)$ (2.21)
N = atmospheric density

n = proton density
p = impulse or collision parameter
Q = proton-source function (4.2)
q = differential collision cross sections
R_e = terrestrial radius
R_g = gyration radius
r = distance from magnetic dipole

s = distance from center of earth
t = time
v = velocity, $\mathbf{v} = |\mathbf{v}|$
W_k = angular distribution of neutrons (7.1) in the energy range k
$W(\tau, \zeta)$ = probability of locus (2.19)
Z = nuclear charge number
$\alpha = \frac{E}{m_o c^2}$
β = magnetic latitude
$\gamma = \left(1 - \frac{v^2}{c^2}\right)^{-1/2}$
ε = deceleration cross section
ζ = sin β
η = sin ψ_o
λ = magnetic latitude
μ = first adiabatic invariant (2.5)
ν = frequency (indices: g = gyration, Osz = oscillation $\parallel \mathfrak{B}$, D = drift around earth)
ξ = phase angle in gyration circle
ϱ = field line distance at Equator
σ = collision cross section
τ = life span
Φ = third adiabatic invariant (2.9)
Φ_n = energy spectrum of albedo neutrons (7.1)
φ = angle of orbital inclination
φ_o = angle of orbital inclination at Equator
χ = $\frac{\pi}{2}\nu$

10. - Literature References

Abbreviations: J.G.R.: Journal of Geophysical Research
Space Research I: Proc. 1st International Space Science Symposium, Nice, ed. H. K. Kallman-Bijl, Amsterdam (1960)
Space Research II: Proc. 2nd International Space Science Symposium, Florence, ed. H. C. van de Hulst, C. de Jager, A. F. Moore, Amsterdam (1961)
Kyoto II: Proc. of the Internat. Conf. on Cosmic Rays and the Earth Storm, Kyoto, J. Phys. Soc. Japan 17, Supplement A II (1962).

ALBERT, R., C. GILBERT, W. N. HESS (Abstr.) J.G.R. 67, 3537 (1962).
ALFVEN, H., Cosmical Electrodynamics, Claredon Press, Oxford (1950).
ALLISON, S. K., Rev. Mod. Phys., 30, 1137 (1958).
ARMSTRONG, A. H., F. B. HARRISON, H. H. HECKMAN, L. ROSEN, J.G.R. 66, 351 (1961).
BACKUS, G., A. LENARD, R. KULSRUD, Z. Naturforsch. 15a, 1007 (1960).
BAME, S. J., J. P. CONNER, F. B. BRUMLEY, R. L. HOSTETLER, A. C. GREEN (1962), J.G.R. 68, 1221 (1963).
BARTELS, J., Collection of Geomagnetic Planetary Indices K and Derived Daily Indices, A_p and C_p for the Years 1932 to 1961, Amsterdam 1963.
BETHE, H. A., Ann. Phys. 5, 325 (1930).
CAMPINI, U., P. H. FOWLER, W. O. LOCK, H. MUIRHEAD, Phil. Mag. 41, 413 (1950).
CHANDRASEKHAR, S., Rev. mod. Phys. 15, 1 (1943).
CHEW, G. F., M. L. GOLDBERGER, F. E. LOW, The Individual Particle Equations of Motion in the Adiabatic Approximation, Los Alamos 2055, VIII E (1955).
COHEN, R. S., L. SPITZER, P. McR. ROUTLY, Phys. Rev. 80, 830 (1950).
COLEMAN, P. J. Jr., C. P. SONETT, D. L. JUDGE, E. J. SMITH, J.G.R. 67, 1191 (1962).
DAVIS, L. Jr., D. B. CHANG, J.G.R. 67, 2169 (1962).
DAVIS, L. R., C. E. FICHTEL, D. E. GUSS, K. W. OGILVIE, Kyoto II, 326 (1962).
DESSLER, A. J., E. H. VESTINE, J.G.R. 65, 1069 (1960).
DRAGT, A. J., J.G.R. 66, 1641 (1961).
FAN, C. Y., P. MEYER, J. A. SIMPSON, J.G.R. 66, 2607 (1961).
FREDEN, S. C., R. S. WHITE, Phys. Rev. Letters 3, 9 (1959).
FREDEN, S. C., R. S. WHITE, J.G.R. 65, 1377 (1960).
FREDEN, S. C., R. S. WHITE, J.G.R. 67, 25 (1962).
FREEMAN, J. W., J.G.R. 67, 921 (1962).
GALL, R., Kyoto II, 139 (1962).
GARREN, A., R. J. RIDELL, L. SMITH, G. BING, L. R. HENRICH, T. G. NORTHROP, J. E. ROBERTS, 2nd United Nations International Conf. on the Peaceful Uses of Atomic Energy, Genf (1958).
GINZBURG, V. L., L. V. KURNOSOVA, V. I. LOGACHEV, L. A. RAZORENOV, M. I. FRADKIN, Kyoto II, 128 (1962).
GRAD, H., R. VAN NORTON, Conf. on Plasma Physics and controlled Nuclear Fusion Research, CN-10/172, Salzburg (1961).
HAERENDEL, G., J.G.R. 67, 1173 (1962); corrig. J.G.R. 67, 1697 (1962).
HAMLIN, D. A., R. KARPLUS, R. C. VIK, K. M. WATSON, J.G.R. 66, 1 (1961).
HANSON, W. B., J.G.R. 67, 183 (1962).
HARRIS, I., V. PRIESTER, J.G.R. 67, 4583 (1962).
HECKMAN, H. H., A. H. ARMSTRONG, J.G.R. 67, 1255 (1962).

HELLWIG, G., Z. Naturforsch. 10a, 508 (1955).
HERRING, J., L. KYLE, J.G.R. 66, 1980 (1961).
HERTWECK, F., A. SCHLUETER, Z. Naturforsch. 12a, 844 (1957).
HESS, W. N., Rev. Mod. Phys. 30, 368 (1958).
HESS, W. N., Phys. Rev. Letters 3, 11 (1959).
HESS, W. N., J.G.R. 67, 4886 (1962).
HESS, W. N., E. H. CANFIELD, R. E. LINGENFELTER, J.G.R. 66, 665 (1961).
HESS, W. N., H. W. PATTERSON, R. WALLACE, E. L. CHUPP, Phys. Rev. 116, 445 (1959).
HESS, W. N., A. J. STARNES, Phys. Rev. Letters, 5, 48 (1960).
HOFFMAN, R. A., R. L. ARNOLDY, J. R. WINCKLER, J.G.R. 67, 1 (1962).
HOLLY, F. E., R. G. JOHNSON, J.G.R. 65, 771 (1960).
JENSEN, D. C., R. W. MURRAY, J. A. WELCH, Jr., "Tables of Adiabatic Invariants for the Geomagnetic Field 1955.0", Air Force Special Weapons Center, Kirtland Air Force Base, New Mexico (1960).
JOHNSON, F. S., Satellite Environment Handbook, 9, Stanford (1961).
JOHNSON, F. S., R. A. FISH, Ap. J. 131, 502 (1960).
KALLMAN-BIJL, H. K., J.G.R. 66, 787 (1961).
KALLMAN-BIJL, H. K., J. atmos. terrest. Phys. 24, 831 (1962).
KATO, Y., T. SAITO, Kyoto II, 34 (1962).
KATO, Y., T. TAMAO, Kyoto II, 39 (1962).
KELLOGG, P. J., Nuovo Cimento 11, 48 (1959).
KING-HELE, D. G., D. M. C. WALKER, Space Research II, 913 (1961).
KRUSKAL, M., Rendiconti del Terzo Congresso Internazionale sui Fenomeni D'Ionizzazione nei Gas tenuto a Venezia, Societa Italiana di Fisica Milano (1957).
KRUSKAL, M., J. Math. Phys. 3, 806 (1962).
LENCHEK, A. M., J.G.R. 67, 2145 (1962).
LENCHEK, A. M., S. F. SINGER, Kyoto II, 123 (1962a).
LENCHEK, A. M., S. F. SINGER, J.G.R. 67, 1263 (1962b).
LENCHEK, A. M., S. F. SINGER, J.G.R. 67, 4073 (1962c).
LUEST, R., Fortschr. Phys. 7, 503 (1959).
LUEST, R., A. SCHLUETER, Z. Naturforsch. 12a, 841 (1957).
McDONALD, F. B., W. R. WEBBER, J.G.R. 67, 2119 (1962).
McDONALD, W. M., M. WALT, Ann. Phys. 15, 44 (1961).
McILWAIN, C. E., J.G.R. 66, 3681 (1961).
NAUGLE, J.E., D. A. KNIFFEN, Phys. Rev. Letters 7, 3 (1961).
NAUGLE, J. E., D. A. KNIFFEN, Kyoto II, 118 (1962).
NEHER, H. V., H. R. ANDERSON, J.G.R. 67, 1309 (1962).
NICOLET, M., J.G.R. 66, 2263 (1961).
NORTHROP, T. G., E. TELLER, Phys. Rev. 117, 215 (1960).
OBAYASHI, T., J. A. JACOBS, Geophys. J. 1, 53 (1958).
OGILVIE, K. W., D. A. BRYANT, L. R. DAVIS, J.G.R. 67, 929 (1962).
PAETZOLD, H. K., H. ZSCHOERNER, Space Research II, 968 (1961).
PARKER, E. N., Phys. Fluids 1, 171 (1958).
PARKER, E. N., J.G.R. 65, 2117 (1960).
PARKER, E. N., J.G.R. 66, 693 (1961).
PARKINSON, W. D., J. CLEARY, Geophys. J. 1, 346 (1958).
PIZZELLA, G., C. E. McILWAIN, J. A. VAN ALLEN, J.G.R. 67, 1235 (1962a).
PIZZELLA, G., C. E. McILWAIN, J. A. VAN ALLEN, J.G.R. 67, 4888 (1962b).
SERGELI, J. D., R. TOUSEY, Space Research I, 590 (1960).
SERIFF, V. P., R. C. HAYMES, S. A. KORFF, J.G.R. 67, 459 (1962).
SMITH, N., Nature 191, 238 (1961).
SOSS, D. C., S. ZIAUDDIN, Space Science Rev. 1, 115 (1962).
SCHLUETER, A., "Plasmaphysik", ["Plasma Physics"], Vorlesungen an der Universitaet Muenchen [Lectures at Munich University] SS 1959.

SIMPSON, J. A. Phys. Rev. 83, 1175 (1951).
SINGER, S. F., Phys. Rev. Letters 1, 171 (1958a).
SINGER, S. F., Phys. Rev. Letters 1, 181 (1958b).
SINGER, S. F., Phys. Rev. Letters 2, 188 (1959).
SONETT, C. P., D. L. JUDGE, A. R. SMITH, J. M. KELSO, J.G.R. 65, 55 (1960).
SONETT, C. P., A. R. SIMS, I. J. ABRAMS, J.G.R. 67, 1191 (1962).
STIX, T. H., Phys. Fluids 1, 308 (1958).
STOERMER, C., The Polar Aurora, Clarendon Press, Oxford (1955).
STUART, G. W., Phys. Rev. Letters 2, 417 (1959).
VAN ALLEN, J. A., L. A. FRANK, Nature 183, 430 (1959a).
VAN ALLEN, J. A., L. A. FRANK, Nature 184, 219 (1959b).
VAN ALLEN, J. A., C. E. McILWAIN, G. H. LUDWIG, J.G.R., 64, 271 (1959).
VERNOV, S. N., E. V. GORCHAKOV, YU. I. LOGACHEV, V. E. NESTEROV, N. F. PISARENKO, I. A. SAVENKO, A. E. CHUDAKOV, P. I. SHAVRIN, Kyoto II, 162 (1962).
VERNOV, S. N., N. L. GRIGOREV, I. P. IVANENKO, A. I. LEBEDINSKII, V. S. MURZIN, A. E. CHUDAKOV, Soviet Physics -- "Doklady" 4, 154 (1959) (Doklady Akad. Nauk SSSR 124, 1022 (1959).
WATTENBERG, A., Handb. Phys. XL, 450 (1957).
WELCH, J. A., W. A. WHITAKER, J.G.R. 64, 909 (1959).
WENTWORTH, R. C., S. F. SINGER, Phys. Rev. 98, 1546 (1955).
WENTZEL, D. G., J.G.R. 66, 359, 363 (1961).
WENTZEL, D. G., J.G.R. 67, 485, (1962).
WHALING, W., Handb. Phys. XXXIV, 193 (1958).
WINCKLER, J. R., Kyoto II, 353 (1962).